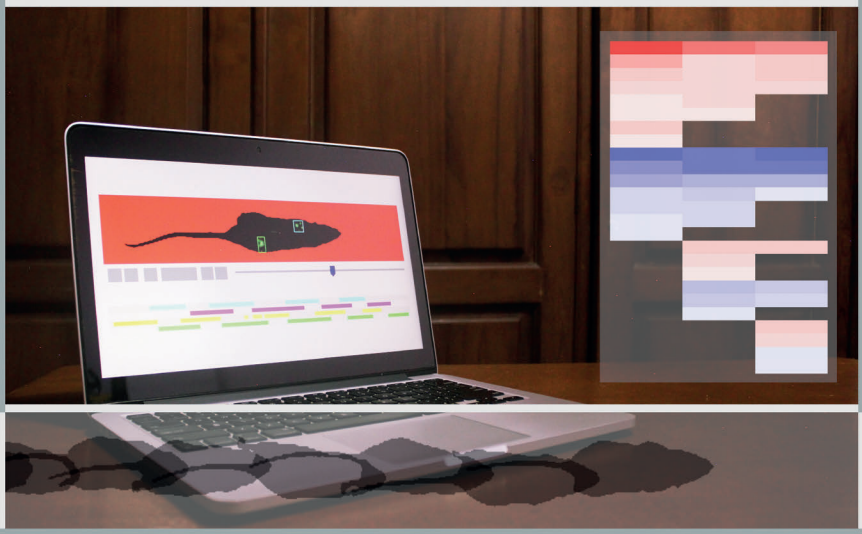

FAU Studien aus der Informatik 12

Ivanna Kristianti Timotius

Computational Methods for Gait Analysis in Rodents

FAU UNIVERSITY PRESS

Ivanna Kristianti Timotius

Computational Methods for Gait Analysis in Rodents

FAU Studien aus der Informatik

Band 12

Ivanna Kristianti Timotius

Computational Methods for Gait Analysis in Rodents

Erlangen
FAU University Press
2020

Bibliografische Information der Deutschen Nationalbibliothek:
Die Deutsche Nationalbibliothek verzeichnet diese Publikation in der Deutschen Nationalbibliografie; detaillierte bibliografische Daten sind im Internet über http://dnb.d-nb.de abrufbar.

Der vollständige Inhalt des Buchs ist als PDF über den OPUS-Server der Friedrich-Alexander-Universität Erlangen-Nürnberg abrufbar:
https://opus4.kobv.de/opus4-fau/home

Bitte zitieren als
Timotius, Ivanna Kristianti. 2020. *Computational Methods for Gait Analysis in Rodents*. FAU Studien aus der Informatik Band 12. Erlangen: FAU University Press. DOI: 10.25593/978-3-96147-321-2

Verlag und Auslieferung:
FAU University Press, Universitätsstraße 4, 91054 Erlangen

Druck: docupoint GmbH

ISBN: 978-3-96147-320-5 (Druckausgabe)
eISBN: 978-3-96147-321-2 (Online-Ausgabe)
ISSN: 2509-9981
DOI: 10.25593/978-3-96147-321-2

Computational Methods for Gait Analysis in Rodents

Rechenmethoden zur Ganganalyse bei Nagetieren

Der Technischen Fakultät der
Friedrich-Alexander-Universität Erlangen-Nürnberg

zur
Erlangung des Doktorgrades Dr.-Ing.
vorgelegt von

Ivanna Kristianti Timotius

aus Semarang, Indonesien

Als Dissertation genehmigt von der
Technischen Fakultät der
Friedrich-Alexander-Universität Erlangen-Nürnberg

Tag der mündlichen Prüfung:	04.03.2020
Vorsitzender des Promotionsorgans:	Prof. Dr.-Ing. habil. Andreas Paul Fröba
Gutachter:	Prof. Dr. Björn Eskofier Prof. Dr. Gernot Riedel Prof. Dr. med. Stephan von Hörsten

Abstract

Gait analysis is important for the investigation of gait progression and the development for therapies in disorders characterized by gait impairments, such as Parkinson's disease (PD), Huntington disease (HD), and Spinal Cord Injury (SCI). Describing gait quantitatively helps researchers to analyze gait impairment in a more consistent, reliable, and precise manner compared to qualitative description. For this reason, apparatus and computation methods are continuously developed for both clinical and preclinical studies.

Preclinical studies often use rodents to study human diseases because of the genetic, physiological, and psychological similarities between rodents and humans, rodents' compactness, relatively low-costs, availability, diminutive lifespan, as well as the possibility of conducting controlled experiments without harming any human. For assessing gait in preclinical studies, both apparatus and computational methods need to be specialized for rodents and to be designed according to the disorder under study.

One of the gait analysis apparatus for rodents is called CatWalk. The system is equipped with a transparent glass floor walkway, where rodents can walk from one to the opposite end. Using a camera located under the walkway, the system records a video, which contains the information of the paw contact positions. Based on the recorded video, this CatWalk system computes several gait parameters.

For analyzing gait, computational methods are developed, which include gait characteristic quantification, gait parameter scaling or normalization, initial data analysis, and multiple gait parameter analysis.

The gait parameters, which are measured and quantified, should characterize the important gait pattern. In the study of PD in humans, sway is one of the crucial gait characteristics considering that it is related to the risk of falling. Here, three methods for quantifying the sway-

relevant characteristic in mice are presented. The methods were developed based on the paw position information by utilizing signal processing approaches, such as the short time fast Fourier transform (STFFT) and the low pass filtering (LPF). The three methods were applied to paw position data taken from all paws as well as from front-/hind-paws separately, yielding a total of nine sway-related parameters. These methods were applied to differentiate two different transgenic PD-relevant mouse models (α-synuclein mice) and their wild-type littermates. The sway-related parameters revealed higher sway in the PD-relevant mouse models compared to their wild-type littermates. One of the PD-relevant mouse models revealed significantly higher sway compared with their wild-type littermates in eight of the nine sway-related parameters.

The analysis of gait often becomes complicated by the fact that several gait parameters relate to body size. A gait parameter normalization for the individual body-size can therefore improve the reliability of the analysis. Here, a video-derived body silhouette length calculation method based on image processing techniques was developed. Subsequently, a correlation study between several gait parameters and calculated body silhouette length in wild-type rodents across age is presented. The correlation study shows the relation of the silhouette-lengths to rodents' stride lengths, swing speeds, and body speed. Therefore, an intra-assay method of silhouette-length-based gait parameter scaling for rodents is presented. The silhouette-length-based scaling method was systematically compared with several other scaling methods and was applied to data collected from HD-relevant mice and PD-relevant rats, which identifies the presence and the effect of genotype-driven body size differences. In general, the scaled gait parameters improve the reliability of gait analysis especially in rodent models with genotype-driven body-size differences and therefore is suitable to become a standard approach in rodent gait analysis.

Complications in data analysis and reporting of CatWalk gait parameters arise additionally due to the large number of parameters. The complications often lead to premature parameter selection and to the omission of negative result reporting. Alternatively, a systematic initial data analysis (IDA) for exploring all gait parameters, including a data reporting approach by utilizing heat mapping, is presented here. The approach is exemplified in PD-relevant mouse models, PD-relevant rat model, and HD-relevant mouse model. The resulting heat maps give

a visualization of gait parameter differences within one single chart, which is advantageous in highlighting important parameters.

Furthermore, as several gait parameters need to be analyzed simultaneously, analyzing several gait parameters, as well as their clustering, are often challenging. One possible way to deal with this is by making a linear combination of the parameters that is able to reflect the disease progression. Therefore, a method of making a linear combination of the gait parameters that reflects the motor recovery of rat SCI models based on the Linear Discriminant Analysis (LDA) is presented. The resulting linear combination was applied in CatWalk gait parameters from three rat thoracic contusion SCI studies, a rat thoracic dorsal hemisection SCI study, and a rat cervical dorsal column lesion SCI study. It is presented here that this CatWalk gait parameter linear combination can depict gait recovery progression after injuries as shown in the rat thoracic contusion SCI studies and the rat thoracic dorsal hemisection SCI study. Therefore, this parameter combination gives an alternative to the standardized subjective gait assessment, i.e. Basso, Beattie, Bresnahan (BBB)-score.

In this dissertation, the implementation of signal processing, image processing, initial data mining, and discriminant analysis concepts on the CatWalk gait data are presented. These methods enrich and improve the outcome of the current Catwalk data acquisition by providing methods in identifying gait patterns related to PD, providing a silhouette-length-based intra-assay scaling method, an initial data analysis method, and a parametric gait recovery progression score for rat SCI models.

Zusammenfassung

Ganganalyse ist wichtig für die Untersuchung des Gangverlaufs und die Entwicklung von Therapien bei Erkrankungen, die durch Gehbehinderungen charakterisiert sind. Beispiele für solche Erkrankungen sind die Parkinson-Krankheit (Parkinson's disease, PD), Huntington-Krankheit (Huntington disease, HD) und Rückenmarksverletzungen (Spinal Cord Injury, SCI). Eine quantitative Beschreibung des Gehens hilft Forschern, die Gangstörung konsistenter, verlässlicher und genauer als die qualitative Beschreibung zu analysieren. Aus diesem Grund werden kontinuierlich Geräte und Berechnungsmethoden sowohl für klinische als auch für präklinische Studien weiterentwickelt.

Präklinische Studien verwenden oft Nagetiere, um menschliche Krankheiten zu untersuchen. Gründe dafür sind die genetische, physiologische und psychologische Ähnlichkeit zwischen Nagetieren und Menschen, die Kompaktheit der Nagetiere, die relativ niedrigen Kosten, die Verfügbarkeit, die geringe Lebensdauer sowie die Möglichkeit, kontrollierte Experimente durchzuführen, ohne einen Menschen zu schädigen. Für die Gangbeurteilung in präklinischen Studien müssen sowohl Geräte als auch Rechenmethoden für Nagetiere spezialisiert und entsprechend auf die zu untersuchende Erkrankung ausgelegt sein.

Eines der Ganganalysegeräte für Nagetiere wird CatWalk genannt. Das System ist mit einem Gang mit Glasboden ausgestattet, in dem die Nagetiere von einem zum anderen Ende gehen können. Mit einer Kamera, die sich unter dem Gehweg befindet, kann das System Videoaufnahmen erzeugen, die Informationen über die Kontaktpositionen der Pfoten enthält. Basierend auf den aufgezeichneten Videodaten berechnet dieses CatWalk-System mehrere Gangparameter.

Für die Ganganalyse werden Berechnungsmethoden entwickelt, die die Quantifizierung der Gangcharakteristik, die Skalierung oder

Normalisierung der Gangparameter, die anfängliche Datenanalyse und die Analyse mehrerer Gangparameter umfassen.

Die Gangparameter, die gemessen und quantifiziert werden, charakterisieren das wichtige Gangmuster. In der Studie von PD beim Menschen ist Schwanken eines der entscheidenden Gangmerkmale, da es mit dem Sturzrisiko verbunden ist. Hier werden drei Methoden zur Beurteilung schwankungsrelevanter Charakteristiken bei Mäusen vorgestellt. Die Methoden wurden basierend auf den Informationen der Pfotenposition unter Verwendung von Signalverarbeitungsansätzen, wie der Fast Fourier-Transformation (FFT) und der Tiefpassfilterung (LPF) aufgebaut. Die drei Methoden wurden auf CatWalk-Daten angewendet, die sowohl von allen Pfoten sowie von Vorder-/Hinterpfoten separat entnommen wurden. Daraus ergaben sich insgesamt neun schwankungsbezogene Parameter. Diese Methoden wurden angewandt, um zwei verschiedene transgene PD-relevante Mausmodelle (α-synuclein Mäuse) und deren Wildtyp-Verwandten zu unterschieden. Die schwingungsbezogenen Parameter zeigten bei den PD-relevanten Mausmodellen eine höhere Schwankung im Vergleich zu ihren Wildtyp-Verwandten. Eines der PD-relevanten Mausmodelle zeigte bei acht der neun schwingungsbezogenen Parameter eine signifikant höhere Schwankung im Vergleich zu ihren Wildtyp-Verwandten.

Die Ganganalyse wird oft dadurch kompliziert, dass sich mehrere Gangparameter auf die Körpergröße beziehen. Eine Normalisierung der Gangparameter für individuelle Körpergrößen kann daher die Reliabilität der Analyse verbessern. Hier wird ein videogestütztes Verfahren zur Längenberechnung der Körpersilhouette auf Basis von Bildverarbeitungstechniken vorgestellt. Daraufhin wird eine Korrelationsstudie zwischen mehreren Gangparametern und der berechneten Länge der Körpersilhouette bei Wildtyp-Nagetieren über die Lebenszeit vorgestellt. Die Korrelationsstudie zeigt den Einfluss der Silhouettenlänge zu Schrittlängen, Schwunggeschwindigkeiten und Körpergeschwindigkeit der Nagetiere. Daher wird eine Intra-Assay-Methode zur Skalierung von Gangparametern basierend auf der Silhouettenlänge für Nagetiere vorgestellt. Diese Skalierungsmethode wurde systematisch mit mehreren anderen Skalierungsmethoden verglichen. Zusätzlich wurde die Skalierungsmethode auf Daten von HD-relevanten Mäusen und PD-relevanten Ratten angewendet, was das Vorhandensein und die Wirkung von genotypbedingten Körpergrößenunterschieden identifiziert. Im Allgemeinen verbessern die skalierten Gangparameter die

Reliabilität der Ganganalyse insbesondere in Nagetier-Modellen mit genotypbedingten Körpergrößenunterschieden und eignen sich daher als Standard in der Ganganalyse von Nagetieren.

Komplikationen bei der Datenanalyse und dem Reporting von CatWalk-Gang-parametern ergeben sich zusätzlich durch die große Anzahl von Parametern. Die Komplikationen führen oft zu einer vorzeitigen Parameterauswahl und zum Wegfall der negativen Ergebnisberichterstattung. Alternativ wird hier eine systematische Initialdatenanalyse (IDA) zur Untersuchung aller Gangparameter, einschließlich eines Datenberichtsansatzes unter Verwendung von Heat Mapping, vorgestellt. Der Ansatz wird anhand von PD-relevanten Mäusen, PD-relevanten Ratten und HD-relevanten Mäusen veranschaulicht. Die daraus resultierenden Heat Maps ermöglichen eine Visualisierung der Unterschiede zwischen Gangparametern in einem einzigen Chart, was bei der Hervorhebung wichtiger Parameter von Vorteil ist.

Da zudem mehrere Gangparameter gleichzeitig analysiert werden müssen, ist die Analyse mehrerer Gangparameter sowie deren Clusterung oft eine Herausforderung. Eine Möglichkeit, damit umzugehen, besteht darin, eine lineare Kombination der Parameter zu bilden, welche den Krankheitsverlauf widerspiegeln kann. Daher wird ein Verfahren zur Erstellung einer linearen Kombination der Gangparameter entwickelt, das den motorischen Verlauf von Ratten mit SCI basierend auf der Linear Discriminant Analysis (LDA) widerspiegelt. Die resultierende lineare Kombination wurde in CatWalk-Gangparametern aus drei Ratten-Thorax-Kontusion-SCI-Studien, einer Ratten-Thorax-Dorsalhämisektions-SCI-Studie und einer Ratten-Halswirbelsäule-Läsion-SCI-Studie angewendet. Es wird hier gezeigt, dass diese Gangparameter-Linar-kombination den Gangsteigerung nach Verletzungen der Ratten-Thorax-SCI-Studien darstellen kann. Daher ist diese Parameterkombination eine Alternative zur subjektiven Gangbewertung mittels Basso-Beattie-Bresnahan (BBB)-Score.

In dieser Arbeit wird die Implementierung von Signalverarbeitung, Bildverar-beitung, initialem Data Mining und Diskriminanzanalyse für CatWalk Gangdaten vorgestellt. Diese Methoden erweitern der aktuellen Catwalk-Datenerfassung, indem sie Methoden zur Identifizierung von Gangmustern im Zusammenhang mit PD, eine Intra-Assay Methode zur Skalierung, ein anfängliches Datenanalyseverfahren und einen parametrischen Gangwert für SCI-Rattenmodelle bereitstellen.

Acknowledgment

I am deeply grateful to God for His presence in every moment from the doctoral study preparation to the finishing this dissertation and for surrounding me with incredible people that make this study and dissertation possible.

I would like to thank Björn Eskofier for having me in the Machine Learning and Data Analytics (MaD) Lab and for his support and feedback during my study toward this dissertation. Special thanks to Stephan von Hörsten for his advice, knowledge, patience, help, encouragement, and for giving the preclinical view that forms the key insights of this dissertation. I would like to express my gratitude to Radhika Puttagunta for her help and for enriching the preclinical view for this dissertation. I would like to acknowledge the support and the clinical view given by Jochen Klucken. Furthermore, I am grateful to Gernot Riedel for reviewing this dissertation and to Reinko Roelofs (Noldus Information Technology) for his interest in the research works described in this dissertation.

I would like to express my deepest appreciation to the coauthors of all the scientific publications related to this dissertation and for everyone who was involved in the preclinical data collection: Fabio Canneva, Georgia Minakaki, Sandra Moceri, Anne-Christine Plank, Johanna Habermeyer, Cristian Pasluosta, Nicolas Casadei, Olaf Riess, Silke Nuber, Jürgen Winkler, Beatrice Sandner, Veronica Estrada, Daniel Garcia-Ovejero, Lara Bieler, Sebastien Couillard–Despres, Florencia Labombarda, and Hans W. Müller.

Special gratitude to Shira Richman (FAU Writing Center) for triggering sentences out of me, teaching writing philosophy, transferring writing energy, and all the time spent in helping me. Thanks to Nadine Jendrusch (FAU Writing Center), Matthias Ring, Wolfgang Mehringer, Vinicius Facco Rodrigues, and Vera Lanaia for the constructive

comments and help in writing. Thank you to all the readers of this dissertation for your interest in this research work.

This doctoral study would not possible without the financial support from Deutscher Akademischer Austauschdienst (DAAD) and Satya Wacana Christian University (SWCU) Indonesia.

Thanks to all the brilliant colleagues I have, especially in Machine Learning and Data Analytics (MaD) Lab, Motion Group, Preclinical Experimental Center (PETZ) and Pattern Recognition (LME) Lab. There were so many things I learned from all of you. Thank you for your help, support and feedback. I would particularly like to thank Christine Martindale for the enormous help, encouragement and suggestions during my doctoral study.

Thank you to my family (Kris H. Timotius, Rita Widayanti, Anne I. Timotius, Yusepaldo Pasharibu, Alexander T. Yonatan, and Arthur T. Yonatan) for the support, help, patience, trust, prayers, and everything you have done for me. Thank you to Teddy Sutanto's family that help me in adapting to life in Germany. Your kindness and support are great blessings to me. Thank you from the bottom of my heart to my second family in Erlangen, i.e. the International Jesus Gemeinde (IJG) Church pastor, leaders, worship team, technical team, kitchen team, and home group, especially to Christian Fricke's family, Stephan Klöcker's family, and Olatunji Ojuola. Thank you for the love, trust, connecting time, and every prayer that bring strength and spiritual growth in me.

Erlangen, March 2020 Ivanna K. Timotius

Contents

1 Introduction

1.1 Overview and Motivation

Animals serve as models of humans in a wide range of studies [Eric 13] and they are frequently used in biomedical research [Dutt 16]. The animals, used as human representations to investigate diseases, are often called animal models of diseases. In a preclinical experiment, animal modeling is especially useful to understand humans without risking an actual human.

Among all animals, mice and rats are the most widely used living experiment system [Dutt 16], because of sharing some similarity with humans' genes [Pete 07] [Wahl 11], physiology, and psychology, as well as their relatively compact size, low cost, availability, and diminutive lifespan (compared to humans) [Dutt 16]. Rodent models of humans for several diseases are continually being developed [Anto 11] [Jack 12] [Kjel 16] [Cher 14]. This includes the transgenic (genetically engineered) mouse that was first created in 1974 [Jaen 74] [Vand 14].

Characterizing animal models of diseases is essential for understanding the diseases and developing new therapies [Broo 09]. Therefore, clinical tests including behavior tests, histology, and electrophysiology are commonly performed. The behavior tests include a wide-range of tests, such as exploration tests, anxiety tests, motor function tests, gait tests, and learning tests [Wahl 11]. From all of the available behavior tests, gait-related tests are especially important for the investigation of disorders that are characterized by gait deficiencies, including neurological disorders such as Parkinson's disease (PD), Huntington disease (HD), and spinal cord injury (SCI). Moreover, gait test is one of the tests that can be translated from animal to human studies [Broo 09]. Rodents' gaits are commonly tested in an open field, on a runway, on a treadmill, or in a running wheel. Several runway-based gait tests exist, namely

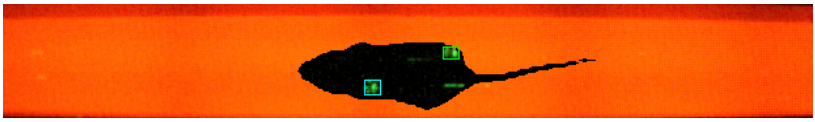

(a) Mouse

(b) Rat

Figure 1.1: Examples of CatWalk-based captured images: The detected paw contacts are marked by the colored rectangles.

ink-based foot-print test, CatWalk, Walkway, MotoRater, GaitLab, and MouseWalker.

The CatWalk^{TM} gait analysis system was initially developed by Frank Hamers [Hame 01] [Hame 06] and is now commercially available by Noldus Information Technology (Wageningen, The Netherlands) [Nold 12]. The system is designed to be used in a darkened room. It comes with a glass floor walkway on which a rodent can walk from one side to the other. Green light enters the long edge of this glass floor and reflects internally. The light escapes and scatters at the point where paws make contact with the glass floor. As a result, the paw contact areas are illuminated. In addition, red light is illuminated from the ceiling above the rodent. Therefore, the rodent's body silhouette is visible, which simplify the paw labeling. This visualization is then recorded by a camera located beneath the walkway. Image samples captured by recorded CatWalk videos are depicted in Figure 1.1, where the rodent's body silhouette is shown and the paw positions are marked. Accordingly, this markerless video-based gait analysis system quantifies several gait parameters based on the animal's paw positions and body silhouette, such as stride length, body speed, swing speed, duty cycle, regularity index [Koop 05], and the number of paws supporting the body. Further description regarding the CatWalk gait test system is given in Section 2.4.

Although the basis of gait analysis in rodents is similar to the gait analysis in humans, quadrupedal gait varies from bipedal gait [Lake 16]. Therefore, data processing and analysis for quadrupedal gait pattern

Figure 1.2: The series of CatWalk-based data processing presented in this dissertation

need to be uniquely designed. The data processing and analysis include gait parameter generation, selection, scaling, and reporting, as well as multiple gait parameter analysis. In this dissertation, several computational methods for CatWalk-based gait analysis are presented. The methods can be grouped into four main categories as visualized in Figure 1.2.

The ability to quantify clinically relevant gait characteristics is essential for a parametric gait analysis system. Despite the large number of CatWalk gait parameters, the rodent's locomotion sway pattern had not been assessed specifically in the CatWalk system. Sway, a body movement in side-to-side mediolateral axis, is associated with body stability and can be translated to balance in humans. Balance is related to the interaction of the body center of mass (COM) and the body base of support (BOS) [Luga 11]. In humans, a reduced balance during walking contributes to a higher risk of falling [Mati 07]. For this reason, investigating the balance-related characteristic in rodent models of humans' diseases is interesting. As quadrupeds, rodents have larger total BOS, and therefore they have a lower risk of falling caused by the unstable COM sway. Nevertheless, locomotion sway descriptors in rodents can reveal the walking stability, which is important to be assessed for the reason that instability is one of the motor characteristics that appeared in diseases such as PD [Jank 08] [Kluc 13] [Lope 10] [Morr 01] [Park 02] [Stol 04]. Therefore, computational methods for assessing locomotion sway in mice were designed by the author of this dissertation and are described in Chapter 3. The methods were applied in α-synuclein (α-Syn) transgenic mice with relevance for PD.

Moreover, as in humans [Hof 96], several rodents' gait parameters are corresponds to the rodents' body size [Hegl 74] [Tayl 78] [Mach 15] [Jaco 14]. This factor needs to be considered in the analysis. In most cases, the body size difference arises due to animal growth. Therefore, many researchers use adult rodents, in which body sizes are relatively

stable [Hame 01] [Wang 12] [Casa 14] [Cao 08] [Chen 14] [Ishi 14]. Alternatively, they use a same-age control group, which have similar body size as the disease-relevant group [Vand 10] [Jaco 14]. However, body size difference can also arise due to diseases, such as in animal models of HD [Hors 03] [Clem 17] and PD [Kohl 16]. Therefore, even though it is not yet common, body-size-scaled gait parameters are needed for a reliable analysis. Several researchers use body weight information to scale several gait parameters [Frah 18] [Mach 15]. Nonetheless, since the body-height- or leg-length-based scaling method is applied in several humans' gait parameters [Hof 96], it is hypothesized that body-length-based gait parameter scaling is more reliable for gait analysis compared with the body-weight-based scaling. To make the body-length-based scaling possible, body-length-related parameter need to be calculated.

The calculation of rodent's body-length (nose-tip–to–anus or nose-tip–to–base-of-tail) appeared in several research works, in which anesthesia was performed [Nove 07] [Chak 17] [Dunn 09]. Anesthesia in a preclinical study should as far as possible be avoided as it might affect the overall results [Karw 01]. Therefore, an intra-assay in-vivo body-length-related parameter computation will enable body-length-based gait-parameter normalization, that is necessary especially in a longitudinal study and in a study involving genotype-related body-size difference. The CatWalk gait analysis system provides gait parameters and silhouette information of the rodents walking above the glass walkway. By computing the length of this silhouette, an intra-assay CatWalk gait parameter scaling can be developed. A computational method for this intra-assay gait parameter scaling was developed by the author of this dissertation and is presented in Chapter 4. In addition, a comparison study of the utilization of silhouette-length, silhouette-area-, body-weight-, and age-based gait parameter scaling was performed and is presented in Chapter 4. The body-silhouette-length-based scaling method was exemplified in rodents with genotype-related body size difference, i.e. human α-Syn overexpressing transgenic rats with relevance to PD and transgenic mice expressing mutant human huntingtin (HTT) modeling HD. As shown in Chapter 4, this gait parameter scaling improves the reliability of gait analysis in rodents, especially in preclinical longitudinal studies and in preclinical studies with genotype-related body size difference.

Furthermore, the CatWalk gait analysis system computes a number of gait parameters, which are often needed for describing a complex

motion. The large number of gait parameters, the complication of formal multivariate statistical analysis that come with the large number of gait parameters, along with the attempt for condensing the published manuscript often lead to the selection of reported gait parameters based on previous research or expert's presumption. In addition, it often lead to the removal of reporting negative results, which associate with the parameters that do not show any between-cohort significant difference and are also important to be reported [Earp 17] [Kann 14a] [Mast 16]. For instance, a set of CatWalk gait parameters was recommended for the evaluation of nerve injured rat models [Chen 17] [Kapp 17], which demonstrate a hypothesis-driven approach. Alternatively, an initial visualization of all gait parameters can serve as a non-hypothesis-driven approach and in addition can avoid the practice of manipulation by selecting the reported parameters [Head 15]. A method for systematic initial data analysis (IDA) which includes visualizing the gait parameter differences in a single chart by heat mapping was formulated by the author of this dissertation and is described in Chapter 5. The method is exemplified in α-Syn transgenic mice with relevance for PD, human α-Syn overexpressing transgenic rats with relevance to PD, as well as transgenic mice expressing mutant human HTT modeling HD.

Generally, disorders affect multiple gait parameters and it is recommended to analyze these parameters simultaneously. Observing gait progression based on all these gait parameters is often challenging. Therefore, it is valuable to develop a gait parameter linear combination, which is able to express gait progression by a single score. For instance, in preclinical studies of SCI, gait is commonly assessed using a non-parametric (observation-based) locomotion scale, which is characterized by several gait characteristics [Bass 95][Bass 06][Ande 09][Sing 14]. For SCI preclinical studies, combining several CatWalk gait parameter into a single score is an alternative to the standardized non-parametric gait score, BBB score. Therefore, a method of gait parameter combination for assessing gait of rat SCI models was developed by the author of this dissertation and is described in Chapter 6.

In this dissertation, computational methods for CatWalk-based gait analysis are developed based on signal processing, image processing, data visualization, and data analysis concepts. The computational methods can be grouped into four main categories as visualized in Figure 1.2 and can be briefly described as follows.

- **Gait characteristic quantification** Methods for quantifying locomotor-sway-related characteristic in mice based on signal processing approaches are presented in Chapter 3 and applied on PD-relevant mouse models.
- **Gait parameter scaling/normalization** A method for the computation of silhouette length based on image processing approaches is presented in Chapter 4. Additionally, a method for silhouette-length-based gait parameter scaling is described and systematically compared with some other body-size-related scaling methods. Subsequently, the silhouette-length-based scaling method is applied to a PD-relevant rat model and a HD-relevant mouse model.
- **Initial data analysis** A method of systematic initial data analysis (IDA) using heat map for data visualization is presented in Chapter 5 and exemplified in PD-relevant mouse models, a PD-relevant rat model, and a HD-relevant mouse model.
- **Multiple parameter analysis** A method for combining CatWalk parameters based on linear discriminant analysis (LDA) for assessing gait in rat SCI models is presented in Chapter 6.

1.2 Related Literature

This section describes the preceding works related to the contributions of this thesis. The section starts with the overview of existing CatWalk-based research studies and their additional data processing (Subsection 1.2.1). This subsection is then followed by the existing literature regarding gait characteristic quantification (Subsection 1.2.2), gait parameter scaling and body length assessment (Subsection 1.2.3), initial data analysis by heat mapping (Subsection 1.2.4), as well as multiple gait parameter analysis (Subsection 1.2.5).

1.2.1 Gait Analysis for the CatWalk System

The CatWalk gait analysis system [Hame 01] [Hame 06] has been widely used in many preclinical studies, as shown in Table 1.1. The CatWalk system generates several gait parameters, that can be directly used for analyzing gait in rodents [Nold 12]. Therefore, most of the researchers analyze the parameters directly, without any additional data processing.

As shown in Table 1.1, a limited number of researchers include additional data processing beyond the available CatWalk gait parameters. Similarly, few have used the raw CatWalk video to develop computational methods. Those who have developed additional data processing or computational methods have done so to quantify new gait parameters, scale/normalize gait parameter, perform between-parameter ratio and averaging, as well as design a classifier.

In this dissertation, several additional data processing methods for the CatWalk gait analysis system are presented, which include quantifying a new clinically relevant gait parameter, gait parameter scaling/normalization, initial data analysis, and multiple gait parameter analyses. The description of the related literature regarding these aforementioned methods is explained in detail in the following subchapters.

1.2.2 Gait Characteristic Quantification: Sway Assessment

In humans, sway-related gait characteristics are often assessed in clinical studies, both while standing still [Manc 12a] [Rocc 04] and during locomotion [Gago 15], [Manc 12b], [Rocc 14]. Sway characteristic in rodents can be also assessed during both quite stance and locomotion. To assess postural sway in mice, a center of pressure (CoP) assay was introduced [Hutc 07]. The assessment of sway in mice during locomotion was done by calculating the sway index [Geld 15]. This sway index, also known as the sinuosity coefficient of a path, is computed by the ratio of the horizontal path distance and straight-line displacement. Sway index computation in the aforementioned research was based on an estimated COM position, chosen from a point at the nose-tip to base-of-tail line. This sway index was calculated based on experiments recorded in a bright room from an apparatus with a white wooden trackway and a camera placed above [Geld 15]. Another sway assessment method is called stance linearity index, which was applied to studies in mice [Mend 15] and in drosophila [Mend 13]. The stance linearity index in mice was calculated based on the average difference of the actual stance trace and the trace's smoothed version of a tracked body points recorded by an apparatus named MouseWalker [Mend 15]. A locomotion sway assessment based on the mouse paw positions had not been previously proposed. Therefore, in this dissertation (Chapter 3), several methods to assess locomotion sway in mice based on their paw positions are presented.

Table 1.1: Overview of literature on preclinical gait analysis using the CatWalk system and their additional data processing methods

Article	Disease Model	Study	Additional Data Processing
[Vlam 07]	PD: 6-OHDA rats	Application of bilateral HFS with different stimulation amplitudes to the STN	–
[Vand 10]	PD: 6-OHDA rats, HD: transgenic rats Stroke: photothrombotic rats	Motor impairment	–
[West 12]	PD: 6-OHDA rats,	Role of levodopa (l-DOPA)	–
[Saal 15]	PD: 6-OHDA mice	PBS, control-shRNA vs. ROCK2-shRNA	–
[Zhou 15]	PD: 6-OHDA rats	CPU, MFB vs. SNC	–
[Boix 18]	PD: 6-OHDA rats	MFB vs. striatal lesion	Scaled by the average of speed
[Froh 18]	PD: 6-OHDA & PFF mice	Time points, brain lesions, brain regions	Generating global features, Step seq. align.: DTW-based Classifier: Rand.For., EN, GBM

Continued on next page

Table 1.1 – continued from previous page

Article	Disease Model	Study	Additional Data Processing
[Wang 12]	PD: MPTP-induced mice	Correlation of gait & neurochemical	–
[Tsik 14]	PD: R1441C LRRK2 mice	Effect of R1441C LRRK2	–
[Casa 14]	PD: α-Syn transgenic mice	Co-expression of synphilin-1	–
[Rote 14]	PD: α-Syn transgenic mice	Diet-induced obesity	–
[Tate 16]	PD: α-Syn transgenic mice	Fasudil treatment	–
[Frah 18]	PD: α-Syn transgenic mice	Accumulation of α-Syn aggregation	Scaled by body weight
[Abad 13]	HD: BACHD mice	Motor, gait, emotional & cognitive deficits	–
[Pluc 14]	AD: hBACE1 knock-in mice	Behavioral traits	–
[Hero 16]	MS: MOG-induced EAE	Gait analysis and MPS treatment	–
[Bern 17]	MS: EAE mice	Treadmill exercise	Scaled by basal value (%)
[Haas 16]	LD: Ndufs$^{-/-}$ mice	Motor impairment	–

Continued on next page

Table 1.1 – continued from previous page

Article	Disease Model	Study	Additional Data Processing
[Maim 18]	ALS: HB9::GFP mice	Alterations in miR126-5p	Scaled by the values from the control animals
[Salv 14]	Ataxia: EA2 mice	Lentiviral based-vector RNA interference	–
[Hodg 15]	Menkes disease: ATP7A mice	Effect of ATP7A loss	–
[Hame 01]	Th8 SCI rats	Comparing contusion and transection injuries	–
[Kloo 05]	Th8 contusive SCI rats	Association of locomotor and sensory features with lesion severity	–
[Koop 05]	Th10 contusive SCI rats	Introducing Regularity Index (RI)	New parameter: Regularity Index (RI)
[Cao 08]	C4 lateral funiculotomy SCI rats	Motor, sensory & immunohistochemistry	–
[Sedy 08]	SCI rats	Review paper	–
[Hill 12]	Th9 contusive SCI rats	dPDN transplantation	–

Continued on next page

Table 1.1 – continued from previous page

Article	Disease Model	Study	Additional Data Processing
[Huna 13]	Th10 contusive SCI rats	Combination of ChABC and AAV-NT_3	–
[Neck 13]	C4–5 overhemisection SCI rats	Gait analysis, Velocity dependency	Double-tap merging, Coordinate frame rotation, & Gait parameter in body coordinate frame.
[Garc 14]	Th8 contusive SCI rats	Progesterone treatment	–
[Gorp 14]	Th9 contusive SCI rats	Different severity of SCI	–
[Kann 14b]	Th8 contusive SCI rats	Transplantation of SC	–
[Forg 14]	C6 contusion-compression SCI rats	Model characterization	–
[Mond 15]	C4 hemi-contusive SCI rats	Moderate & large disp., sham, control.	Scaled by the pre-injured value
[Haya 15]	Th9 contusive SCI mice	SCI treatment with BDNF-expressing pDNA	Scaled by the average of non-injured intact control

Continued on next page

Table 1.1 – continued from previous page

Article	Disease Model	Study	Additional Data Processing
[Datt 15] & [Datt 16]	Th8 contusive SCI rats	Gender	Change from baseline (%)
[Jala 17]	Th10 contusive SCI rats	Effects of early surgical decompression	–
[Tan 17]	Th10 contusive SCI rats	Local injection of Lenti-Olig2	–
[Slus 17]	Th11 contusive SCI rats	Gait	–
[Bhim 17]	Contusive SCI	Review paper	–
[Vida 17]	C5–C6 DCM mice	Effect of early and delayed decompression	–
[Biel 18]	C4 transection SCI rats	Sham, complete CST lesion & iDC-lesion	–
[Crow 18]	Th11 contusive SCI mice	Develop combination of CatWalk parameters based on BMS scores	Calculate the correlation of 104 CatWalk parameters with the BMS scores. Then, combine the 104 linear regression equations according to R^2.

Continued on next page

Table 1.1 – continued from previous page

Article	Disease Model	Study	Additional Data Processing
[Miya 13]	L5–L6 needle IVD injury rats	Gait (compared with controls)	–
[Chen 14]	Peripheral nerve injury rats, Vessel clamp crushing on the left sciatic nerve	Hyaluronic acid effect	Left-right ratio
[Fago 16]	Cervical & thoracic dorsal column transection	Evaluating of five behavioral tests	–
[Chen 17]	Peripheral nerve injury rats, sciatic nerve segment removal	Standard data processing & set of CatWalk parameter formulation.	Left-right ratio
[Kapp 17]	Central and peripheral nerve injuries	Recommendation on the choice of CatWalk parameters	–
[Chia 14]	CCI rats with ligature on left sciatic nerve	Different intensities of nerve damage	–
[Parv 13]	Arthritis: CFA-induced mice	Gait (CFA vs. PBS contr.)	Left-right ratio
[Lake 16]	Arthritic disorders rodents	Review paper	–

Continued on next page

Table 1.1 – continued from previous page

Article	Disease Model	Study	Additional Data Processing
[Ferl 11]	OA: ACLT-pMMx rats & MIA rats	Gait analysis & pain response	Change from baseline (%)
[Ferr 12]	OA: MIA-induced rats	Effects of lidocaine, morphine & diclofenac on nociceptive behavior	Ratio of total intensity of the ipsilateral hindpaw to the total intensity of both hind paws.
[Mura 14]	OA: DMM mice	Effect of IAI-HA	Left-right ratio
[Ishi 14]	OA: MIA-induced rats	Effect of several drugs	Scaled by the values from the control animals, Right-left subtraction
[Qin 14a]	OA: ACLT-induced rats	Low magnitude high frequency vibration	–
[Piel 14]	OA animals	Review paper	–
[Adae 14]	OA: rats with intra-articular injections of 250 U & 500 U of type II collagenase	The use of the rat model for nociception study	Calculation of the percentage of the total ipsilateral paw print intensity (%TIPPI)

Continued on next page

Table 1.1 – continued from previous page

Article	Disease Model	Study	Additional Data Processing
[Adae 15]	OA: rats with intra-articular injections of 500 U of type II collagenase	Effect of sensory neurons injury	Calculation of %TIPPI
[Miya 11]	Myofascial Inflammation: rats with paraformaldehyde buffer	Gait (compared with controls)	–
[Ange 12]	Inflammation: rats with FCA or carrageenan injection	Gait (compared with controls)	New parameters: weight bearing, guarding index.
[Dupl 18]	Bone pain at hind limb of rats	Effect of analgesic bone cement: unloaded, ropivacaine-loaded, and bupivacaine-loaded CPCs	Scaled by pre-operative baseline (%)
[Kame 17]	Lumber disc herniation: NP applied rats	Gait analysis & mechanical withdrawal thresholds	–
[Liu 13]	Unilateral ICH stroke rats: Type IV collagenase infusion	Gait analysis	Left-right ratio

Continued on next page

Table 1.1 – continued from previous page

Article	Disease Model	Study	Additional Data Processing
[Hetz 12]	Stroke: mice with MCAo	Gait analysis	Scale swing speed by run speed
[Qin 14b]	Stroke: mice contains human BDNF Val66Met	Impact of BDNF SNP	Scaled by pre-ischemic baseline (%)
[Madi 14]	Stroke: rats with PT induction	Effect of enriched environment/housing	–
[Caba 17]	Stroke: mice with dMCAO	post-dMCAO gait assessment, correlation study between gait parameters and body weight, as well as body speed.	–
[Robi 12]	Rett syndrome: MeCP2 mice	Activation of a quiescent MeCP2 gene in adults	–
[Yoo 15]	Brain structure: St3gal2- & St2gal3-null mice	Sialoglycan function	–
[Stel 15]	Obesity: mice	Oleuropein supplementation	–

Continued on next page

Table 1.1 – continued from previous page

Article	Disease Model	Study	Additional Data Processing
[Zimp 18]	Intact mice	CatWalk version, gender weight, age & strain. Investigating the redundancy between tests.	PCA
[Koop 07]	Intact rats	Strain & Locomotor speed	–

* The abbreviations are listed in List of Abbreviations on page 211.

1.2.3 Gait Parameter Scaling and Body Length Assessment

Aside from diseases, there are several factors that relates to animals' gait parameters, such as body size [Hegl 74] [Mach 15] [Tayl 78] [Jaco 14], walking speed [Koop 07] [Neck 13] [Neck 15] [Mach 15] [Tayl 78], strain/breed [Koop 07] [Webb 03] [Hegl 74], and gender [Datt 16]. These factors need to be included in the analysis. Gait parameter scaling/normalization is one possible approach to handle this circumstance.

Parameter scaling in the study of gait in humans has become a common practice [Hof 96]. As shown in Table 1.1, CatWalk gait parameter scaling appeared in several preclinical studies, i.e. scaling based on body weight [Frah 18], by control/pre-injured/basal value [Bern 17] [Maim 18] [Mond 15] [Haya 15] [Ishi 14] [Qin 14b], as well as based on the average of speed [Boix 18]. In addition, body-weight-based scaling also appeared in gait parameters measured by the LocoMouse assay in a non-darkened room [Mach 15]. Since body-height or leg-length-based scaling is applied in human gait studies [Hof 96], it is hypothesized in this dissertation that body-length-based scaling is more suitable for the analysis of several gait parameters than the other body-size-related parameters.

The body-length-related parameter has to be first calculated to implement a body-length-based scaling. Anesthesia-based body length calculation was performed in several preclinical studies [Chak 17] [Dunn 09] [Nove 07]. Additionally, after-death body length measurement was performed in a preclinical study [Lang 05]. A marker-based body-length-related parameter can be easily computed based on markers drawn on rodent's body recorded by the video in a bright room. However, an in-vivo body-length-related parameter computed from a markerless gait analysis system (such as the CatWalk system) as well as body-length-based gait parameter scaling had not previously been studied and is described in this dissertation (Chapter 4).

1.2.4 Initial Data Analysis (IDA) by Heat Mapping

Since CatWalk gait parameter selection is often unavoidable, researchers frequently report only a selected cluster of gait parameters [Haya 15] [Ishi 14] [Salv 14] [Tate 16] [Fago 16], which leaves a query on how important are the unselected gait parameters. The selection was commonly based on the previous publications or the expert presumption. For

instance, a standard set of CatWalk gait parameters is suggested for assessing gait in nerve injured rat models [Chen 17] [Kapp 17].

All of the CatWalk gait parameters can also be reported by using a table/map, in which the presence of changes are reported [Caba 17]. Alternatively, an approach of IDA of all gait parameters using heat map visualization, in which colors are used to indicate the amounts of differences, is presented in this dissertation (Chapter 5).

IDA was described by [Hueb 16] as a systematic data inspection approach performed before the formal statistical analysis. This approach consists of data cleaning, data screening, and data reporting. Data cleaning [Demp 71] [Broe 05] is practiced by identifying inconsistencies, faulty or outlying data. Data screening is performed to describe the data. Data reporting aims to depict information for the following analysis.

A heat map is defined as a two-dimensional color-shade matrix for displaying data in many rows and columns simultaneously [Gehl 12] [Wilk 09]. This heat map technique has been used for data visualization in many study field, such as biology [Wein 08], behavioral science [Ande 14] [Kas 11], social statistic [Loua 73], accounting, graphic design, computer engineering, and others [Wilk 09]. In the field of gait analysis, it is used for depicting principal components resulting from principal component analysis (PCA) algorithm [Cour 09] [Heik 15a] [Heik 15b] [Mond 15] [Nurm 15] [Swee 15] [Zain 15] [Zimp 18], as well as to report correlation coefficients [Mach 15] [Caba 17].

1.2.5 Multiple Gait Parameter Analysis

Multiple aspects of gait are affected by diseases. Therefore, in preclinical studies of SCI, locomotor rating scales based on several gait characteristics were developed for observing gait recovery progression. In the study of middle/lower thoracic SCI in rats, gait is commonly evaluated using the 21-point Basso, Beattie, and Bresnahan (BBB) locomotor rating scale [Bass 95]. In the study of middle thoracic SCI in mice, another non-parametric locomotion test is normally performed, known as the Basso mouse scale (BMS) [Bass 06]. Furthermore, in the study of cervical SCI in rats, the forelimb locomotor assessment scale (FLAS) [Ande 09] or the forelimb locomotor scale (FLS) [Sing 14] is performed to evaluate their gait.

The BBB test (which was also used to assess rat SCI models in Chapter 6) is performed by experienced human observers who score the walk

of a rat placed in a circular open field according to several characteristics, such as hindlimb movement, joint movement, body–weight–supported plantar stepping, forelimb (FL)–hindlimb (HL) coordination, toe clearance, trunk stability, and tail placement. The BBB scoring system is relatively easy to be learned by inexperienced observers and is also relatively inexpensive. However, this scoring system relies on the observation of how consistent specific gait characteristics occurred and generates non-parametric scores [Bhim 17].

The CatWalk system [Hame 01] [Hame 06] provides an alternative of movement assessment for rodent SCI models. The advantages of using the CatWalk system are the objective computerized data generation and the possibility of assessing FL-HL coordination by its ability to observe four paws simultaneously [Hame 06] [Koop 05] [Bhim 17].

In analyzing gait parameters obtained from the CatWalk system, many studies (as listed in Table 1.1) observed several gait parameters individually. However, several approaches for parameter combination are available to be used depending on the research goal, including taking the ratio, difference, average, as well as making a linear combination. In studies related to diseases that affect both the left and right sides of the body with similar severity, it is reasonable to calculate the average of the left and right parameters. On the contrary, in diseases which affect only one side of the body, it will be interesting to analyze the ratio or the difference between left and right gait parameters [Chen 14] [Chen 17] [Ishi 14] [Liu 13] [Mura 14] [Parv 13]. On the other hand, in studies where uninjured data are available, the baseline/uninjured gait parameter ratio is often applied [Datt 15] [Datt 16] [Haya 15] [Mond 15].

Often, ratio, difference, and average are insufficient for handling numerous gait parameters. Therefore, some researchers have used linear combinations based on principal component analysis (PCA) [Zimp 18] or based on linear regression [Crow 18], and others have used approaches based on machine learning [Froh 18]. PCA was used in a study involving intact/uninjured mice [Zimp 18]. In a mice SCI study, the correlation and linear regression of 104 CatWalk parameters with the BMS scores were used to develop the CCI-score [Crow 18]. Approaches based on machine learning were used in a study involving PD-relevant mice to define features from the recorded raw CatWalk data. These features were used to classify an animal into the following groups: vehicle/sham, 6-OHDA, murine PFFs, and non-lesioned [Froh 18].

One approach of combining diverse parameters is by determining a linear combination based on linear discriminant analysis (LDA). LDA is a method, which attempts to form a linear function that discriminates between two groups, introduced by R.A. Fisher in 1936 [Fish 36]. LDA, to the best of the author's knowledge, had not been applied to analyze results obtained from the CatWalk system, including in the studies relating to SCI. Therefore, a method of combining CatWalk gait parameters based on LDA for assessing gait in rat SCI models is presented in this dissertation (Chapter 6).

1.3 Aims and Scientific Contributions

This dissertation aims to contribute computational methods that will enrich the information extracted from the present CatWalk gait analysis system, with a possibility to be applied to other systems. The main contributions of the dissertation are grouped into four main components: gait characteristic quantification (Chapter 3), gait parameter scaling/normalization (Chapter 4), initial data analysis (Chapter 5), and multiple gait parameter analysis (Chapter 6).

1. **Gait characteristic quantification.** As described in Section 1.2.2, locomotion sway was previously assessed based on the estimated COM position [Geld 15] or some tracked body points [Mend 15]. In this dissertation (Chapter 3), locomotion sway-related gait parameters are quantified based on the paw positions recorded by the CatWalk gait analysis system. Three computational methods in assessing locomotion sway based on mouse paw positions in the CatWalk gait analysis system are presented. The methods are based on signal processing approaches, i.e. fast Fourier transform (FFT) and low pass filter (LPF). These methods are applied on CatWalk data taken from two PD-relevant transgenic mouse models and their wild-type mates. This research work was published in the Journal of Neuroscience Methods [Timo 18b] and the related data was published in the journal Data in Brief [Timo 18c]. The computational methods and the analysis described in these publications were originally developed by the author of this dissertation. In addition, the publications were substantially written by the author of this dissertation in a collaboration with the coauthors of the publications.

2. **Gait parameter scaling/normalization.** As described in Section 1.2.3, computational methods for CatWalk-based body-length-related parameters had not been proposed. Moreover, a body-length-based CatWalk gait parameter scaling had not been studied. In addition to the various paw-position-based gait parameters, the Catwalk system provides body-silhouette information. Therefore, CatWalk body-silhouette length can serve as a body-length-related parameter and hence could promote an intra-assay silhouette-length-based scaling in several gait parameters. Accordingly, the following contributions are presented and analyzed (Chapter 4).
    - Image-processing-based silhouette-length and -area computation methods.
    - Correlation analysis between silhouette length and several gait parameters (i.e. stride lengths, temporal gait parameters, and speed-related gait parameters).
    - Gait-parameter scaling method based on silhouette length.
    - Comparison study of silhouette-length-, silhouette-area-, age-, as well as body-weight-based gait- parameter scaling.
    - Application of the silhouette-length-based scaling method in longitudinal data obtained from wild-type rats and mice, as well as PD-relevant rats and HD-relevant mice.

    The part of this research work was presented at the Measuring Behavior Conference 2018 [Timo 18d]. The complete study is published in the journal eNeuro [Timo 19b]. The computational methods, implementation as well as the analysis in these publications were performed by the author of the dissertation. The manuscript writing was performed by the author of the dissertation in a collaboration with the coauthors of the publication.

3. **Initial data analysis.** As described in Section 1.2.4, often only a selection of gait parameters is reported. Negative results are often not reported. Alternatively, a non-hypothesis-driven approach of IDA using heat mapping for gait parameter reporting is presented in this dissertation (Chapter 5). Heat mapping used in this approach is able to present between-group differences in one single chart. This IDA approach is exemplified in an intervention study

in mice modeling PD, as well as longitudinal studies in rats modeling PD and mice modeling HD. This contribution was presented at the Measuring Behavior Conference 2018 [Timo 18a] and published in the Special Issue of Measuring Behavior in the Journal of Neuroscience Methods [Timo 19a]. The publications were written mainly by the author of this dissertation in a collaboration with the coauthors of the publications.

4. **Multiple parameter analysis.** As described in Section 1.2.5, LDA had not been used for combining CatWalk parameters. Moreover, the CatWalk gait parameters of rat SCI models are often observed individually. In this dissertation (Chapter 6), a linear combination of several CatWalk gait parameter is presented. The parameter combination is developed based on LDA and is designed for observing gait recovery progression in rat SCI models objectively. This parameter combination approach was applied in the analysis of CatWalk data taken from three thoracic contusion SCI models, a thoracic dorsal hemisection SCI model, and a cervical dorsal column lesion SCI model. The manuscript based on this research work is expected to be submitted to a journal in 2020 [Timo 19c].

1.4 Structure of this Dissertation

The remainder of this dissertation is structured as follows:

- Chapter 2 covers the fundamentals relevant to the topic and methods described in the dissertation.
- Chapter 3 describes the study related to gait characteristic quantification, which focuses on several dynamic-footprint-based locomotion-sway assessment methods. These methods are applied to CatWalk data collected from PD-relevant mouse models.
- Chapter 4 covers the study related to parameter scaling/normalization. In this chapter, silhouette-length and -area computation methods are described. The results were then used in a correlation study between silhouette-length and several gait parameters. This chapter also covers a comparison study of several body-size-based gait parameter scaling. The application of silhouette-length-based scaling on CatWalk data obtained from PD-relevant rats and HD-relevant mice is then described.

- Chapter 5 describes the use of heat mapping for the gait parameter difference reporting in initial data analysis (IDA). The approach is exemplified in PD-relevant mouse models, a PD-relevant rat model, and a HD-relevant mouse model.
- Chapter 6 reports the multiple-parameter-analysis study, in which the linear gait parameter combination resulted from LDA is applied to describe gait recovery progression in several rat SCI models.
- Chapter 7 summarized the studies presented in this dissertation.

2 Fundamentals

Here the fundamentals for the understanding of the subsequent chapters are presented. This chapter starts with a brief introduction of laboratory rodents (Section 2.1), followed by a brief overview of several existing behavior tests (Section 2.2), including gait tests (Section 2.3) and particularly the CatWalk gait test (Section 2.4). The basics of several central nervous system (CNS) disorders are described in Section 2.5. Finally, the fundamentals of the computational methods used in this dissertation are described in Section 2.6, 2.7, and 2.8, which include digital image processing, signal processing, and linear discriminant analysis (LDA).

2.1 Rodents as Models of Humans

Animals have been used as models of humans since 600 BCE, their use increasing substantially at the beginning of the twentieth century [Eric 13]. Rodents (mice and rats) are the most widely used animals for representing (modeling) humans in scientific research [Eric 13] [Dutt 16].

The main ancestors of mice used in the scientific research are the *Mus musculus domesticus*, the *Mus musculus musculus*, the *Mus musculus castaneus*, and the *Mus musculus molossinus* [Wahl 11]. They are all often referred as the laboratory mice (the *Mus musculus laboratorius*) [Wahl 11].

Based on the types of animal breeding, the laboratory mice can be grouped into outcross, backcross, intercross, and incross animals [Silv 95]. An outcross or outbred animal is a result of the mating between two animals that are considered unrelated [Silv 95]. An incross or inbred animal is a result of the mating between two animals having a close genetic relation (commonly between two siblings). A backcross animal is a result of the mating between an animal with one of its

parents or an animal genetically similar to its parents [Silv 95]. An intercross animal is a result of the mating between two incross animals or between outcross siblings [Silv 95].

An inbred mouse strain is normally named by its strain and sub-strain. The strain name is given in capital letters and integers before a slash ('/') and the sub-strain is given after the slash [Wahl 11]. The C57BL/6 (C57 black 6) mouse is the most widely used inbred strain [Meka 09]. The C57BL/6 sub-strain developed by the Jackson Laboratory is named C57BL/6J. The one developed by National Institute of Health (NIH) is named C57BL/6N, which was established from C57BL/6J mice sent to NIH.

The laboratory or Norway rats (*Rattus norvegicus*) includes several strains, such as the Wistar rats (first developed by the Wistar Institute), the Sprague-Dawley rats, the Long-Evans rats, the Fischer rats, and the Lewis rats [Lind 06].

In this dissertation, C57BL/6N mice, Sprague-Dawley rats, Fischer rats, and Wistar rats are used as animal subjects in Chapter 3, 4, 5, and 6.

2.2 Behavior Assessment Methods in Rodents

The study of animal behavior has started as early as humans began to hunt [Vale 07]. Behavior-related studies are especially interesting for neuroscientists due to the relationship between the brain and behavior [Krak 17] [Staa 06] as well as the relationship between the genotype (genetic composition) and phenotype (observed physical and behavioral characteristics) [Vale 07]. Traditionally, behaviors are identified through careful human observation and are described accordingly. Nonetheless, objective quantification of behavior is needed for interpreting and characterizing behavior [Brow 18] [Gris 17].

In studies involving rodents, several standardized behavior assessment methods were developed (Table 2.1). These assessment methods are essential for characterizing rodent models, especially for the understanding of behavior-affecting diseases and the effect of their therapies.

In a preclinical study, rodent models usually undergo several behavior tests. The tests can be arranged according to a designed test protocol (series of tests), such as SHIRPA (an assessment protocol designed by SmithKline Beecham, Harwell, Imperial College, and Royal London

Hospital) [Roge 97] [Roge 01], test protocol for HD rat model [Manf 17], and other self-designed protocols.

The varieties of behavior tests for rodents are continuously being developed. Technologies have been incorporated in the test design to gain more information, such as

- The utilization of 3D-imaging in a circular-open-field test, a square-open-field test, or above a cage [Wilt 15] [Naka 15] [Hong 15].
- The utilization of motion capture systems (VICON or SIMI) for kinematic analysis in rats [Cour 09].
- The utilization of virtual reality for visual simulation in the study of mice [Stow 17].
- The utilization of robotics in an interaction study involving rats [Wile 12].
- The utilization of head-mounted camera system for observing eye movement, whisker pad movement, and head accelerometry [Meye 18].
- The utilization of head accelerometry, intranasal pressure, ultrasonic vocalization, and video tracking in observing freely behaving rat [Alve 16].

For analysis, the information collected from behavior tests often needs further data processing. In extracting information resulting from those behavior tests, computational methods can be used. The computational methods include signal processing (Section 2.7), image processing [Bell 18] [Robi 17] [Mazu 11] [Reev 16] [Pere 14] [Ben 17] (Section 2.6), data analysis methods, and machine learning approaches [Vall 17] [Puri 18] [Robi 17] [Roia 16] [Arac 19].

In preclinical studies, gait tests are one type of the existing behavior assessment methods, which are often used in studies related to neurological disorders. The following section (Section 2.3) will focus on the existing gait tests for rodents, which is used for assessing the characteristics of animals during walking.

Table 2.1: Examples of rodents' behavior assessment methods

Category	Examples
Exploration tests (tests for measuring rodents' surrounding exploratory behavior) [Belz 99] [Wahl 11] [Broo 09] [Sedy 08] [Sous 06]	Squared and circular open field, cylinder test, nose poke hole board, home cage activity, symmetrical Y-maze, Y-maze with foot-shock reinforcement [Ried 94].
Anxiety-related behavior tests (most of the anxiety-related behavior tests measure the time of avoiding places that entail risk) [Wahl 11] [Sous 06] [Bail 09]	Light-dark box, elevated plus maze, elevated zero maze, elevated square maze, the Vogel conflict test, the Geller conflict test, social interaction, ultrasonic vocalization, freezing, startle response, shock-probe test, light spot test [Aart 15].
Motor function and gait tests (tests for characterizing motor-related ability or movement) [Wahl 11] [Broo 09] [Sedy 08] [Sous 06]	Motor observation in an open field (SCI observation: the BBB scale [Bass 95], the BMS scale [Bass 06], the FLAS scale [Ande 09], the FLS scale [Sing 14]; knee arthritis observation [Lake 16]; PD-relevant observation: the AIMs scale [Lund 04]; Ataxia-relevant observation [Mett 04]), the BLG scale [Pajo 10], grip strength test, wire hang test, isometric pull test [Hays 13], inverted grid test [Niew 16], rotarod, gait test (foot print test, runway locomotion test, treadmill locomotion test [Wool 09], wheel walk test), swim test, climbing test (vertical-pole, inclined pole or grid,

Continued on next page

Table 2.1 – continued from previous page

Category	Examples
	rope or string climbing, coat hanger), the CoP assay [Hutc 07], dynamic weight bearing test, kinematic test, thoracolumbar height test, forelimb asymmetry test, rearing test in a cylinder place.
Skilled limb use tests (assessing the use of limbs for a task)	Pellet reaching test [Broo 09], the Collins test [Coll 68], staircase reaching test [Broo 09].
Sensory tests (assessing hyper- and hypo-activities of the sense of touch, cold, heat, or pain) [Sedy 08] [Sous 06]	Plantar hot plate-based test, tail-flick test, cold sensitivity-based test, Von Frey filaments, paw compression test (analgesia meter or Randall-Selitto test), withdrawal reflexes test.
Sensory-motor tests (assessing the sensory and motor functions, as well as their relation)[Sedy 08]	Rope walking test, balanced beam [Broo 09] or raised beam test, grid test (horizontal grid, ladder rung task [Metz 02] or foot slip test), inclined rolling ladder [Fago 16], grooming test.
Reflex response-based tests (detecting absent, normal, or abnormal reflex responses)[Sedy 08]	Toe spread reflex test, contact placing response test, static reflex test, acoustic startle response test [Broo 09] [Sous 06].

Continued on next page

Table 2.1 – continued from previous page

Category	Examples
Learning tests (assessing learning and memory processes)[Wahl 11] [Sous 06]	Operant learning (Skinner box [Skin 38], nine-hole box [Humb 99], five-choice serial reaction time test, sequence learning), mazes, spatial memory (Barnes maze, 8-arm radial maze, morris water maze [Morr 84], visual learning water maze [Robi 01]).
Behavior information in their housing/a cage (observing cage activities or disease-related activities)	PhenoTyper (Noldus), IntelliCage and PhenoMaster (TSE Systems), IVC-RackScan (CleverSys), magnetic-coil-based system [Krem 10], floor-movement-based system, RFID-based system [Rich 15].
Movement tracking (track the positions of animals)	Observation [Nold 91], joy-stick-based locomotion tracking [Brod 95], Ethovision [Nold 01], VideoMot2 (TSE Systems), 3D-imaging-based tracking [Naka 15].
Social behavior observation (assessing the interaction between animals) [Sous 06]	Reproduction activity, aggressive behavior, submissive behavior, avoidance behavior.
Autonomic tests (behavioral assessments of autonomic system disturbance) [Sedy 08]	Urinary bladder function tests, erection-based tests, autonomic dysreflexia (hyperreflexia) tests.

2.3 Gait Tests in Rodents

Conventionally, gait is assessed subjectively by observers. Manuscripts relating to gait analysis by human observation can be traced to before the modern computer era [Bake 07]. Subsection 2.3.1 introduces a common observation-based gait test in SCI studies, namely the BBB test [Bass 95]. For assessing gait objectively, several methods and tools were developed. These methods and tools are designed to quantify walking patterns and generate corresponding gait parameters. Therefore, several parametric gait tests are introduced in Subsection 2.3.2.

2.3.1 Non-Parametric (Observation-based) Gait Tests

Visual examinations (sometimes together with a video recording) are traditionally used in identifying gait abnormalities [Whit 96]. Therefore, observation without any exact measurement is still common in describing gait.

Unlike in PD and HD, there are standard non-parametric gait tests used in SCI studies depending on the species and placement of the injury. In these tests, human observers match gait characteristic of rodents according to a standardized scale. The Basso, Beattie, and Bresnahan (BBB) test [Bass 95] is used to assess gait in rat middle/lower-thoracic SCI models. The Basso mouse scale (BMS) test [Bass 06] is used to assess gait in mouse thoracic SCI models. The forelimb locomotor assessment scale FLAS test [Ande 09] or the forelimb locomotor scale (FLS) [Sing 14] is used to assess gait in rat cervical SCI models.

The 21-point BBB locomotor rating scale [Bass 95] is the most common method used for evaluating locomotor recovery in middle/lower thoracic SCI rats. This scale is therefore also used to assess gait of the rats described in Chapter 6. This scale is divided into three major categories of recovery: early (0–7), intermediate (8–13), and late (14–21). In this locomotion evaluation, rats are placed in an open field environment. The locomotor assessment is then performed by two examiners positioned across to each other. The examiners score the locomotion recovery according to the description given in Table 2.2. This BBB scoring system can be learned quickly. However, experience is needed to assure the reliability and the consistency of scoring [Bass 96].

Table 2.2: The BBB locomotor scale [Bass 95]

Score	Description
0	No observable hindlimb (HL) movement
1	Slight movement of one or two joines, usually hip and/or knee
2	Extensive movement of one joint, or Extensive movement of one joint and slight movement of other joint
3	Extensive movement of two joints
4	Slight movement of all three joints of the HL
5	Slight movement of two joints and extensive movement of the third
6	Extensive movement of two joints and slight movement of the third
7	Extensive movement of all three joints of the HL
8	Sweeping with no weight support, or plantar placement of the paw with no weight support
9	Plantar placement of the paw with weight support in stance only (i.e., when stationary), or occasional, frequent, or consistent weight supported dorsal stepping and no plantar stepping
10	Occasional weight supported plantar steps, no forelimb (FL) - HL coordination
11	Frequent to consistent weight supported plantar step and no FL - HL coordination
12	Frequent to consistent weight supported plantar step and occasional FL - HL coordination
13	Frequent to consistent weight supported plantar step and frequent FL - HL coordination
14	Consistent weight supported plantar step, consistent FL - HL coordination; and predominant paw position during locomotion is rotated (internally or externally) when it makes initial contact with the surface as well as just before it is lifted off at the end of the stance, or

Continued on next page

Table 2.2 – continued from previous page

Score	Description
	frequent plantar stepping, consistent FL - HL coordination, and occasional dorsal stepping
15	Consistent plantar stepping and consistent FL - HL coordination; and no toe clearance or occasional toe clearance during forward limb advancement; predominant paw position is parallel to the body at initial contact
16	Consistent plantar stepping and consistent FL - HL coordination during gait; and toe clearance occurs frequently during forward limb advancement; predominant paw position is parallel at initial contact and rotated at lift off
17	Consistent plantar stepping and consistent FL - HL coordination during gait; and toe clearance occurs frequently during forward limb advancement; predominant paw position is parallel at initial contact and lift off
18	Consistent plantar stepping and consistent FL - HL coordination during gait; and toe clearance occurs consistently during forward limb advancement; predominant paw position is parallel at initial contact and rotated at lift off
19	Consistent plantar stepping and consistent FL - HL coordination during gait; and toe clearance occurs consistently during forward limb advancement; predominant paw position is parallel at initial contact and lift off; and tail is down part or all of the time
20	Consistent plantar stepping and consistent coordination gait; consistent toe clearance;

Continued on next page

Table 2.2 – continued from previous page

Score	Description
	predominant paw position is parallel at initial contact and lift off; tail consistently up; and trunk instability
21	Consistent plantar stepping and coordination gait consistent toe clearance; predominant paw position is parallel throughout stance, consistent trunk instability, tail consistently up

Definitions

Slight: partial joint movement through less than half the range of joint motion

Extensive: movement through more than half of the range of joint motion

Sweeping: rhythmic movement of HL in which all three joints are extended, then fully flex and extend again; animal is usually side-lying, the plantar surface of paw may or may not contact the ground; no weight support across the HL is evident

No Weight Support: no contraction of the extensor muscles of the HL during plantar placement of the paw, or no elevation of the hindquarter

Weight Support: contraction of the extensor muscles of the HL during plantar placement of the paw, or elevation of the hindquarter

Plantar Stepping: the paw is in plantar contact with weight support then the HL is advanced forward and plantar contact with weight support is reestablished

Dorsal Stepping: weight is supported through the dorsal surface of the paw at some point in the step cycle

FL–HL Coordination: for every FL step, an HL step is taken and the HLs alternate

Occasional: less than or equal to half; $\leq 50\%$

Frequent: more than half but not always; 51–94%

Consistent: nearly always of always; 95–100%

Trunk Instability: lateral weight shifts that cause waddling from side to side or a partial collapse of the trunk

2.3.2 Parametric Gait Tests

A classical method in quantifying rodent's gait is by using a footprint test [Broo 09], where the positions of paws are documented by dyes on a paper. In this test, the rodent's paws are dyed in different colors, then they walk in a narrow corridor over an absorbent paper. Then, the rodent's stride lengths, base width, overlap between front-hind paws, and finger splay can be analyzed.

Gait analysis tools for rodents are continuously being developed. Several existing spatio-temporal/kinematic gait analysis systems for rodents are listed in Table 2.3, some of which are described by several review works [Lake 16] [Jaco 14].

The following section (Section 2.4) will describe the CatWalk gait test system, which is one of the runway-based markerless parametric gait tests for rodents.

Table 2.3: Several gait analysis systems for rodents

Gait Analysis System	Company/References	Specification
Ink-based foot-print test	–	Paw print analysis, paper.
CatWalk	Noldus, Netherlands	Paw print and silhouette analysis, camera, markerless, runway, glass floor, ventral view, darkened room.
Walkway	TekScan, USA	Paw print analysis, pressure sensor mat, markerless.
DigiGait	Mouse Specifics, USA	Paw print analysis, camera, markerless, treadmill or overground, transparent belt, ventral view, bright room.
TreadScan	CleverSys, USA	Paw print and body analysis, camera, markerless, treadmill, transparent belt, ventral view, bright room.
GaitScan	CleverSys, USA	Paw print and body analysis, camera, markerless, runway or treadmill, transparent floor/belt, ventral view, bright room.

Continued on next page

Table 2.3 – continued from previous page

Gait Analysis System	Company/References	Specification
KinemaScan	CleverSys, USA	Paw print, body and kinematic analysis, camera, treadmill, transparent belt, ventral and sagittal view, bright room.
MotoRater	TSE System, Germany	Paw print, body and kinematic analysis, camera, runway, transparent floor, ventral and sagittal view, bright room.
Gait	Noveltec Inc., Japan	Transparent running wheel with speed controller, camera, ventral view, bright room.
GaitLab	ViewPoint, France	Paw print and silhouette analysis, camera, markerless, runway, glass floor, ventral and sagittal view, bright room.
MouseWalker	[Mend 15]	Paw print and body analysis, camera, markerless, runway, glass floor, ventral view.
Gaitor: Agatha & Edgar	[Kloe 17] [Jaco 17] [Jaco 18]	Paw print and body analysis, camera, markerless, runway, transparent floor, ventral and sagittal view.

Continued on next page

Table 2.3 – continued from previous page

Gait Analysis System	Company/References	Specification
LocoMouse	[Mach 15]	Paw print and kinematic analysis, camera, markerless, runway, transparent floor, ventral and sagittal view.
Transparent-runway-based system	[Chen 97]	Paw Print analysis, runway, transparent floor with lined transparent film, video recording, ventral view, semidark room.
White wooden trackway-based system	[Geld 15]	Body analysis, camera, white wooden runway, dorsal and sagittal view, bright room.
Inverted U-shaped tunnel-based system	[Clar 99] [Coul 02] [Clar 95] [Clar 91] [Clar 86]	Paw print analysis, 2 cameras, markerless, runway, glass floor, ventral view.
Treadmill-based system	[Magh 16] [Magh 15]	Kinematic analysis, 4 side-cameras, markerless, treadmill, bright room
Force-sensing exercise wheel	[Smit 15]	Footfall analysis with force sensors, kinematic analysis with camera, exercise wheel.
Depth-sensor-based foot-print tracking	[Naka 15]	Foot print tracker, square open field, 3D imaging, markerless.

Continued on next page

Table 2.3 – continued from previous page

Gait Analysis System	Company/References	Specification
Open-arena gait analysis	[Alle 09] [Alle 12] [Alle 11] [Kloe 15]	Paw print, camera, markerless, open field, transparent floor, ventral and sagittal view.
Treadmill & running wheel -based system	[Cost 10]	Camera, ventral and sagittal view, wheel or treadmill

* Rodents do not walk in the same way on overground/on a runway, on a treadmill [Guil 08], as well as in a wheel [Smit 15]. Rodents tends to have lower anxiety in dark environment [Aart 15] [Leza 17].

2.4 CatWalk Gait Test System

The CatWalk™ system (Noldus, Wageningen, The Netherlands) is a paw-position-based assessment system for rodents, which was first developed by Frank Hamers [Hame 01] [Hame 06]. The development idea of the CatWalk system was raised by the difficulty of observing FL-HL coordination in the well-known BBB test [Bass 95], because an observer is only able to see a maximum of three paws simultaneously [Nold 12]. Compared with other available gait tests, the CatWalk gait test has the advantage of evaluating gait in a darkened room without any mark on the rodent body needed.

The CatWalk gait test system consists of a glass walkway where rodents can traverse from one end to the other in a darkened room. Since it uses the Illuminated Footprints Technology™, footprints are illuminated at the actual location where the paws make contact with the glass walkway. The operation principle of the Illuminated Footprints technology in the CatWalk system is illustrated in Figure 2.1. Similar with the principle of optical fiber, green light is sent into the long edge of a glass plate and radiates inside the plate. Since the light rays strike the surface below the critical angle, they reflect internally. The light escapes only at the areas where the animal paws touch the plate. Therefore, the footprints become visible.

From the ceiling above the walking rodent, red light is illuminated (as illustrated in Figure 2.1). As a result, the rodent's body silhouette is visible from beneath the walkway. This body silhouette is used to facilitate the labeling of the footprints (designate if they originated from RF, LF, RH, or LH paws).

The footprints and body silhouette information is recorded by a camera with a sampling rate (f_s) of 100 Hz placed underneath the walkway. CatWalk-based captured image samples are shown in Figure 1.1. This recorded video is processed by the CatWalk software [Nold 12]. First, the CatWalk software automatically checks the compliance of the rodent's run based on the walking speed and its variation. The walking-speed maximum and minimum thresholds for this compliance check can be selected by the researchers. The same applies to the walking-speed variation thresholds. Typically, researchers select these thresholds to assure that the rodents walk in the walking speed range and not performing any other activity. The footprint information recorded by the videos is then labeled automatically by the software and can be

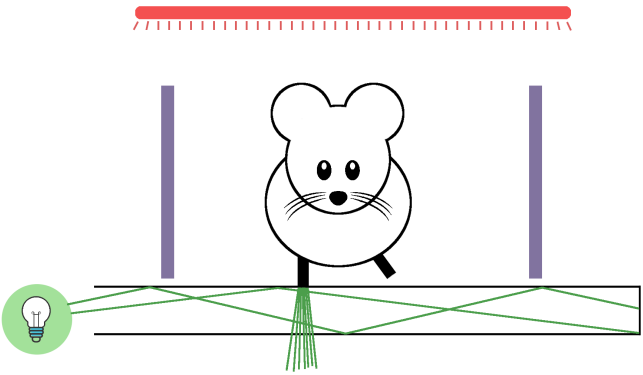

Figure 2.1: An illustration of the operation principle of the Illuminated Footprints technology and the placement of red light source in the CatWalk gait test system.

revised manually by an experienced observer. Based on labeled footprints in a video, several gait parameters are computed. Part of the CatWalk gait parameters [Nold 12] are:

- Stride length (cm) is calculated by the distance between the center points of two consecutive positions of the same paw.
- Stand time (s) is calculated by the contact duration with the walkway of a specific paw.
- Swing time (s) is calculated by the non-contact duration with the walkway of a specific paw.
- Step cycle (s) is calculated by the duration of two consecutive initial contacts of a specific paw (step cycle = stand time + swing time).
- Body speed (cm/s) is calculated from each paw by dividing the distance to the time of two consecutive initial contacts.
- Swing speed (cm/s) is calculated from each paw by dividing the distance to the time during swing (swing speed = stride length/ swing time).

- Duty cycle (%) is the ratio of stand time to step cycle (duty cycle = stand time/step cycle). This is calculated from each paw.
- 'Max contact at (%)' is the ratio of 'max contact at (s)' to the stand time (s), where 'max contact at (s)' is the time when maximum paw-intensity is measured. This is calculated from each paw.
- Base of support (BOS) (cm) is calculated by averaging the width on the y-axis between either front paws or hind paws (BOS front paws = $\bar{y}_{RF} - \bar{y}_{LF}$; BOS hind paws = $\bar{y}_{\mathrm{RH}} - \bar{y}_{\mathrm{LH}}$).
- Sequence AB (%) is the percentage of a specific LF–RH–RF–LH paw sequence.
- Regularity index (RI) (%) is the ratio of the number of normal step sequence pattern (NSSP) times four and the total number of paw placement (PP) [Koop 05] (RI = NSSP$\times$4/PP). There are six patterns that are considered as NSSP [Chen 97]: cruciate (CA: RF–LF–RH–LH; CB: LF–RF–LH–RH), alternate (AA: RF–RH–LF–LH; AB: LF–RH–RF–LH), and rotary (RA: RF–LF–LH–RH; RB: LF–RF–RH–LH).
- 'Print position (cm)' is the distance between the position of a hind paw and the previously placed front paw on the same side of the body calculated on the x-axis. If a rodent walks from left to the right, this print position is equal to $x_{\mathrm{F}} - x_{\mathrm{H}}$.

All CatWalk gait parameters, including parameters calculated from each paw (also known as paw statistics), are individually reported in exported output files, namely 'Run Statistics' and 'Trial Statistics'. In addition, paw position information from all video frames (also known as the dynamic paw placements or footfalls) can be accessed from a exported output file, namely 'Run Data'.

2.5 Central Nervous System (CNS) Disorders

The brain and the spinal cord collectively form the central nervous system (CNS), which integrates and coordinates the information received from and sent to all parts of the body. The CNS influences body movement and activities. Therefore, damage in the brain or spinal cord often results in movement disorders. The CNS disorders are part of the neurological disorders, which includes Parkinson's disease (PD), Huntington

disease (HD), and spinal cord injuries (SCI). In this dissertation, computational methods were applied in rodents modeling PD, HD, an SCI. Therefore, this section is continued by the fundamentals of these disorders and their rodent models.

2.5.1 Parkinson's Disease (PD)

PD in humans, first described by James Parkinson in 1817 [Park 02], is a neurodegenerative disorder that is characterized by typical motor symptoms called parkinsonism, which includes resting tremor, bradykinesia, muscular rigidity, and postural instability [Mcca 14] [Beit 14] [Jank 08] [Tolo 06]. Other motor symptoms of PD include shuffling gait, freezing, festination, flexed posture, gait instability, reduced stride length, reduced gait speed, and poor balance [Jank 08] [Kluc 13]. Besides these motor symptoms, some non-motor symptoms also appear in PD such as hallucinations, depression, dementia, sleep disorder, speech disorder, pain, constipation, and olfactory disturbance [Mcca 14].

A validated biomarker such as a blood test is not yet available for assessing the progression of PD in humans [Haus 18] [Jank 08]. The progression assessment and the disease staging of PD in humans is scored commonly based on the observed symptoms by standardized scores, such as the unified Parkinson's disease rating scale (UPDRS) as well as the Hoehn & Yahr (H&Y) scale [Jank 08] [Kluc 13] [Goet 03].

The cause of PD is still unknown [Kali 15] [Macp 01]. However, it can be related to Lewy bodies as well as the loss of dopaminergic neurons in substantia nigra compact (SNC), which might be developed from genetic or environmental factors [Macp 01] [Lees 09] [Kluc 12]. Lewy bodies are abnormal aggregates of α-synuclein (α-Syn) protein inside the nerve cell [Mcca 14] [Spil 97]. This protein formed by 140 amino acids and is encoded by the SNCA gene.

Several animal models are utilized in experiments related to PD. Ideally, PD-relevant animal models should closely match human pathology, especially in their motor symptoms, non-motor symptoms, Lewy body formation (abnormal formation of protein in the nerve cells), neuronal cell loss in the basal ganglia, and disease progression. However, none of the current PD-relevant models can replicate all of the criteria [Anto 11]. The currently existing neurotoxin (nerve tissue destructive toxin)-based animal models of PD include the 6-hydroxydopamine (6-OHDA) model, the methyl-4-phenyl-1,2,3,6-tetrahydropyridine (MPTP) model, the rotenone model, and the paraquat model [Bove 12]. The

currently existing PD-relevant transgenic (genetically engineered) models include the α-Syn models, the DJ-1 model, the Parkin model, the PTEN-induced putative kinase 1 (PINK1) model, and the MitoPark model [Harv 08] [Mage 10].

In this dissertation, PD-relevant transgenic rodent models (α-Syn models [Kohl 16] [Nube 13] [Wass 18]) are used in the studies described in Chapter 3, 4, and 5.

2.5.2 Huntington Disease (HD)

In humans, HD, also known as chorea, is a neurodegenerative disorder caused by an expansion of the cytosine, adenine, and guanine (CAG) trinucleotide repeat within the Huntingtin (HTT) gene, which leads to an abnormal protein called the HTT protein [McCo 18]. This HTT mutation is mostly inherited from one generation to the next.

The early descriptions of HD-relevant disease in humans appeared in some research works and reports particularly by Paracelsus, Thomas Sydenham, Charcot, Mitchell, Osler, Gowers, Charles Waters, George Huntington and Americo Negrette [Vale 15] [Roos 10]. HD is characterized by some motor symptoms such as choreatic involuntary movement, lack of coordination, and unsteady gait, as well as non-motor symptoms such as cognitive impairment, emotional problems, depression, irritability, abnormal facial expression, abnormal posturing, sleep disturbance, and trouble in speaking [Roos 10] [Hunt 96]. The stride lengths of HD patients are usually shorter compared with healthy controls [Dano 14]. The progression of HD in humans is normally assessed using a standardized scale, namely the unified Huntington disease rating scale (UHDRS) [Hunt 96].

Several animals are utilized to the HD-relevant experimental studies including worms (*Caenorhabditis elegans*), fruitflies (*Drosophila melangaster*), mice, rats, sheep, pigs, and monkeys [Poul 13]. Before the development of transgenic models, HD-relevant animal models were based on neurotoxins (nerve tissue destructive toxin), such as ibotenic acid or kainic acid [Poul 13]. The first transgenic HD-relevant mouse model was described by Mangiarini et al. [Mang 96] [Bate 05]. There are currently over 20 different HD-relevant rodent models, including truncated N-terminal fragment of mutant HTT (mHTT) models (such as R6/1, R6/2, and N171-Q82) and full-length mHTT models (such as knock-in models, as well as transgenic models created using YAC or BAC technology) [Poul 13].

In this dissertation, a HD-relevant transgenic rodent model (BACHD [Gray 08]) is used in the studies described in Chapter 4 and 5.

2.5.3 Spinal Cord Injury (SCI)

Approximately 291.000 persons suffered from SCI in the US in 2018 [Nati 19]. This injury occurs mostly due to vehicle crashes, falls, violence, and sport-related incidents [Nati 19] [Silv 14] [Ahuj 17] [Kjel 16].

The spinal cord sends information between the brain and peripheral nerves. Therefore, an injury in the spinal cord affects the patient's motor control and sensory capabilities. Injury is often followed by infections [Silv 14] and affects the quality of life of both patients and caretakers/family. The motor and sensory impairments of an SCI patient are strongly influenced by the position and severity of the injury. The quality of life in SCI patients is mostly assessed using a subjective measure called the satisfaction with life scale (SWLS), which is defined by the patients' independence [Ahuj 17].

For developing therapies to repair injured spinal cords, animal models are often used. The most common animal SCI model are rats due to their low cost, accessibility, handling, and the availability of well-established analysis techniques [Silv 14] [Ahuj 17] [Kjel 16] [Cher 14]. In addition, rats develop similar SCI-related symptoms as seen in humans. As in humans, gait recovery in rats is a visible indicator of post-SCI recovery [Kjel 16].

The rat's spinal cord is surrounded by three meninges (the pia mater, arachnoida mater, and dura mater) [Kjel 16] and by a bony structure/vertebrae (a part of this bony structure is called lamina and a surgery removing this part is called a laminectomy). This rat's spinal cord consists of the white matter and the gray matter, which surround the central canal. A sketch of cross sectional views of a spinal cord is shown in Figure 2.2a. The white matter is the location of the sensory (ascending) and motor (descending) nerve tracts/axons as shown in Figure 2.2b. Ascending nerve tracts in spinal cord include the dorsal columns, spinothalamic, and spinocerebellar tracts [Kjel 16]. Descending nerve tracts in spinal cord include the corticospinal, rubrospinal, reticulospinal, vestibulospinal, raphespinal tracts [Kjel 16]. The location of these nerve tracts in rats differs from the location in humans [Kjel 16].

The locomotion assessment of animal SCI models needs to be adjusted according to the animal strain/breed and, in some cases, to the location of injuries (cervical, thoracic, lumbar, sacral, or coccygeal).

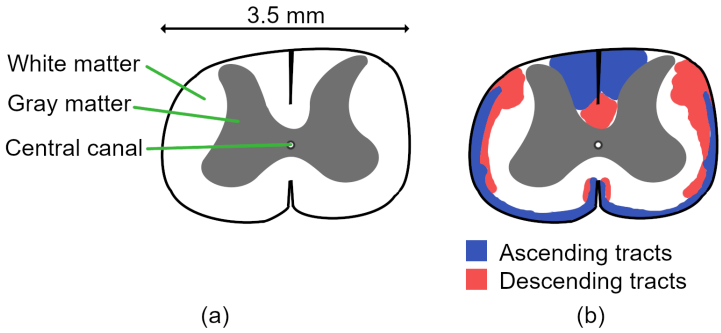

Figure 2.2: Sketch of cross sectional views of a rat spinal cord: (a) The white matter, gray matter, and central canal (b) Approximate locations of ascending (sensory) and descending (motor) nerve tracts.

For assessing locomotion of rat middle/lower-thoracic SCI models, the 21-point subjective BBB scale is commonly used [Bass 95] (as described in Section 2.3.1). For analyzing locomotion of rat cervical SCI models, the subjective forelimb locomotor assessment scale (FLAS) [Ande 09] or the 17-point subjective forelimb locomotor scale (FLS) can be used [Sing 14]. The locomotion of mouse middle-thoracic SCI models is commonly assessed by using the 9-point subjective Basso mouse scale (BMS) [Bass 06] or the 30-point subjective Toyama mouse score (TMS) [Shig 14]. The BMS can be combined with the results from other motor tests to form a combined motor function score, BLG [Pajo 10].

The injuries/lesions of a spinal cord can be generated in animal models by contusion (by using a weight-drop device), transection (by using knives or scissors), and compression (by using a clip, forceps, or balloon) [Rose 04] [Silv 14] [Kjel 16]. The method of generating the lesion will correspond to the affected nerve tracts, as well as to the motor and sensory impairments. A transection will typically generate a precise lesion [Kjel 16], such as dorsal column lesions (Figure 2.3a), dorsal hemisection lesions (Figure 2.3b), and lesions of specific nerve tracts. A contusion will typically generate a non-nerve-tract-specific lesion as illustrated in Figure 2.3c.

In this dissertation, rat SCI models (contusion or transection, middle/lower-thoracic or cervical) are used in the studies described in Chapter 6.

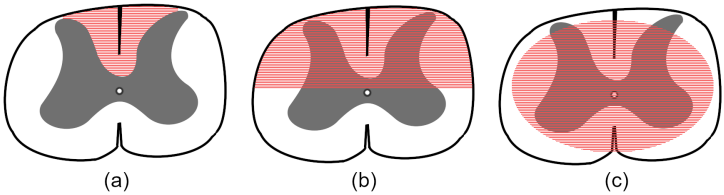

Figure 2.3: Illustrations of the area affected by the spinal cord injury, lesion (a) Dorsal column lesion (b) Dorsal hemisection lesion (c) Contusion lesion.

2.6 Digital Image Processing

Due to the ability to replay movement slowly, the innovation of motion image (video) recording brings a breakthrough in gait observation of both animals [Hild 89] [Muyb 99] as well as humans [Whit 96] [Cout 99]. The information from the recorded video can be extracted by using video and image processing approaches. In this dissertation, the concepts of digital image processing were used to extract information (specifically morphological image processing approaches and background subtraction) from the recorded CatWalk videos (Chapter 4).

A digital video is a three-dimensional function $f_{video}(x, y, t)$, composed of a sequence of digital images $f_{image}(x, y)$. The images structuring a video are often referred as frames. The rate or frequency at which the frames are displayed or recorded is expressed in frames per second (fps) or in Hz.

An image is a two-dimensional function $f_{image}(x, y)$, where x and y are spatial coordinates, and f_{image} is the intensity of the image at that point [Gonz 08]. When f_{image}, x, and y are discrete quantities, the image is referred as a digital image. This digital image is composed of picture elements (pixels). A digital gray-scale image commonly uses 8 bits to store the light intensity of each pixel. A binary image has only two possible intensities (black and white, b/w) for each pixel, and therefore the pixel can be stored as a single bit. In addition, a digital color image includes color information by representing each pixel in three layers (24-bit pixel depth). A color image can be represented in different color spaces (also known as color models or color systems). Red-green-blue (RGB) color space is a hardware-oriented most-commonly-used color space [Gonz 08], in which pixels are represented in red, green, and blue layers.

The term digital image processing refers to the use of computer algorithms in processing digital images. One of the techniques in digital image processing is morphological image processing, which aims to change the shape or morphology of image components. Here an object in a binary image can be represented as a set of pixels, e.g. in a binary image, the coordinates of all white pixels are members of a set A_i. A connected area or object in a binary image is called a binary large object (blob). The area or the size of a blob often refers to the number of pixels in the blob. In performing morphological operations of an image, a small binary object called structuring element S_e is often used. By applying morphological image processing on an image, a new object A_r is generated. The techniques of morphological image processing include but are not limited to [Gonz 08]:

- Translation: Translates the origin of A_i by a point/vector z.

$$(A_i)_z = \{a_r | a_r = a_i + z, \text{for } a_i \in A_i\} \tag{2.1}$$

- Reflection: Reflects all elements of A_i about the origin of this set.

$$\hat{A}_i = \{a_r | a_r = -a_i, \text{for } a_i \in A_i\} \tag{2.2}$$

- Complement: Selects set of points, that are not in A_i.

$$A^c = \{a_r | a_r \notin A_i\} \tag{2.3}$$

- Dilation: Expands the boundary of A_i by S_e.

$$A_i \oplus S_e = \{z | [(\hat{S_e})_z \cap A_i] \neq \varnothing\} \tag{2.4}$$

- Erosion: Contracts the boundary of A_i by S_e.

$$A_i \ominus S_e = \{z | (S_e)_z \subseteq A_i\} \tag{2.5}$$

- Opening: Smooths contours, eliminates small islands, and sharp peaks of A_i by S_e.

$$A_i \circ S_e = (A_i \ominus S_e) \oplus S_e \tag{2.6}$$

- Hole/region filling: Fills a region in A_i by S_e, given a starting point $X_0 = p$ inside the region.

$$\begin{aligned} X_k &= (X_{k-1} \oplus B) \cap A^c \quad k = 1, 2, 3, \ldots \\ A_{filled} &= A \cup X_k \end{aligned} \tag{2.7}$$

  The iteration in Eq. 2.7 stops at k (number of iterations), where $X_k = X_{k-1}$.

Another technique in digital image processing is called background subtraction, which aims to detect changes (foreground) from a background image. A simple approach to implement this in a gray-scale image is by subtracting the pixel intensity of an image I_{frame} by its corresponding background image $I_{background}$, which yields the following equation:

$$I_{FB} = |I_{frame} - I_{background}| \tag{2.8}$$

The pixels in I_{FB} that have non-zero intensity are appointed as the foreground area. A threshold is often used to decrease the over-sensitivity of the approach. This yields:

$$I_{foreground,area} = |I_{frame} - I_{background}| > \text{Threshold} \tag{2.9}$$

The foreground image $I_{foreground}$ is the collection of pixels from the original image I_{frame} in the foreground area $I_{foreground,area}$.

2.7 Signal Processing

Signal processing approaches were used in developing computational methods described in Chapter 3. Therefore, this section starts with the fundamentals regarding signals and different types of signals. This section is continued by the fundamentals regarding signal processing approaches, specifically regarding the low pas filter (LPF) and the Fourier transform.

A signal is generally described as a function (or a clue, a message, an indicator) that expresses information [Oppe 14], which also could be behavior-related information. When a signal is described as a function, the independent variable(s) can be continuous or discrete. Continuous-time signals or analog signals refer to signals defined along continuous independent variable(s). An example of an one-dimensional continuous-time signal is shown in Figure 2.4a. Discrete-time signals refer to signals

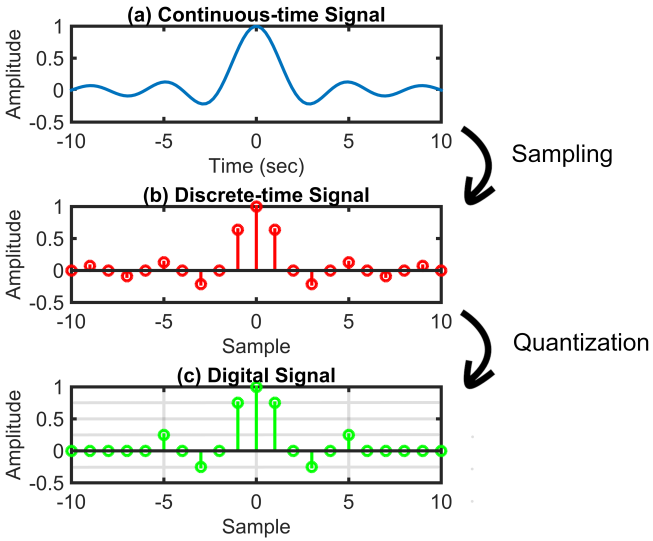

Figure 2.4: Examples of signals (a) Continuous-time signal (b) Discrete-time signal, can be also represented as a sequence of numerical values, [0, 0.07, 0, -0.09, 0, 0.13, ...] (c) Digital signal

defined at discrete independent variable(s), commonly integer variable(s). Discrete-time signals are often represented by sequences of numerical values. A discrete-time signal can be generated from a continuous-time signal by the approach of sampling. An one-dimensional discrete-time signal example is given in Figure 2.4b. The amplitude or the dependent variable of a signal can be also continuous or discrete. Digital signals are signals, which both independent variable(s) and dependent variable(s) are discrete. A digital signal can be generated from a discrete-time signal by the approach of quantization as shown in Figure 2.4c.

The term signal processing refers to the representation, transformation, manipulation, analysis, and synthesis of signals [Oppe 14]. A transformation that maps an input sequence $x[n]$ into an output sequence $y[n]$ is often referred to a discrete-time system. In this dissertation, two approaches in discrete-time signal processing are introduced, namely the discrete-time LPF and the short time fast Fourier transform (STFFT).

2.7.1 Low Pass Filter (LPF)

The approach of Hamming windowing is used in Chapter 3 as a LPF. The Hamming window is a discrete-time finite impulse response (FIR) system, that is often used as a filter. Therefore, this subsection starts with the fundamental regarding filters, FIR filters, and the Hamming windowing.

Filters are linear time-invariant systems that select or modify signals according to their frequency components. Specifically, the LPF passes the low-frequency component of a signal and attenuates the high-frequency components of the signal. As discrete-time systems can be categorized into infinite impulse response (IIR) and finite impulse response (FIR), discrete-time filters can be also categorized by IIR filters and FIR filters. IIR filters are designed commonly by applying transformation from continuous-time filters into discrete-time IIR filters, whereas FIR filters are designed commonly by approximating the desired frequency response and impulse response [Oppe 14].

The simplest FIR filter designing method is based on windowing. The rectangular window, the Bartlett (triangular) window, the Hanning window, the Hamming window, and the Blackman window are windows that are frequently used as filters [Oppe 14]. The rectangular window, Hanning window, and Hamming window with a length of $M_w + 1$ can be expressed as Eq.2.10, Eq.2.11 and Eq. 2.12, respectively.

$$w_{\text{rectangular}}[n] = \begin{cases} 1, & 0 \leq n \leq M_w \\ 0, & \text{otherwise} \end{cases} \tag{2.10}$$

$$w_{\text{Hanning}}[n] = \begin{cases} 0.5 - 0.5\cos(2\pi n/M_w), & 0 \leq n \leq M_w \\ 0, & \text{otherwise} \end{cases} \tag{2.11}$$

$$w_{\text{Hamming}}[n] = \begin{cases} 0.54 - 0.46\cos(2\pi n/M_w), & 0 \leq n \leq M_w \\ 0, & \text{otherwise} \end{cases} \tag{2.12}$$

Compared with the rectangular window, the Hamming and Hanning windows have lower side lobes in the frequency-domain and a smoother transition in the time-domain [Oppe 14] [Blac 58]. The Hamming window does not touch zero at the end point in the time-domain such as the Hanning window. The representations of these windows in the time- and frequency-domains are illustrated in Figure 2.5.

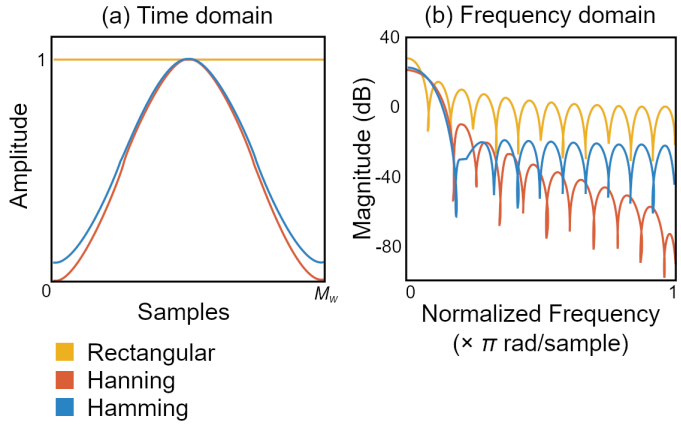

Figure 2.5: The rectangular, Hanning, and Hamming windows in the time and frequency domains with $M_w = 23$.

2.7.2 Fourier Transform

The approach of short time fast Fourier transform (STFFT) is used in Chapter 3. The Fourier analysis is typically used to convert a signal or a system from the time-domain to the frequency-domain. The use of the Fourier analysis in discrete-time systems is affected by the sampling approach (the approach of obtaining a discrete-time signal/system from a continuous-time signal/system). Therefore, this subsection starts with the fundamental of the Nyquist frequency, which is the maximum frequency that can be described by a discrete-time signal. It is followed by the fundamentals of several Fourier analysis, including the discrete-time Fourier transform (DTFT), the discrete Fourier transform (DFT), the fast Fourier transform (FFT) as well as the short time fast Fourier transform (STFFT).

As introduced in Figure 2.4, a discrete-time sequence $x[n]$ can be obtained by sampling a continuous-time signal $x(t)$ according to $x[n] = x(nT_s)$, where T_s represents the sampling period, $f_s = 1/T_s$ is the sampling frequency in Hz, and $\omega_s = 2\pi/T_s$ is the sampling frequency in rad/s. In case that $x(t)$ is a band-limited signal with a maximum frequency of $|\omega| = \omega_M$, the sampling theorem describes that $x(t)$ is uniquely determined by its samples $x[n] = x(nT_s)$ if $\omega_s > 2\omega_M$

[Nyqu 28] [Oppe 96]. The frequency $2\omega_M$ is often referred as the Nyquist rate and the frequency ω_M is often referred as the Nyquist frequency.

The discrete-time Fourier transform (DTFT) of a sequence $x[n]$ provides information about the composition of various-frequency complex-exponentials. This DTFT is often referred as spectrum and is described in Eq.2.13 [Oppe 96]. The resulting Fourier transform $X(e^{j\omega})$ is a periodic function with a period of 2π. The high-frequency components of $x[n]$ are represented by the values of $X(e^{j\omega})$ with ω near the odd multiplies of π. When $x[n]$ is real, $||X(e^{j\omega})|| = ||X(e^{-j\omega})||$. Moreover, the energy-density spectrum of $x[n]$ is defined by $||X(e^{j\omega})||^2$.

$$X(e^{j\omega}) = \sum_{n=-\infty}^{+\infty} x[n]e^{-j\omega n} \tag{2.13}$$

A DTFT version of finite-length signals is represented by the discrete Fourier transform (DFT). The DFT of an N_l-length sequence is described in Eq. 2.14 [Oppe 14]. The spacing between DFT frequencies is $2\pi/N_l$, and therefore the frequencies related to those frequencies are $\omega_k = 2\pi k/N_l$. The computation of all the values of $X[k]$ requires N_l^2 complex multiplications and $N_l(N_l - 1)$ complex additions.

$$\begin{aligned} X[k] &= \sum_{n=0}^{N_l-1} x[n]W_N^{kn}, \qquad 0 \leq k \leq N_l - 1 \\ W_N &= e^{-j(2\pi/N_l)} \end{aligned} \tag{2.14}$$

The fast Fourier transform (FFT) is an efficient computational algorithm to compute the DFT. By exploiting its symmetry and periodicity properties, the computation of the FFT requires roughly $N_l \log_2 N_l$ complex multiplication. One of the FFT algorithms is the Cooley-Tukey algorithm [Cool 65] [Duha 90], which has several variations, such as the decimation in time and the decimation in frequency [Oppe 14].

The time-varying Fourier transform was introduced by considering that the Fourier transform is not directly applicable for the analysis of a signal, which has properties that change as a function of time. For example, in the analysis of speech processing, short-time analysis principle is seen as a valid approach [Rabi 78]. Here, the temporal properties are assumed fixed over a short time and the spectral properties are

assumed to change relatively slowly. The time-varying Fourier transform is described by Eq. 2.15, where $w[m]$ is a real window sequence and n is a particular time index. The length of the window $w[m]$ is often finite [Rabi 78]. If $w[m]$ is a rectangular window with a length of M_w+1, the time-varying Fourier transform can be described by Eq. 2.16

$$X_n(e^{j\omega}) = \sum_{m=-\infty}^{+\infty} w[m-n]x[m]e^{-j\omega m} \tag{2.15}$$

$$X_{n,r}(e^{j\omega}) = \sum_{m=n}^{n+M_w} x[m]e^{-j\omega m} \tag{2.16}$$

The efficient computation algorithm to compute a time-varying Fourier transform is called short time fast Fourier transform (STFFT).

2.8 Linear Discriminant Analysis (LDA)

The linear discriminant analysis (LDA), also known as the Fisher discriminant analysis (FDA), was first designed by Fisher [Fish 36] to find a linear function that best discriminates between two groups. In addition to the use in data analysis, the LDA is also applied for extracting features and for reducing dimensionality [Li 05].

Given samples with a number of independent parameters, the LDA generates a linear combination of the parameters, which yields the largest differences between the two groups [Mart 01]. To achieve this, two different measures are defined:

- Within-class scatter matrix

$$S_w = \sum_{j=1}^{c} \sum_{i=1}^{N_j} (\mathbf{x}_i^j - \mu_j)(\mathbf{x}_i^j - \mu_j)^T \tag{2.17}$$

- Between-class scatter matrix

$$S_b = \sum_{j=1}^{c} (\mu_j - \mu)(\mu_j - \mu)^T \tag{2.18}$$

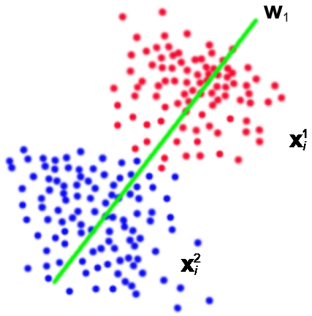

Figure 2.6: An illustration of the LDA principle.

In Eq. 2.17 and Eq. 2.18, $\mathbf{x}_i^j \in \mathbb{R}^k$ is the i–th sample of group j, μ_j is the mean of group j, $c = 2$ is the number of groups, N_j is the number of samples in the groups j, μ represents the mean of all groups, and k is the number of parameters.

The LDA aims to maximize the between-class scatter and minimize the within-class scatter, which can be done by maximizing the ratio $(\det|S_b|/\det|S_w|)$. This can be achieved by solving the eigen-value problem as stated in Eq. 2.19, where $\mathbf{w}$ represents the eigen-vector and λ represents the eigen-value. The eigen-vector with the highest eigen-value $\mathbf{w}_1 \in \mathbb{R}^k$ will typically represent the vector that best discriminates the two groups (illustrated in Figure 2.6). For a new unseen data $\mathbf{z} \in \mathbb{R}^k$, its projection to the resulting eigen-vector is equal to the linear combination of parameters as expressed in Eq. 2.20.

$$S_w^{-1} S_b \mathbf{w} = \lambda \mathbf{w} \tag{2.19}$$

$$|\mathbf{w}_1||\mathbf{z}|cos\theta = \mathbf{w}_1 \cdot \mathbf{z} = \sum_{i=1}^{k} w_{1,i} z_i \tag{2.20}$$

In this dissertation (Chapter 6), the LDA is used as the basis of developing a linear combination of gait parameters.

3 Dynamic-Footprint-based Locomotion Sway Assessment in Mice

This chapter presents computational methods designed for quantifying sway-related gait parameters in mice. The material, methods, results, and discussion of this chapter are closely based on manuscripts published in the Journal of Neuroscience Methods [Timo 18b] and the journal Data in Brief [Timo 18c], which were written by the author of this dissertation in collaboration with the coauthors of the manuscripts.

The CatWalk data used in this chapter were collected primarily by the coauthors, Fabio Canneva and Georgia Minakaki. The author of this dissertation subsequently developed computational methods through which the data were evaluated. The same mouse models were also involved in an intervention study published in the journal Behavioral Brain Research [Mina 19], where the author of this dissertation is a coauthor of the publication. In addition, this mouse models is also used in a study described in Chapter 5, presented in the proceeding of the Measuring Behavior Conference 2018 [Timo 18a], and published in the Journal of Neuroscience Methods [Timo 19a].

The author of this dissertation implemented signal processing approaches for assessing sway and applied the methods to CatWalk data of PD-relevant mice. The fundamentals relating to this chapter are given in Section 2.5.1 (PD) and Section 2.7 (signal processing).

3.1 Overview

Sway during locomotion is one of the gait characteristics related to PD. Therefore, assessing sway during gait tests is valuable for the observation of gait progression in preclinical studies related to PD. Three computational methods for assessing locomotion sway based on the recorded paw positions are described here. The methods were applied to

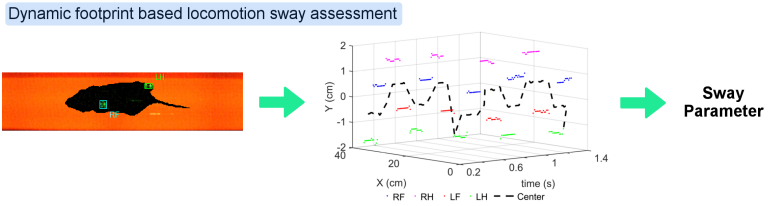

Figure 3.1: Graphical overview: Dynamic-footprint-based locomotion sway assessment in mice. Three computational methods are presented in this chapter: (i) FFT-based sway parameter (ii) FFT-based intensity sway parameter (iii) LPF-based sway parameter or sway index. This image was reproduced from [Timo 18b] with permission.

the CatWalk dynamic footprint data collected from two α-synuclein (α-Syn) mouse models and their wild-type littermates.

The CatWalk dynamic footprint data provide the temporal and spatial information of the paw contacts to the transparent walkway. Using signal processing approaches based on the FFT and the LPF, three computational methods for generating sway-related gait parameters were developed: (i) FFT-based sway parameter (ii) FFT-based intensity sway parameter (iii) LPF-based sway parameter or sway index. An overview of the methodological pipeline is depicted in Figure 3.1.

The three methods were applied to dynamic footprint data recorded from all paws as well as from front-/hind-paws separately, resulting in total nine sway-related parameters. These parameters were used to differentiate the mouse models, α-Syn mouse models and their wild-type littermates. Higher sway-related parameters were observed in the α-Syn mouse models compared with the wild-type mice.

The computational methods presented here quantify sway-related characteristic during walking. These methods add new gait information, which was obtained from data collected from the standard gait analysis system, CatWalk.

3.2 Material and Methods

3.2.1 Animals and Data Acquisition

A total of 33 male mice, all backcrossed on to C57BL/6N genetic background, were used at 7 months of age. The mice were grouped into three cohorts:

- 12 non-transgenic mice (wild-type, "WT" mice).
- 13 mice bearing a knock-out for the endogenous murine α-Syn ("KO" mice, described in [Abel 00]).
- 8 double transgenic mice, with compensatory expression of human α-synuclein (α-Syn) protein, under the control of a bacterial artificial chromosome (BAC) construct (described in [Kohl 16] [Nube 13] [Wass 18]), on the mouse α-Syn knock-out background ("huWT/KO" mice).

These α-Syn mouse models were generated by mating male huWT/KO with female α-Syn knock-out mice [Mina 19]. There were no significant body weight differences across the three cohorts (31 $\pm$ 2.47 g, mean $\pm$ SD). These same mice were involved in an intervention study published in [Mina 19].

The mice were kept under the standard specific-pathogen-free (SPF) laboratory conditions on a 12h:12h light:dark cycle, where food and water were available *ad libitum*. All procedures were approved by the local Animal Welfare and Ethics committee of Bavaria, Germany (RegUFr#55.2-2532-2-218).

Each mouse can explore and walk freely above the CatWalk walkway. Experimental sessions typically lasted 5–10 min, after which each mouse was returned to its own home-cage, in order to reduce habituation of the mice to the environment and the appearance of unwanted behaviors (e.g. sniffing, rearing, sitting). All runs were recorded in the dark at a minimum level of external disturbing factors and 2–4 compliant runs were recorded from each mouse. A total of 34, 32, and 24 compliant runs were collected for this study, from WT, KO, and huWT/KO mice, respectively. In this chapter, the information of paw positions and their intensities in each frame of the CatWalk videos is used to describe locomotion sway of each mouse.

3.2.2 FFT–based Locomotion Sway Descriptors

The first two methods describe sway based on the recorded paw positions in lateral (y-axis) as a function of time. Examples of these recorded paw positions from all paws (RF, RH, LF, and LH) are depicted in Figure 3.2. Subsequently, the mean of the paw positions in every frame is computed, resulting the center of paw positions $x_{c0}[n]$ (black lines in Figure 3.2), with $n = 1, 2, ..., N$, where N is the number of frames with labeled paws in the captured video. The values of N were 112 and 234 for the WT mouse in Figure 3.2a and the huWT/KO mouse in Figure 3.2b, respectively.

The center position $x_{c0}[n]$ was subtracted by its mean value. This mean value of $x_{c0}[n]$ reflects the walking middle path and does not convey any sway-related information. Therefore, it is eliminated and the resulting function is then denoted by $x_c[n]$.

$$x_c[n] = x_{c0}[n] - \overline{x_{c0}[n]} \tag{3.1}$$

In these methods, sway is characterized by the lateral movement at a specific frequency range. The frequency content of $x_c[n]$ was analyzed by using the short time fast Fourier transform (STFFT) [Rabi 78], which was computed for every shift N_S samples of N_W window size (N_S: the amount of window shift; N_W: the size of window), resulting the frequency-domain function $X_W[f, m]$, with $f = 0, 1, 2, ..., N_w - 1$ and $m = 1, 2, ..., M$, where $M = \lfloor (N - N_W)/N_S \rfloor$ is the number of the windowed signal.

$$X_W[f, m] = \text{STFFT}(x_c[n]) \tag{3.2}$$

The spectrum information, $X_c[f]$, of the complete signal, $x_c[n]$, was computed by averaging the absolute value of $X_W[f, m]$ over all m.

$$X_c[f] = \overline{\|X_W[f, m]\|} \tag{3.3}$$

This spectrum information is used to examine normal gait cycle and sway associated signals. The frequency content associated with a normal gait cycle was chosen by analyzing the mean of WT step cycle, which is 0.28 $\pm$ 0.05 second (mean $\pm$ SD) and leads to 3.60 $\pm$ 0.66 step/sec (mean $\pm$ SD). The frequency contents, lower than this normal gait cycle (3.60 $\pm$ 0.66 step/sec), are considered associated with the body locomotion sway. This assumption is based on knowledge that the

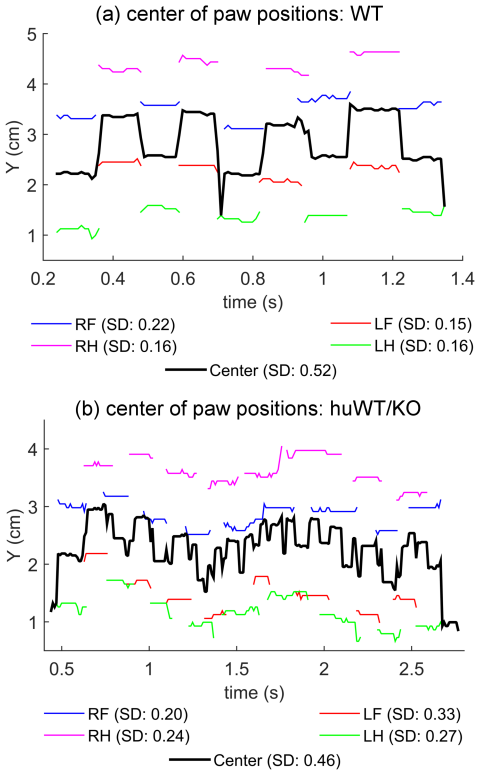

Figure 3.2: Examples of paw positions and their center positions as functions of time (blue: RF; magenta: LF; red: RH; and green: LH). (a) a WT mouse (b) a huWT/KO mouse. The SD of the center and paw positions were also shown in the figure and serves as additional information, which were impacted by the mouse movement. This image was reproduced from [Timo 18b] with permission.

postural sway components are typically concentrated at the lower spectrum (0–1 Hz) [Morr 08]. A shift of $N_S = 5$ samples was used and a window size of $N_W = 64$ was chosen concerning the normal step frequency range and the limitation of labeled frame numbers, N. Thus, with a video sampling rate (f_s) of 100 Hz, each sample in the frequency domain is separated by 1.56 Hz. Using the information given by the resulting $X_c[f]$, the normal gait cycle was associated with $f = 2, 3$ (frequency

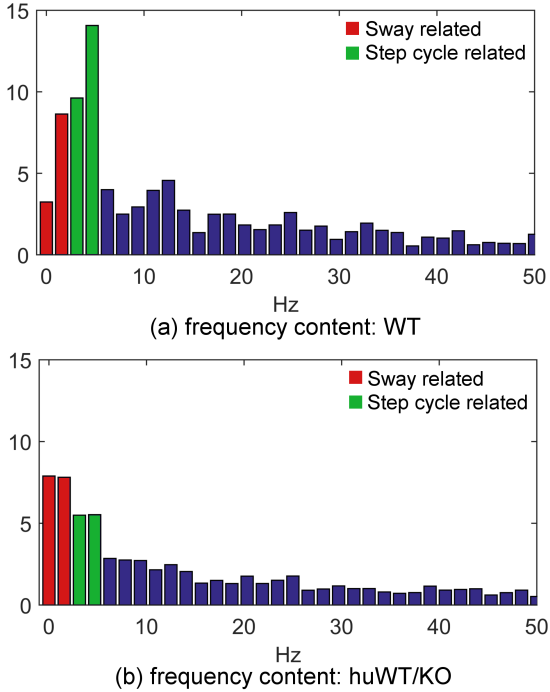

Figure 3.3: Examples of frequency contents, $X_c[f]$ for $f = 0, 1, 2, ..., N_W/2$, computed from the signal in Figure 3.2 (a) a WT mouse (b) a huWT/KO mouse. This image was reproduced from [Timo 18b] with permission.

bin center of 3.13 and 4.69 Hz, respectively) and the locomotion body sway is associated with $f = 0, 1$ (frequency bin center of 0 and 1.56 Hz, respectively). Since the step frequency averages for KO and huWT/KO are respectively 3.1 and 2.7 step/sec, it can be expected that the normal gait cycle for KO and huWT/KO is expressed in $X_c[f]$ with $f = 2, 3$ as well. The frequency content, $X_c[f]$ for $f = 0, 1, 2, ..., N_W/2$, as a function of frequency of the signals in Figure 3.2 are shown in Figure 3.3.

The energy of these frequency components were then calculated as follows:

$$E_n = \text{sum}(X_c^2[f]), \quad \text{with } f = 2, 3 \tag{3.4}$$

$$E_s = \text{sum}(X_c^2[f]), \quad \text{with } f = 0, 1 \tag{3.5}$$

The locomotion sway was then described by the ratio of body sway energy, E_s, and normal cycle energy, E_n:

$$S_{p,FFT} = \frac{E_s}{E_n} \tag{3.6}$$

In addition to the positions of the labeled paws, the CatWalk system also provides information about the mean, the minimum and the maximum intensity of each labeled paw within a 0–255 range. The information regarding the intensity corresponds to the amount of pressure exerted by the paws over the glass surface. For developing the second FFT-based locomotion sway descriptor, the same approach as described above was also performed on the product of the paw positions and their related intensity means on the y-axis, resulting on an intensity locomotion sway parameter, $S_{(i,FFT)}$. In this second locomotion sway descriptor, the means of paw intensities were first scaled by the minimum intensity to eliminate the effect of different minimum footprint intensity thresholds.

Finally, the locomotion sway descriptors were calculated based on the front paws and hind paws separately. Figure 3.4 shows the paw positions and their center positions from front- and hind- paws of paw positions of both WT and huWT/KO mice shown in Figure 3.2. The frequency contents of those positions are shown in Figure 3.5. The FFT-based locomotion sway parameters of the paw positions shown in Figure 3.2 are also listed in Table 3.1.

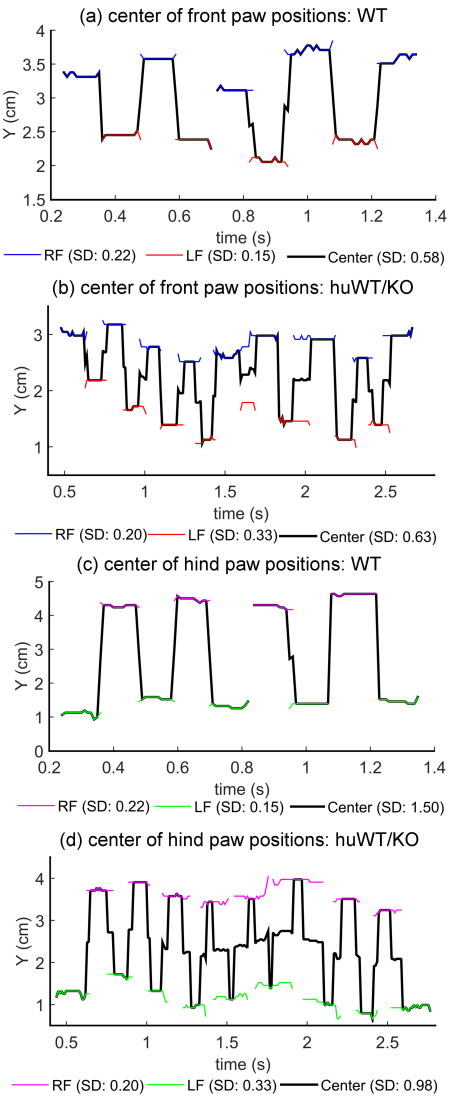

Figure 3.4: Examples of front- and hind- paw positions and their center positions as functions of time taken from the same paw positions as in Figure 3.2 (a) a WT mouse, front (b) a huWT/KO mouse, front (c) a WT mouse, hind (d) a huWT/KO mouse, hind. This image was reproduced from [Timo 18b] with permission.

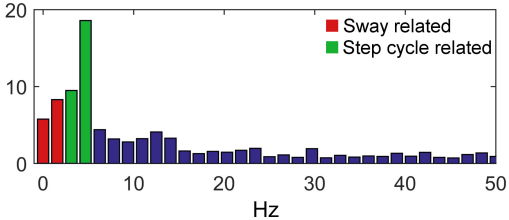

(a) frequency content: WT, front paws

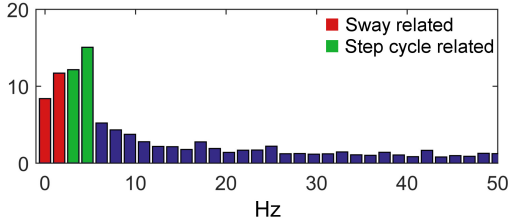

(b) frequency content: huWT/KO, front paws

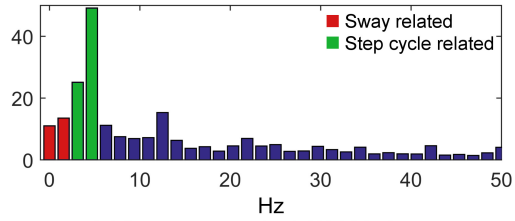

(c) frequency content: WT, hind paws

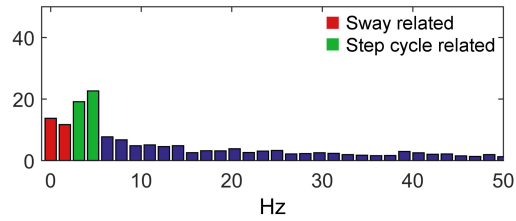

(d) frequency content: huWT/KO, hind paws

Figure 3.5: Examples of frequency contents, $X_c[f]$ for $f = 0, 1, 2, ..., N_W/2$, of the front- and hind- paws as function of frequency taken from the same paw positions as in Figure 3.2 (a) a WT mouse, front (b) a huWT/KO mouse, front (c) a WT mouse, hind (d) a huWT/KO mouse, hind. This image was reproduced from [Timo 18b] with permission.

Table 3.1: The FFT-based locomotion sway parameters of the paw positions shown in Figure 3.2

Algorithm	WT mouse	huWT/KO mouse
$S_{p,FFT}$	0.29	2.03
$S_{i,FFT}$	0.22	1.45
$S_{p,FFT,front}$	0.24	0.55
$S_{i,FFT,front}$	0.48	0.64
$S_{p,FFT,hind}$	0.10	0.37
$S_{i,FFT,hind}$	0.10	0.42

$S_{p,FFT}$: FFT-based locomotion sway parameter
$S_{i,FFT}$: FFT-based intensity locomotion sway parameter

3.2.3 Estimated Locomotion Sway Index

The third method describes sway in a straight walkway based on the estimated path, which was calculated by employing a LPF on the paw positions on both the x-axis and y-axis as a function of time. In this method, the LPF is used mainly to reduce the effect of normal gait cycle paw positions on the estimated path.

The locomotion sway index is defined as the ratio of the horizontal path distance and the straight-line displacement [Geld 15]. In this work, the path distance was estimated by the labeled paw positions. This method is based on the paw positions on the x-axis and the y-axis as a function of time and it was implemented as follows.

First, the center point of the labeled paws for every frame, $(x[n], y[n])$ with $n = 1, 2, ..., N$ was computed (where N is the total number of frames with labeled paws). Then, the mean of the center point position on the y-axis $\overline{y[n]}$ was removed, because this mean only contain the information of walking middle path.

$$(x_p[n], y_p[n]) = (x[n], y[n] - \overline{y[n]}) \tag{3.7}$$

The center paw position on the y-axis $y_p[n]$ was then filtered using a symmetric low pass Hamming filter [Oppe 14] (20th order, cutoff frequency of 1 Hz) to describe the walking path, $y_h[n]$.

The center paw position on the x-axis $x_p[n]$ was also filtered by a symmetric Hamming low pass filter (3rd order, cutoff frequency of 20 Hz) to smooth the signal and eliminate high frequency fluctuations. The

filtered signal of $x_p[n]$ is denoted by $x_h[n]$. Figure 3.6 shows the filtered signal $(x_h[n], y_h[n])$ and the labeled paw positions from the mice, which paw positions were depicted in Figure 3.2. This filtered signal $(x_h[n], y_h[n])$ is referred as the estimated path of the locomotion.

The horizontal path distance, p, from the signal $(x[n], y[n])$ was estimated by calculating the Euclidean distance of the adjacent points (Equation 3.8).

$$p = \sum_{n=\left\lfloor \frac{N_y}{2} \right\rfloor + 1}^{N - \left\lfloor \frac{N_y}{2} \right\rfloor} \sqrt{(x_h[n] - x_h[n-1])^2 + (y_h[n] - y_h[n-1])^2} \tag{3.8}$$

The straight-line displacement was then estimated based on the minimum and the maximum value of paw positions on the x-axis:

$$\begin{aligned} d &= \max(x_h[n]) - \min(x_h[n]) \\ n &= \left\lfloor \frac{N_y}{2} \right\rfloor + 1, \ldots, N - \left\lfloor \frac{N_y}{2} \right\rfloor \end{aligned} \tag{3.9}$$

The locomotion sway index was finally estimated by

$$S_{index} = \frac{p}{d} \tag{3.10}$$

The sway index was estimated for the front paws and hind paws, separately. The estimated path of the front- and hind-paws of the paw positions in Figure 3.2 are shown in Figure 3.7. The estimated sway indexes of the paw positions in Figure 3.2 are also listed in Table 3.2.

Table 3.2: The estimated sway indexes of the paw positions shown in Figure 3.2 and Figure 3.6

Algorithm	WT mouse	huWT/KO mouse
S_{index}	1.03	1.17
$S_{index,front}$	1.04	1.12
$S_{index,hind}$	1.13	1.16

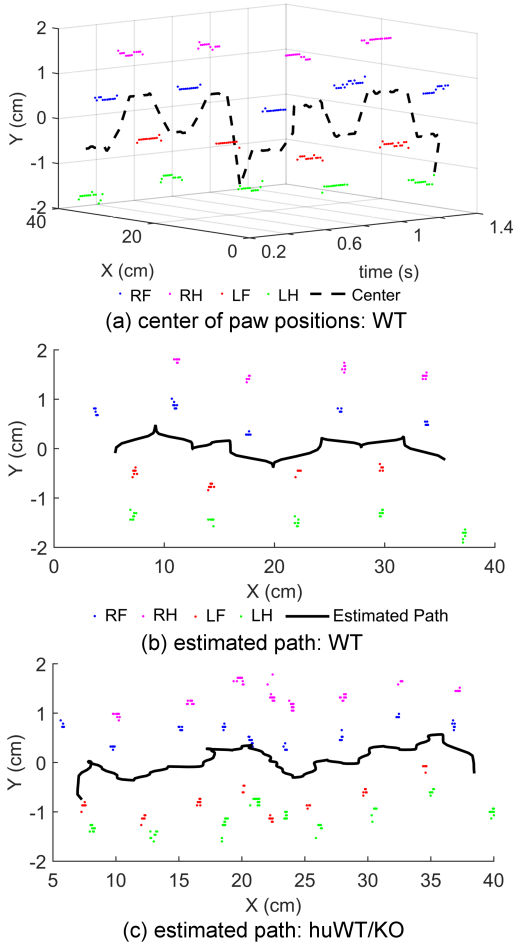

Figure 3.6: Examples of paw positions taken from the same paw positions as in Figure 3.2 and (a) their center of paw positions as a function of time, WT (b) their estimated path, WT (c) their estimated path, huWT/KO. This image was reproduced from [Timo 18b] with permission.

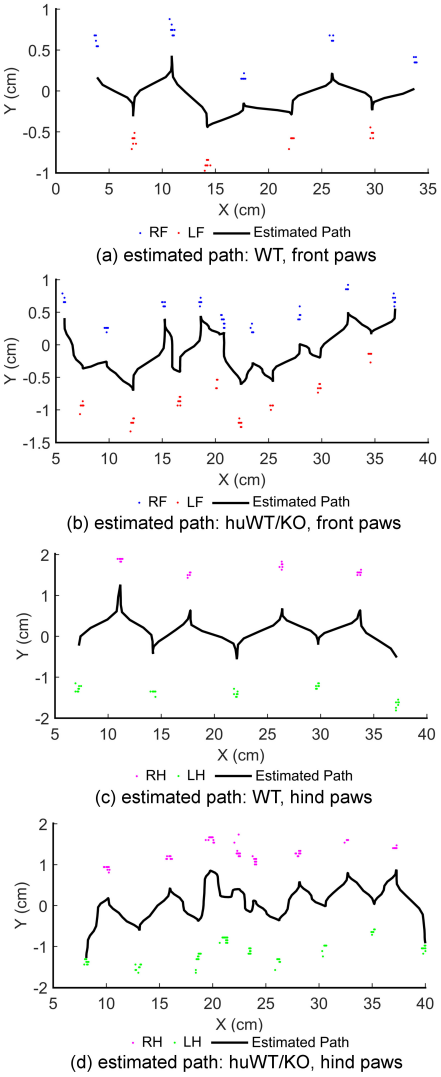

Figure 3.7: Examples of paw positions and the estimated path of front- and hind-paws taken from the same paw positions as in Figure 3.2 and Figure 3.6 (a) a WT mouse, front (b) a huWT/KO mouse, front (c) a WT mouse, hind (d) a huWT/KO mouse, hind. This image was reproduced from [Timo 18b] with permission.

3.2.4 Analysis

For the purpose of the analysis, the sway parameters from the runs of each mouse were averaged. The sway differences between these three cohorts of mice were analyzed by using the one-way analysis of variance (ANOVA) [Arms 00] [Fish 21], [Mull 09] and the multiple comparison tests by Bonferroni correction in Matlab R2015a (8.5.0). These tests return the p-values of the three-cohort-comparison as well as the pairwise comparison. Other comparison analyses were performed by using the unpaired student's t-test [Derr 16] between WT and the combination of KO and huWT/KO, as well as the F-tests. For the correlation analysis of the sway parameters, the p-values as well as the coefficients of determination, R^2 [Nage 91] were computed.

3.3 Results

The mean, standard deviation (SD), and standard mean error (SEM) values of all the locomotion sway parameters in each cohort are given in Table 3.3 and Figure 3.8. By comparing the means of sway parameters with the other cohorts, the WT mice have the lowest sway parameter values and the huWT/KO mice have the highest sway parameter values. A similar trend is shown by the SD values.

The p-values and f-values of the statistical analysis are given in Table 3.4. The corresponding significant differences based on the resulted p-values are also shown in Figure 3.8. Significant differences between the three cohorts as well as significant differences between WT and huWT/KO can be seen in all of the sway parameters, except for $S_{i,FFT}$. This exception is influenced by the relatively low mean values and high SD values of the $S_{i,FFT}$ of huWT/KO mice. A significant difference between WT and KO is only observed in $S_{index,front}$. With the exception of $S_{i,FFT,front}$, significant differences between WT and non-WT are observed in all of the sway parameters.

The p-values and the coefficients of determination (R^2 values) are given in Table 3.5. The R^2 values are mostly low, especially for the correlation between the FFT-based and LPF-based parameters. High R^2 values are observed between the FFT-based sway parameters calculated from the front- and hind- paws. However, among all of the parameters, the p-values show significant correlations ($p < 0.05$).

Table 3.3: The mean ± SD of sway parameters in cohorts of mice

Algorithm	WT	KO	huWT/KO	KO & huWT/KO
$S_{p,FFT}$	0.74 ± 0.36	1.25 ± 0.73	1.57 ± 0.79	1.37 ± 0.75
$S_{i,FFT}$	0.70 ± 0.41	1.26 ± 0.85	1.46 ± 1.00	1.34 ± 0.89
S_{index}	1.09 ± 0.05	1.15 ± 0.08	1.22 ± 0.14	1.17 ± 0.11
$S_{p,FFT,front}$	0.49 ± 0.53	0.96 ± 0.65	1.97 ± 1.90	1.35 ± 1.33
$S_{i,FFT,front}$	0.62 ± 0.36	0.96 ± 0.60	1.91 ± 1.67	1.32 ± 1.19
$S_{index,front}$	1.09 ± 0.02	1.14 ± 0.05	1.18 ± 0.07	1.15 ± 0.06
$S_{p,FFT,hind}$	0.19 ± 0.14	0.53 ± 0.42	0.97 ± 1.15	0.70 ± 0.79
$S_{i,FFT,hind}$	0.19 ± 0.14	0.56 ± 0.44	0.91 ± 1.04	0.69 ± 0.73
$S_{index,hind}$	1.21 ± 0.07	1.29 ± 0.09	1.38 ± 0.16	1.32 ± 0.13

$S_{p,FFT}$: FFT-based locomotion sway parameter
$S_{i,FFT}$: FFT-based intensity locomotion sway parameter
S_{index}: Locomotion sway index

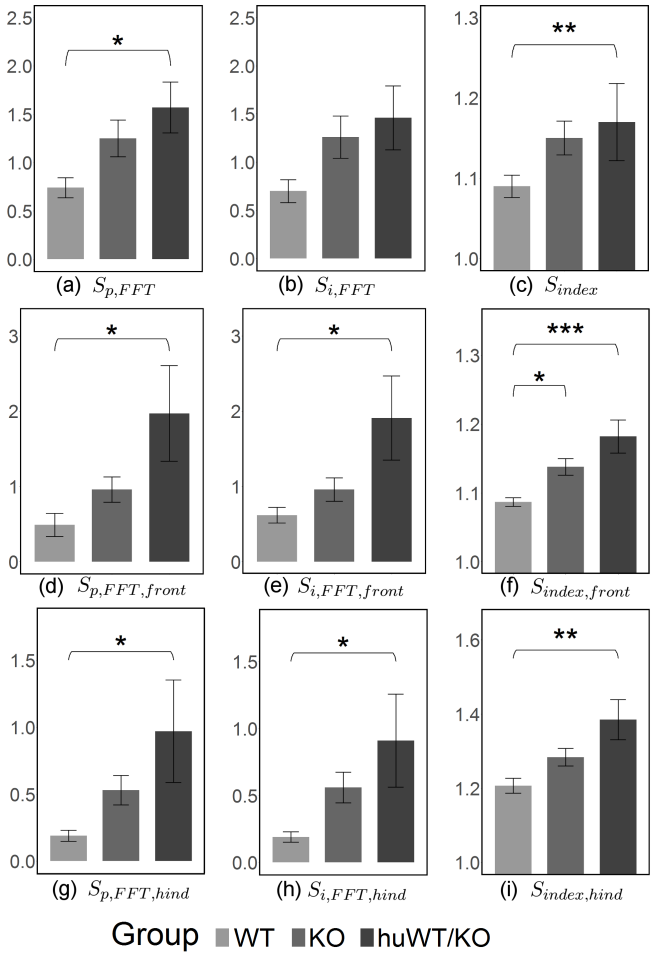

Figure 3.8: Locomotion sway parameters: Mean ± SEM and their significant differences between cohorts (*$p < 0.05$, **$p < 0.01$, ***$p < 0.001$): (a) $S_{(p,FFT)}$ (FFT-based locomotion sway parameter) (b) $S_{(i,FFT)}$ (FFT-based intensity locomotion sway parameter) (c) S_{index} (locomotion sway index) (d) $S_{(p,FFT,front)}$ (e) $S_{(i,FFT,front)}$ (f) $S_{(index,front)}$ (g) $S_{(p,FFT,hind)}$ (h) $S_{(i,FFT,hind)}$ (i) $S_{(index,hind)}$. This image was reproduced from [Timo 18b] with permission.

Table 3.4: Statistical analysis results, p-value (f-value), of the comparison tests between the cohorts. The tests were done using the one-way ANOVA, multiple comparison test by Bonferroni correction, unpaired t-test, and F-test.

	ANOVA and Multiple Comparison Test				**Unpaired t–test**
Algorithm	3 cohorts	WT–KO	WT–huWT/KO	KO–huWT/KO	WT–(KO & huWT/KO)
$S_{p,FFT}$	0.02 (4.3)	0.17 (4.7)	0.03 (10.1)	0.84 (0.9)	0.01 (7.3)
$S_{i,FFT}$	0.07 (2.9)	0.23 (4.3)	0.11 (5.7)	1 (0.2)	0.03 (5.5)
S_{index}	0.01 (5.2)	0.32 (5.1)	0.01 (9.2)	0.25 (2.3)	0.01 (6.8)
$S_{p,FFT,front}$	0.02 (4.8)	0.82 (3.9)	0.01 (6.7)	0.13 (3.2)	0.04 (4.5)
$S_{i,FFT,front}$	0.02 (4.9)	1 (2.7)	0.01 (6.8)	0.08 (3.6)	0.06 (3.8)
$S_{index,front}$	10^{-4} (9.8)	0.04 (11.5)	10^{-4} (18.5)	0.14 (3.0)	10^{-4} (13.8)
$S_{p,FFT,hind}$	0.03 (3.8)	0.53 (7.2)	0.03 (5.6)	0.38 (1.6)	0.03 (5.0)
$S_{i,FFT,hind}$	0.04 (3.8)	0.36 (7.8)	0.03 (5.8)	0.57 (1.2)	0.02 (5.6)
$S_{index,hind}$	10^{-3} (6.7)	0.25 (5.4)	10^{-3} (11.5)	0.13 (3.3)	10^{-3} (8.0)

$S_{p,FFT}$: FFT-based locomotion sway parameter
$S_{i,FFT}$: FFT-based intensity locomotion sway parameter
S_{index}: Locomotion sway index

Table 3.5: Sway parameter correlations calculated by p-values and the coefficients of determination (R^2 values)

		$S_{p,FFT}$	$S_{i,FFT}$	S_{index}	$S_{p,FFT,f}$	$S_{i,FFT,f}$	$S_{index,f}$	$S_{p,FFT,h}$	$S_{i,FFT,h}$	$S_{index,h}$
$S_{p,FFT}$	R^2	1	–	–	–	–	–	–	–	–
	p	0	–	–	–	–	–	–	–	–
$S_{i,FFT}$	R^2	0.55	1	–	–	–	–	–	–	–
	p	10^{-6}	0	–	–	–	–	–	–	–
S_{index}	R^2	0.42	0.45	1	–	–	–	–	–	–
	p	10^{-5}	10^{-5}	0	–	–	–	–	–	–
$S_{p,FFT,f}$	R^2	0.52	0.36	0.67	1	–	–	–	–	–
	p	10^{-6}	10^{-4}	10^{-8}	0	–	–	–	–	–
$S_{i,FFT,f}$	R^2	0.51	0.37	0.67	0.91	1	–	–	–	–
	p	10^{-6}	10^{-4}	10^{-8}	10^{-17}	0	–	–	–	–
$S_{index,f}$	R^2	0.26	0.33	0.75	0.44	0.48	1	–	–	–
	p	0.002	10^{-4}	10^{-10}	10^{-5}	10^{-5}	0	–	–	–
$S_{p,FFT,h}$	R^2	0.55	0.56	0.74	0.77	0.86	0.54	1	–	–
	p	10^{-6}	10^{-6}	10^{-10}	10^{-11}	10^{-14}	10^{-6}	0	–	–
$S_{i,FFT,h}$	R^2	0.53	0.61	0.75	0.74	0.82	0.54	0.98	1	–
	p	10^{-6}	10^{-7}	10^{-10}	10^{-10}	10^{-12}	10^{-6}	10^{-28}	0	–

Continued on next page

Table 3.5 – continued from previous page

		$S_{p,FFT}$	$S_{i,FFT}$	S_{index}	$S_{p,FFT,f}$	$S_{i,FFT,f}$	$S_{index,f}$	$S_{p,FFT,h}$	$S_{i,FFT,h}$	$S_{index,h}$
$S_{index,h}$	R^2	0.25	0.21	0.69	0.53	0.62	0.81	0.61	0.57	1
	p	0.003	0.007	10^{-9}	10^{-6}	10^{-7}	10^{-12}	10^{-7}	10^{-7}	0

$S_{p,FFT}$: FFT-based locomotion sway parameter
$S_{i,FFT}$: FFT-based intensity locomotion sway parameter
S_{index}: Locomotion sway index
$S_{p,FFT,f} = S_{p,FFT,front}$: FFT-based locomotion sway parameter from the front paws
$S_{i,FFT,f} = S_{i,FFT,front}$: FFT-based intensity locomotion sway parameter from the front paws
$S_{index,f} = S_{index,front}$: Locomotion sway index from the front paws
$S_{i,FFT,h} = S_{i,FFT,hind}$: FFT-based intensity locomotion sway parameter from the hind paws
$S_{p,FFT,h} = S_{p,FFT,hind}$: FFT-based locomotion sway parameter from the hind paws
$S_{index,h} = S_{index,hind}$: Locomotion sway index from the hind paws

3.4 Discussion

This study introduces three methods for assessing locomotion sway in mice based on the labeled footprints. The methods were applied on the gait data taken from WT mice and their α-Syn transgenic littermates, which are used as positive controls. The first two methods were based on the paw positions along the y-axis as a function of time and processed based on the FFT, while the third method is based on the estimated path and processed based on the LPF. These methods quantify higher sway-related gait parameters in the α-Syn transgenic mouse models as compared to the WT mice.

The results, presented in Table 3.3 and Figure 3.8, show higher sway-related parameter mean values in the α-Syn transgenic mouse models compared to their non-transgenic littermates. Significant differences between the WT mice and the huWT/KO mice were observed in eight of the nine sway parameters. These sway differences were observed and matched with the recorded videos by the CatWalk system.

The LPF-based sway descriptors showed higher f-values and lower p-values between the WT and huWT/KO mice compared with the FFT-based sway descriptors due to the small SD value of the LPF-based sway descriptors in each cohort. In addition, one of the LPF-based sway descriptors, $S_{index,front}$, can identify significant difference between the KO and huWT/KO mice.

The sway-related gait parameters, described in this study, can also be calculated only from the front- or hind-paws. The α-Syn transgenic mice show higher front- and hind- paw sway-related parameters compared to their non-transgenic littermates. The sway assessment from the front- and hind- paws separately is valuable for obtaining additional information relating to the gait, such as the sway of part of the body. Furthermore, it can be used in the circumstances, in which only front- or hind-paws can be detected.

By comparing the test results of the with- and without- intensity FFT-based sway parameters, shown in Table 3.3 and Figure 3.8, similar or higher p-values are observed in the FFT-based sway parameters that include intensity information. This suggests that the intensity values do not give additional sway-related information for C57BL/6N α-Syn transgenic mouse models. Intensity values correspond to the weight that is put on the glass surface, which depend on the paw pressure and the body weight [Hend 06] [Nold 12]. This intensity might be also influenced

by the moistness of the floor. Dry walkway floor is recommended for assessing the asymmetries in paw loading [Hame 01]. Since the intensity-based locomotion sway parameter $S_{i,FFT}$ depends on the ratio of the energy of different frequency components, the intensity values will influence the sway parameter if there is intensity imbalance between the paws. Although this intensity-based parameter is not adding information for C57BL/6N α-Syn transgenic mouse models, it will be feasible for the study in rodent models with paw loading asymmetries.

In addition, experiments by changing the size of the windows N_W in the FFT-based locomotion sway descriptors were performed. Changing the value of N_W in the range from 55 to 70 shows similar differences between classes, in which no change of the resulted asterisks is observed. The higher value of N_W, the finer frequency information is obtained and the more frames with labeled paws are needed.

Since all of the parameters are related to sway, they significantly correlate to each other ($p < 0.05$). The parameters generated based on the FFT have a higher correlation to each other. However, the relatively low R^2 values for most of the pairwise correlation test indicate that the parameters could not be strongly estimated or explained by each other. Thus, each method models the locomotion sway differently. High R^2 values are observed between the FFT-based sway parameters calculated from the front- and hind-paws, due to the similarity of the method and of the paw-center signal shapes.

A compact comparison of the described methods with the pre-existing method [Geld 15] is provided in Table 3.6. Since the pre-existing method [Geld 15] used a different hardware setting (specifically regarding the type of walkway, lighting, and camera placement), different sway-related computer algorithm was developed. As the CatWalk system provides information related the rodents' body silhouette, it will be possible to further develop a sway index calculation based on the body silhouette. This possibility is briefly described in Table 3.6.

Overall, the described FFT- and LPF-based methods serves as quantitative descriptors of locomotion sway in mouse models, which is an important step towards increasing the translational value of preclinical studies aimed at modeling disease progression.

Table 3.6: Method comparison

	Geldenhuys' [Geld 15]	**Paw-position-based** $S_{p,FFT}$	$S_{i,FFT}$	S_{index}	**Silhouette-based**
Experimental setting	• The walkway is made from a white wood. • The trackway is illuminated with a 250 Watt quartz light. • The camera is placed overhead to allow for a dorsal view.	CatWalk: • The walkway is made from a glass plate. • The video is recorded in a dark room. • The camera is placed below the trackway. • The video gives paw positions and body silhouette information.			
Algorithm	• The positions of the nose tip and tail base are determined by a video analysis software, but no information about the	The algorithm is based on the paw positions in lateral position as a function of time and processed based	The algorithm is similar to $S_{p,FFT}$ with an addition of intensities information.	The algorithm is based on the estimated path and processed based on LPF.	The silhouette is extracted based on image processing, then two possible methods can be implemented: • Estimating COM

Continued on next page

Table 3.6 – continued from previous page

	Geldenhuys' [Geld 15]	**Paw-position-based** $S_{p,FFT}$	$S_{i,FFT}$	S_{index}	**Silhouette-based**
	algorithm is given in [Geld 15]. • The positions are smoothed by a quantic spline function. • The COM position is determined by 41.5%/45.5% (male/female) of nose-tip to tail-base length.	on FFT.			by the center of silhouette. • Tail removal algorithm, followed by estimating COM by the 41.5%/45.5% of estimated nose-tip to tail line.
Discussion	The publication [Geld 15] did not give enough information for reproduction.	The CatWalk system provides the information of the paw positions. Therefore, the algorithms are not influenced by a slight head movement.			The algorithm will probably be very sensitive to head movements compared with the paw-position-based methods.
		The implementation on rodents with	The limitation is similar to the $S_{p,FFT}$.	The results depend on the chosen filter	

Continued on next page

Table 3.6 – continued from previous page

Geldenhuys' [Geld 15]	**Paw-position-based** $S_{p,FFT}$	$S_{i,FFT}$	S_{index}	**Silhouette-based**
	low step frequency is challenging since the normal step cycle and sway share the same spectrum.	The $S_{i,FFT}$ is based on information about paw pressure, which might be influenced by the paw moist.	parameters.	

4 Silhouette-Length-based Gait Parameter Scaling in Rodents

This chapter presents a computational method, developed by the author of this dissertation, which scales gait parameters based on rodents' body silhouette length. The material, datasets, methods, results, and discussion of this chapter are closely based on the manuscript published in the journal eNeuro [Timo 19b], which was written substantially by the author of this dissertation in collaboration with the coauthors of the manuscript. Part of this chapter, i.e. the correlation between rodents' stride lengths and body-size (body silhouette length and body weight), was published in the proceeding of the Measuring Behavior Conference 2018 [Timo 18d].

The CatWalk data used in this chapter were collected primarily by the coauthors, Sandra Moceri and Anne-Christine Plank. The author of this dissertation subsequently developed a method through which the CatWalk data can be scaled. These CatWalk data were also involved in a study presented in Chapter 5, which was published in the proceeding of the Measuring Behavior Conference 2018 [Timo 18a] and in the Journal of Neuroscience Methods [Timo 19a]. The rat model appeared in this chapter were also involved in a longitudinal study presented in the AAT-AD/PD Conference 2018 [Moce 18], where the author of this dissertation is a coauthor of the presented poster.

The author of this dissertation implemented image processing approaches for calculating rodents' silhouette-length. Subsequently, a scaling method was developed and exemplified in rodents modeling PD and HD. The fundamentals relating to this chapter are given in Section 2.5.1 (PD), Section 2.5.2 (HD), and Section 2.6 (image processing).

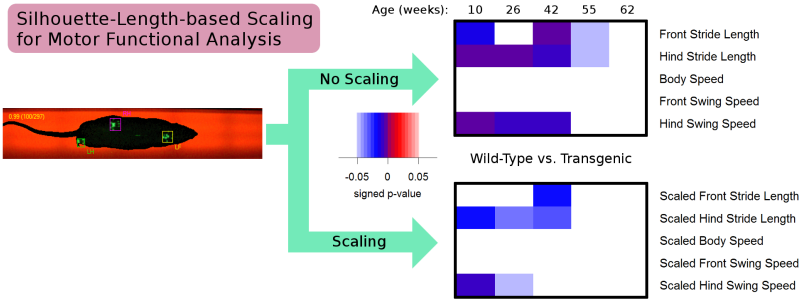

Figure 4.1: Graphical overview: Silhouette-length-based gait parameter scaling/normalization in rodents. Compared with the non-scaled gait parameters, the scaled gait parameters displayed less differences between the transgenic and wild-type animals. This image was reproduced from [Timo 19b] with permission.

4.1 Overview

Motor functional analysis of rodents often suffers from the fact that those models exhibit body size differences. The body size affects gait parameters, and therefore scaling by a body-size-related parameter is able to improve the reliability of gait analysis allowing normalization for individual differences.

Here, body-silhouette-length and -area computation methods based on image-processing techniques on data recorded by the Catwalk system are presented. The silhouette length computation method was applied to data recorded from wild-type rats and mice, where it is shown that both differ in silhouette length across age. This silhouette-length relates to their stride lengths and speed-related gait parameters (body speed and swing speed), but not their duration-related gait parameters (stand time, swing time, and step cycle).

The silhouette length and silhouette area, as well as the body weight and age, were used to scale several gait parameters of mice and rats taken from several age-points. These different scaling approaches were then compared by using correlation studies, which depict the better suitability of the silhouette-length-based scaling approach compared with the other approaches.

Additionally, the silhouette-length-based gait parameter scaling method is applied to an HD-relevant transgenic mouse model and a PD-relevant transgenic rat model. The differences of the silhouette-length and the gait parameters between the transgenic animals and their wild-type littermates are then reported in heat-maps. An overview of the use of this silhouette-length-based scaling on a longitudinal study involving a transgenic rat model is shown in Figure 4.1, where it is displayed that the wild-type and transgenic animals show less differences in scaled gait parameters compared to the non-scaled gait parameters. Overall, this emphasizes the need for silhouette-length-based intra-assay scaling as an improved standard approach in gait analysis.

4.2 Material and Methods

4.2.1 Animals and Data Acquisition

Two neurodegenerative rodent models were involved in this study, i.e.

- male BAC α-synuclein (α-Syn) transgenic rats, with overexpression of human α-Syn protein [Kohl 16] [Nube 13] [Wass 18] [Moce 18], as a PD-relevant transgenic (TG) model and their corresponding wild-type (WT) littermates.
- BAC of mutant Huntingtin (HTT) gene (BACHD) mice [Gray 08], backcrossed to C57BL/6N mice, as an HD-relevant transgenic (TG) model and their corresponding wild-type (WT) littermates.

The number of rodents involved in the study are given in Figure 4.2. Additionally, for the purpose of comparing the video-based measured silhouette length and the corresponding manually measured body length, 10 additional BAC α-Syn rats were used in this study.

The rodents were maintained under specific-pathogen-free (SPF) conditions with a 12h:12h light:dark cycle, where food and water were available *ad libitum*. All research and animal care procedures were performed in compliance with international animal welfare standards and approved by the district of Lower Franconia, Würzburg, Bavaria, Germany (RegUFr#55.2-2532-2-218 / 54-2532.1-49/12).

4.2.2 Data Acquisition

During the data collection process, the rodents were free to walk from one to the opposite end above the CatWalk walkway with no physical

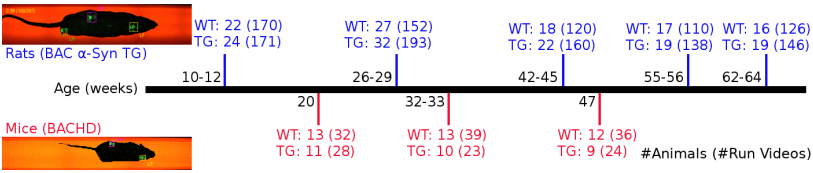

Figure 4.2: Scheme of the experimental design. The timeline displays the number of rodents and run videos analyzed within a longitudinal repeated experimental design spanning five age-points for rats and three age-points for mice. This image was reproduced from [Timo 19b] with permission.

restrictions or rewards. The walking speeds were 30.7 $\pm$ 6.7 cm/s for rats and 30.3 $\pm$ 7.7 cm/s for mice (mean $\pm$ SD). All runs were recorded in the dark at a minimum level of external disturbing factors. Data were acquired between their young and advanced age at five different age points for rats and three different age points for mice, over several acquisition days for each age point. The number of animals and runs for each age point are given in Figure 4.2. The minimum number of individual repeated measures across ages are 16 for rats and 9 for mice.

For the comparison of the different scaling methods, the body weight information of wild-type rodents was measured at $\pm$1 week from the CatWalk gait data acquisition. The number of rats with body weight information are 22, 27, 17, and 16 assessed at the age of 10–12, 26–29, 55–56, and 62–63 weeks, respectively. In addition, the number of mice with body weight information are 13, 13, and 12 assessed at the age of 21, 32, and 46 weeks, respectively.

Manual measurement of the body length for the additional 10 BAC α-Syn rats was performed on isoflurane anesthetized rats by a physically measurement of the nose-tip to tail-base length. All measurements were performed on the consecutive day after the recording of the CatWalk video files for in total 67 runs of these animals.

Based on human motor functional analysis studies [Hof 96], human's gait parameters related to length, duration, frequency, speed/velocity, moment, energy, power, angular velocity, angular acceleration, as well as the moment of inertia should be scaled by the human's leg length or height. Not all of these gait parameters are provided in the Catwalk rodent gait analysis system. Therefore, the following parameters p_g were chosen from the CatWalk-derived parameters for this study:

1. Stride lengths:
   a) Front-Paw Stride Length (cm)
   b) Hind-Paw Stride Length (cm)
2. Parameters relating to duration:
   a) Front-Paw Stand Time (s)
   b) Front-Paw Swing Time (s)
   c) Front-Paw Step Cycle (s)
   d) Hind-Paw Stand Time (s)
   e) Hind-Paw Swing Time (s)
   f) Hind-Paw Step Cycle (s)
3. Speed parameters:
   a) Body Speed (cm/s)
   b) Front-Paw Swing Speed (cm/s)
   c) Hind-Paw Swing Speed (cm/s)

Because of their similarity, the parameters obtained from the left and right paws were averaged, with the exception of the body speed, which was averaged over all four paws.

4.2.3 Silhouette-Length and Silhouette-Area Computation

The silhouette length and silhouette area were computed based on the unlabeled video and its corresponding background image. Representative images are shown in Figure 4.3a-d. The silhouette length computation begins at the first image frame where all paws are detected on the walkway and ends at the image frame where the first paw disappears from the recording area. These start and end points were obtained based on the information given by the CatWalk run data. This run data provides information on the labeled paw positions in each video-frame. Given f_{RH}, f_{LH}, f_{RF}, f_{LF} are vectors containing the frame number in ascending order of video-frames with detected right-hind-, left-hind-, right-front-, and left-front-paws, respectively, $f_{RH}(1)$ and $f_{LH}(1)$ refer to the first appearance of the corresponding paws as well as $f_{RF}(last)$

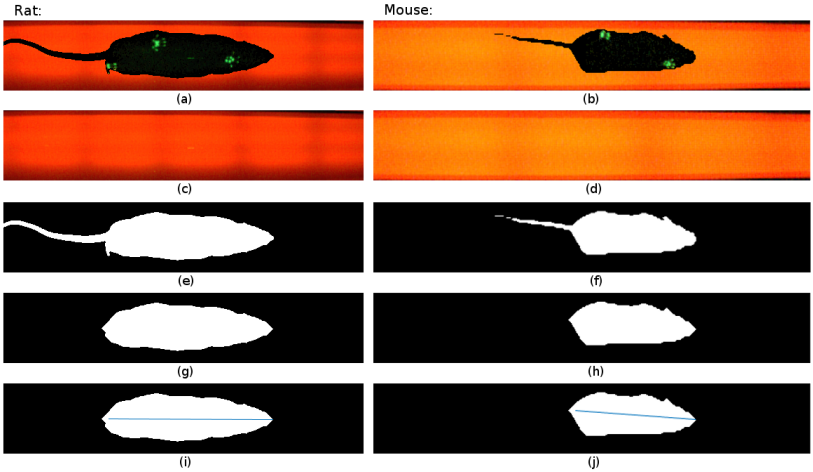

Figure 4.3: Scheme of image-flow analysis. (a)-(b) Images captured from the unlabeled CatWalk videos; (c)-(d) Background images; (e)-(f) Background subtraction results I_{FG}; (g)-(h) Binary largest objects I_R; (i)-(j) Silhouette length illustration: a rat with a silhouette length of 23.9 cm and a mouse with a silhouette length of 9 cm. This image was reproduced from [Timo 19b] with permission.

and $f_{LF}(last)$ refer to the last appearance of the corresponding paws. The start and end frames were therefore obtained as follows:

$$f_{start} = \max\{f_{RH}(1), f_{LH}(1)\} \tag{4.1}$$

$$f_{stop} = \min\{f_{RF}(\text{last}), f_{LF}(\text{last})\} \tag{4.2}$$

For each frame between the start (f_{start}) and end (f_{stop}) points, the methods of silhouette extraction and tail removal were based on image processing techniques (the fundamentals are described in Section 2.6), are depicted in Figure 4.4, and explained as follows:

1. Background subtraction: this technique was performed in order to extract the rodent's body (foreground I_{FG}) from the background I_{BG}. The foreground I_{FG} of each image frame I_O was extracted by choosing the image pixels, which have pixel value difference more than a threshold $T_h = 10$ in at least one of the

color layers ($I_{L,R}$, $I_{L,G}$ or $I_{L,B}$) compared with the background image I_{BG}. The value of the threshold T_h was chosen to avoid noise oversensitivity. Some examples of the resulting images after background subtraction are shown in Figure 4.3e and 4.3f.

$$I_L = \|I_O - I_{BG}\| > T_h \tag{4.3}$$

$$I_{FG} = I_{L,R} \text{ OR } I_{L,G} \text{ OR } I_{L,B} \tag{4.4}$$

2. Morphological image opening [Gonz 08]: removal of the tail part from the image I_{FG} was performed via morphological opening using a diamond structuring element I_{SE}. This diamond shape was chosen to best preserve the without tail body shape. The distance r_d from the structuring element origin to the points of the diamond was adjusted to the tail size of the rodents, which were $r_d = 9$ mm (corresponding to 9 pixels with image resolution, x_{mm} and y_{mm}, 1 mm/pixel) for rats and $r_d = 5$ mm (corresponding to 7 pixels with image resolution, x_{mm} and y_{mm}, 0.7 mm/pixel) for mice. The resulting image is denoted by I_T.

3. Hole Filling [Gonz 08]: this operation filled any hole in the object of the image I_T. The resulting image is denoted by I_H.

4. Retaining the largest object: the largest object in the image I_H is then the body silhouette. Examples from the resulting image I_R are shown in Figure 4.3g and 4.3h.

The length of the silhouette was then calculated by first detecting the positions of the leftmost and rightmost pixels of the body silhouette that is retained in I_R: (x_1, y_1), (x_2, y_2). Then, the Euclidean distance between these two points was calculated:

$$l_{sil} = \sqrt{\{(x_1 - x_2 - r_d) \times x_{mm}\}^2 + \{(y_1 - y_2) \times y_{mm}\}^2} \tag{4.5}$$

The image resolution, x_{mm} and y_{mm}, is indicated by the exported CatWalk data. The subtraction of r_d in Equation 4.5 was performed since in most cases half of the structure element area I_{SE} belongs to the tail area. Illustrations of the length are shown in Figure 4.3i – 4.3j, where the image resolutions for these specific videos are 1 mm/pixel for the rats and 0.7 mm/pixel for the mice.

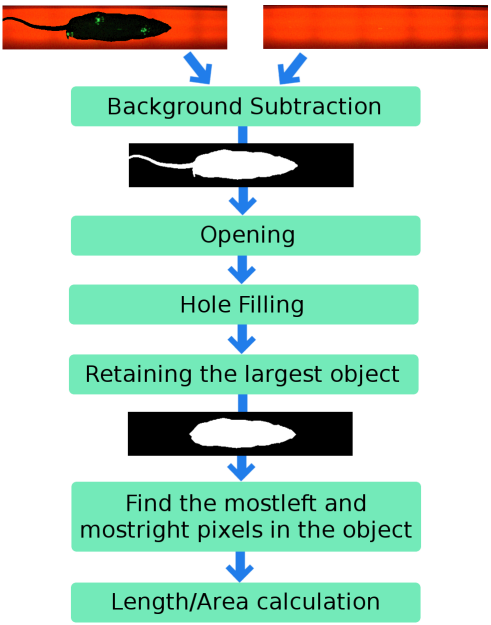

Figure 4.4: The block diagram of the silhouette extraction, tail removal, and silhouette parameters. This image was reproduced from [Timo 19b] with permission.

The area of the silhouette was calculated by counting the number of pixels in the silhouette that is retained in I_R, followed by multiplying it with the image resolution, x_{mm} and y_{mm}. Noteworthy, the silhouette area can be calculated from the silhouette (blob) including the tail, I_{FG}, or excluding the tail, I_R, according to the application needs. After the silhouette length and area were calculated for each frame, the silhouette length and area of the whole run video were finally determined by the maximum length and area values from all the calculated lengths and areas of the video frames. By doing this, a value of silhouette length and a value of silhouette area were specified for every run video.

For each animal, where body weight information w was available, a body-weight silhouette-length index I_{WSL} can also be calculated. As

silhouette length is related to body length, this index resembles the body-mass index [Nove 07].

$$I_{WSL} = \frac{w}{l_{sil}^2} \tag{4.6}$$

4.2.4 Gait Parameter Scaling Methods

The gait parameters p_g were scaled by dividing their values by the silhouette length as indicated in Equation 4.7. This yields the silhouette-length-scaled gait parameters $\hat{p}_g$.

$$\hat{p}_g = \frac{p_g}{l_{sil}} \tag{4.7}$$

For the parameters related to speed, an additional scaling method was also tested. This additional scaling method was adapted from human gait analysis [Hof 96] [Zijl 96]. It is given in Equation 4.8, where g is the acceleration of gravity (= 9.81 m/s^2 on earth). This yields other variation of the silhouette-length-scaled gait parameters $\hat{p}_a$.

$$\hat{p}_a = \frac{p_g}{\sqrt{\frac{g}{l_{sil}}}} \tag{4.8}$$

For the comparison of the different scaling methods, the parameters p_g were also scaled based on silhouette area a_{sil}, body weight w, and age a. The scaling method was performed in the same way as Equation 4.7, by simply replacing silhouette length with silhouette area, body weight, or age. This yields the scaled gait parameters $\hat{p}_g$.

$$\hat{p}_g = \frac{p_g}{a_{sil}} \tag{4.9}$$

$$\hat{p}_g = \frac{p_g}{w} \tag{4.10}$$

$$\hat{p}_g = \frac{p_g}{a} \tag{4.11}$$

4.2.5 Analysis

Silhouette length values were computed for all runs or videos of each animal in accordance with the description in Section 4.2.3. The silhouette length, gait parameters, as well as the scaled gait parameters computed from all run videos were subsequently averaged for each animal. The gait parameter scaling was performed for all the parameters listed in Section 4.2.2. Scaled parameters were calculated for each run and averaged for each animal. The sample Pearson correlation coefficient [Pear 95] r, coefficient of determination r^2 [Nage 91], and the p-value between the silhouette length and gait parameters were computed. The r and p-values before and after scaling were compared. For all gait parameters showing higher p-values (and lower correlation coefficient, r) on their scaled version, a repeated analysis of variance (ANOVA) [Arms 00] [Fish 21] [Mull 09] was performed based on animals which were tested consecutively at all age points. This repeated measures ANOVA was also performed on the silhouette parameters (length and area) to investigate age-related effects.

The computed silhouette length values were compared with the physically measured body length values. This comparison was performed in the small cohort of rats by observing the correlation and the difference between the silhouette length and body length.

The comparison study between the scaling approaches based on silhouette length, silhouette area, body weight, and age was done in accordance with the scaling method in Equation 4.7, by simply replacing the silhouette length with the silhouette area, body weight, or age as shown in Equation 4.9–4.11. Then, both the r and p-values of the correlation between the gait parameters and silhouette-area/weight/age were evaluated. The body-weight-based scaling was done by utilizing the animals with corresponding body weight information.

The genotype-related differences were investigated via the mixed ANOVA (occasionally also called the two-way repeated measures ANOVA) and multiple comparison tests by Bonferroni correction in Matlab R2015a (8.5.0). The p-values with lower bound adjustment were used to detect the presence of significant differences and reported by using heat-maps, as described in Chapter 5 [Timo 18a].

4.3 Results

4.3.1 Silhouette Length and Silhouette-Length-based Gait Parameter Scaling in Wild-Type Rodents

The scatter plots of several gait parameters as a function of silhouette length for rats and mice are depicted in Figure 4.5. The color in the scatter plots denotes the age of the animals, with young rodents showing smaller silhouette lengths compared to older ones. The correlation coefficients between the gait parameters and silhouette length are given in Table 4.1. No significant correlation with the silhouette length was shown for the gait parameters relating to duration. Significant correlations ($p < 0.05$) were observed between the stride length and silhouette length in rats as well as mice. Significant correlations in rats were also shown between the parameters related to speed and silhouette length, where only moderate correlation was shown in mice.

The scaling approaches were performed for all listed parameters in Section 4.2.2. For the stride lengths and the parameters relating to speed, the scaled parameters showed lower correlation coefficients, r (and higher p-values) compared with non-scaled parameters. The speed parameters, which were scaled using Equation 4.7, displayed lower correlation coefficients compared with the parameters scaled using Equation 4.8.

The relation between silhouette length and measured body length calculated from the small cohort of rats is depicted in Figure 4.6b. The body length was measured from the nose-tip to tail-base as shown in Figure 4.6a. Significant correlation between the silhouette length and body length was shown ($p < 0.01$). The mean and SD of the absolute difference between the silhouette length and body length $|\Delta|$ were 0.49 $\pm$ 0.39 cm (mean $\pm$ SD).

The age analysis of the wild-type animals using repeated ANOVA is given in Table 4.2. This analysis was conducted for the gait parameters that show significant correlations in Table 4.1 and for the silhouette parameters. In rats, significant effects of age were shown for silhouette parameters and gait parameters, excluding the body speed. In mice, a significant effect of age was shown for silhouette parameters and swing speeds. All of the scaled gait parameters listed in Table 4.2 showed higher p–values compared with their corresponding non-scaled parameters.

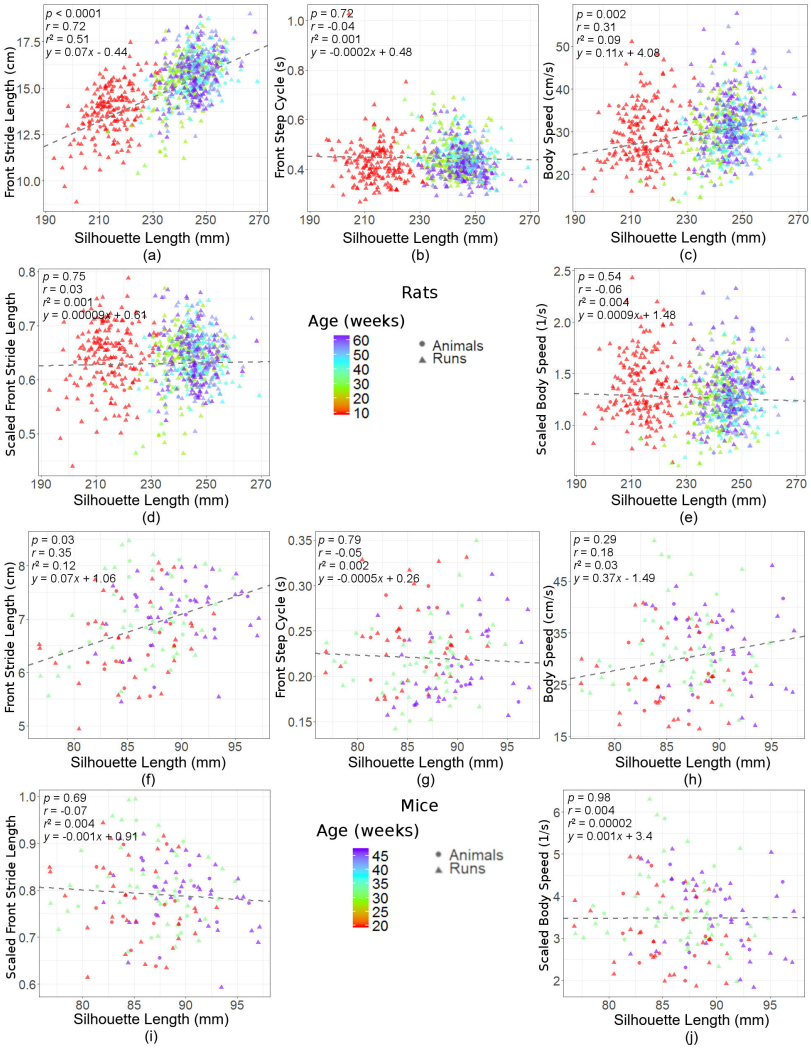

Figure 4.5: Scatter plots for the correlation between the non-scaled and scaled gait parameters with the silhouette length of the wild-type rodents. The number of animals and the number of run videos are given in Figure 4.2. The animal data are the averaging results from their respective CatWalk run data. The sample Pearson correlation coefficient r, coefficient of determination r^2, p-value p, and the regression line were calculated from the animal data. This image was reproduced from [Timo 19b] with permission.

Table 4.1: The sample Pearson correlation coefficients (r) and p-values of the silhouette length and CatWalk gait parameters. The scaled parameters which show higher p-values compared with their non-scaled versions are highlighted.

Gait Parameters	**Rats**				**Mice**			
	non-scaled		scaled		non-scaled		scaled	
	r	p	r	p	r	p	r	p
Stride Lengths:								
Front-Paw Stride Length	0.72	<0.0001	0.03	0.75	0.35	0.03	-0.07	0.69
Hind-Paw Stride Length	0.72	<0.0001	0.02	0.81	0.35	0.03	-0.05	0.76
Parameters relating to duration:								
Front-Paw Stand Time	0.02	0.81	-0.34	<0.001	<0.01	0.97	-0.18	0.28
Front-Paw Swing Time	-0.20	0.05	-0.58	<0.0001	-0.12	0.48	-0.38	0.02
Front-Paw Step Cycle	-0.04	0.72	-0.45	<0.0001	-0.05	0.79	-0.27	0.10
Hind-Paw Stand Time	-0.05	0.59	-0.36	<0.001	<0.01	0.97	-0.16	0.33
Hind-Paw Swing Time	0.07	0.51	-0.57	<0.0001	-0.10	0.56	-0.42	<0.01
Hind-Paw Step Cycle	-0.04	0.70	-0.46	<0.0001	-0.03	0.85	-0.26	0.12
Speed Parameters:								
Body Speed	0.31	<0.01	(i)-0.06 (ii)0.13	(i) 0.54 (ii) 0.20	0.18	0.29	(i)<0.01 (ii) 0.09	(i) 0.98 (ii)0.58

Continued on next page

Table 4.1 – continued from previous page

Gait Parameters	**Rats**				**Mice**			
	non-scaled		scaled		non-scaled		scaled	
	r	p	r	p	r	p	r	p
Front-Paw Swing Speed	0.49	<0.0001	(i)0.09 (ii)0.31	(i) 0.40 (ii)<0.01	0.22	0.18	(i) 0.02 (ii) 0.12	(i) 0.90 (ii)0.46
Hind-Paw Swing Speed	0.51	<0.0001	(i)-0.08 (ii)0.25	(i) 0.43 (ii) 0.01	0.30	0.07	(i) 0.04 (ii) 0.18	(i) 0.80 (ii)0.29

(i) Scaling method: $\hat{p}_g = p_g / l_{sil}$
(ii) Scaling method: $\hat{p}_g = p_g / \sqrt{g / l_{sil}}$

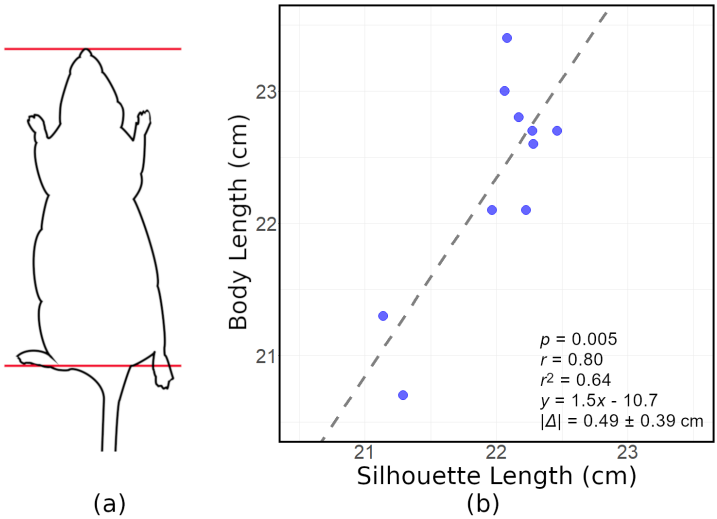

Figure 4.6: (a) The diagram of the body length (nose-tip to tail-base) measurement. (b) The scatter plot for the correlation between the body length and silhouette length of the small cohort of rats. This image was reproduced from [Timo 19b] with permission.

Table 4.2: The effect of age on the silhouette and gait parameters: repeated measures ANOVA (p-values)

Parameters	Rats		Mice	
	non-scaled	scaled*	non-scaled	scaled*
Stride Lengths:				
Front-Paw Stride Length	<0.001	0.69	0.13	0.20
Hind-Paw Stride Length	<0.0001	0.64	0.12	0.18
Speed Parameters:				
Body Speed	0.11	0.24	0.11	0.15
Front-Paw Swing Speed	0.03	0.35	0.04	0.07
Hind-Paw Swing Speed	0.04	0.24	0.04	0.06
Silhouette Parameters:				
Sil. Length	<0.0001		<0.01	
Sil. Area without Tail	<0.0001		<0.001	
Sil. Area with Tail	<0.0001		<0.001	

*Scaling method: $\hat{p}_g = p_g / l_{sil}$
Sil.: Silhouette

4.3.2 Silhouette-Area-, Body-Weight- and Age-based Gait Parameter Scaling in Wild-Type Rodents

As rodents grow, it is reasonable to expect that the body silhouette length, body silhouette area, and the body weight also increase. Correspondingly, high correlation between them, as well as age, were found (Table 4.3). The relationship between the body weight and silhouette length for rats and mice are also reported as scatter plots shown in Figure 4.7.

The correlation coefficients between the silhouette area (a_{sil}) and the CatWalk gait parameters are given in Table 4.4. The parameter scaling in Table 4.4 was performed based on the silhouette area. In rats, significant correlations ($p < 0.05$) with the silhouette area were shown for the gait parameters relating to stride length or speed, but not for the parameters relating to duration. All silhouette-area-based scaled gait parameters showed significant correlations with the silhouette area. In mice, most of the silhouette-area-scaled gait parameters gave lower p-values

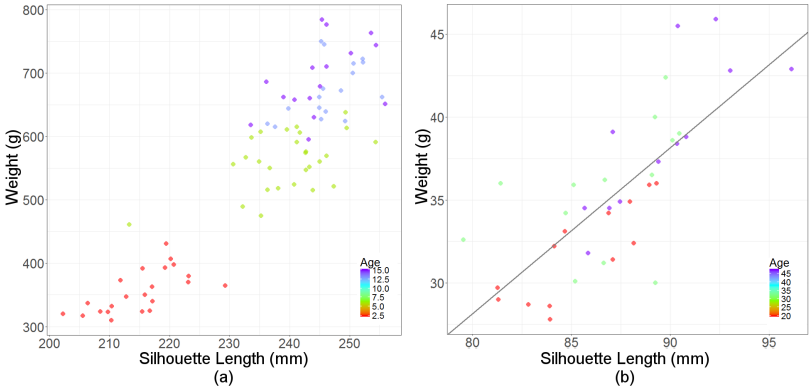

Figure 4.7: The scatter plots for correlation between the body weight with the silhouette length of the wild-type animals: (a) rats (b) mice. This image was reproduced from [Timo 19b] with permission.

compared with the non-scaled parameters. Some exceptions were revealed for the stand time parameters, where both of the non-scaled and scaled gait parameters showed no significant correlation with the silhouette area.

The correlation coefficients between the body weight (w) and the CatWalk gait parameters are given in Table 4.5. The scaling method in Table 4.5 was based on the body weight. Both in rats and mice, significant correlations were found between the body weight and body-weight-scaled gait parameters.

The correlation coefficients and p-values between age and the CatWalk gait parameters are given in Table 4.6. Significant correlations were found between the age and age-scaled gait parameters.

Table 4.3: The correlation between the silhouette length, silhouette area (with tail), body weight, and age: the p-values, sample Pearson correlation coefficients (r), and coefficient of determination (r^2)

	Silhouette Length		**Silhouette Area**		**Body Weight**		**Age**	
	rats	mice	rats	mice	rats	mice	rats	mice
Silhouette Length	$p = 0$ $r = 1$ $r^2 = 1$		–	–	–	–	–	–
Silhouette Area	$p < 0.0001$ $r = 0.93$ $r^2 = 0.87$	$p < 0.0001$ $r = 0.84$ $r^2 = 0.70$	$p = 0$ $r = 1$ $r^2 = 1$		–	–	–	–
Body Weight	$p < 0.0001$ $r = 0.90$ $r^2 = 0.81$	$p < 0.0001$ $r = 0.75$ $r^2 = 0.57$	$p < 0.0001$ $r = 0.98$ $r^2 = 0.96$	$p < 0.0001$ $r = 0.89$ $r^2 = 0.79$	$p = 0$ $r = 1$ $r^2 = 1$		–	–
Age	$p < 0.0001$ $r = 0.74$ $r^2 = 0.55$	$p < 0.01$ $r = 0.49$ $r^2 = 0.24$	$p < 0.0001$ $r = 0.88$ $r^2 = 0.77$	$p < 0.01$ $r = 0.50$ $r^2 = 0.25$	$p < 0.0001$ $r = 0.90$ $r^2 = 0.81$	p<0.0001 $r = 0.61$ $r^2 = 0.37$	$p = 0$ $r = 1$ $r^2 = 1$	

Table 4.4: The sample Pearson correlation coefficients (r) and p-values of the silhouette area (a_{sil}) and CatWalk gait parameters (scaling method: $\hat{p}_g = p_g / a_{sil}$). The scaled parameters which show higher p-values compared with their non-scaled versions are highlighted.

Gait Parameters	Rats				Mice			
	non-scaled		scaled		non-scaled		scaled	
	r	p	r	p	r	p	r	p
Stride Lengths:								
Front-Paw Stride Length	0.59	<0.0001	-0.80	<0.0001	0.31	0.06	-0.37	0.02
Hind-Paw Stride Length	0.59	<0.0001	-0.81	<0.0001	0.31	0.06	-0.35	0.03
Parameters relating to duration:								
Front-Paw Stand Time	0.06	0.57	-0.66	<0.0001	0.19	0.25	-0.14	0.41
Front-Paw Swing Time	-0.14	0.17	-0.80	<0.0001	<0.001	0.99	-0.45	<0.01
Front-Paw Step Cycle	0.01	0.88	-0.74	<0.0001	0.11	0.49	-0.29	0.08
Hind-Paw Stand Time	<0.01	0.94	-0.62	<0.0001	0.15	0.37	-0.13	0.43
Hind-Paw Swing Time	0.02	0.81	-0.88	<0.0001	0.06	0.71	-0.49	<0.01
Hind-Paw Step Cycle	<0.01	0.99	-0.76	<0.0001	0.13	0.44	-0.27	0.10
Speed Parameters:								
Body Speed	0.27	0.02	-0.55	<0.0001	0.03	0.85	-0.24	0.15
Front-Paw Swing Speed	0.38	<0.0001	-0.54	<0.0001	0.13	0.45	-0.20	0.22
Hind-Paw Swing Speed	0.44	<0.0001	-0.72	<0.0001	0.15	0.36	-0.26	0.11

Table 4.5: The sample Pearson correlation coefficients (r) and p-values of the body-weight (w) and CatWalk gait parameters (scaling method: $\hat{p}_g = p_g/w$)

Gait Parameters	**Rats**				**Mice**			
	non-scaled		scaled		non-scaled		scaled	
	r	p	r	p	r	p	r	p
Stride Lengths:								
Front-Paw Stride Length	0.54	<0.0001	-0.95	<0.0001	0.36	0.03	-0.69	<0.0001
Hind-Paw Stride Length	0.54	<0.0001	-0.95	<0.0001	0.37	0.02	-0.67	<0.0001
Parameters relating to duration:								
Front-Paw Stand Time	0.04	0.70	-0.87	<0.0001	0.06	0.73	-0.47	<0.01
Front-Paw Swing Time	-0.11	0.35	-0.92	<0.0001	-0.01	0.95	-0.67	<0.0001
Front-Paw Step Cycle	0.01	0.92	-0.90	<0.0001	0.02	0.88	-0.58	<0.001
Hind-Paw Stand Time	0.01	0.91	-0.84	<0.0001	0.04	0.81	-0.42	<0.01
Hind-Paw Swing Time	-0.01	0.90	-0.95	<0.0001	0.02	0.88	-0.74	<0.0001
Hind-Paw Step Cycle	<0.01	0.98	-0.91	<0.0001	0.03	0.86	-0.57	<0.001
Speed Parameters:								
Body Speed	0.20	0.08	-0.81	<0.0001	0.10	0.54	-0.39	0.02
Front-Paw Swing Speed	0.32	<0.01	-0.83	<0.0001	0.14	0.39	-0.43	<0.01
Hind-Paw Swing Speed	0.41	<0.001	-0.90	<0.0001	0.21	0.21	-0.50	<0.01

Table 4.6: The sample Pearson correlation coefficients (r) and p-values of the age (a) and CatWalk gait parameters (scaling method: $\hat{p}_g = p_g/a$)

Gait Parameters	Rats				Mice			
	non-scaled		scaled		non-scaled		scaled	
	r	p	r	p	r	p	r	p
Stride Lengths:								
Front-Paw Stride Length	0.55	<0.0001	-0.89	<0.0001	0.33	0.046	-0.93	<0.0001
Hind-Paw Stride Length	0.57	<0.0001	-0.89	<0.0001	0.33	0.044	-0.93	<0.0001
Parameters relating to duration:								
Front-Paw Stand Time	-0.05	0.62	-0.88	<0.0001	-0.24	0.14	-0.84	<0.0001
Front-Paw Swing Time	-0.14	0.16	-0.88	<0.0001	-0.33	0.04	-0.91	<0.0001
Front-Paw Step Cycle	-0.07	0.50	-0.89	<0.0001	-0.31	0.06	-0.89	<0.0001
Hind-Paw Stand Time	-0.08	0.44	-0.88	<0.0001	-0.21	0.20	-0.81	<0.0001
Hind-Paw Swing Time	0.08	0.41	-0.89	<0.0001	-0.35	0.03	-0.93	<0.0001
Hind-Paw Step Cycle	-0.08	0.45	-0.89	<0.0001	-0.29	0.07	-0.88	<0.0001
Speed Parameters:								
Body Speed	0.28	<0.01	-0.85	<0.0001	0.32	0.047	-0.74	<0.0001
Front-Paw Swing Speed	0.36	<0.001	-0.86	<0.0001	0.38	0.02	-0.81	<0.0001
Hind-Paw Swing Speed	0.37	<0.001	-0.88	<0.0001	0.44	<0.01	-0.87	<0.0001

4.3.3 Genotype-related Differences in Silhouette Length-based Scaled Gait Parameters in Rodent Models of Neurodegenerative Diseases

As a proof of concept for this scaling approach, genotype-related differences for BAC α-Syn transgenic and BACHD animals as well as the effect of age and their interaction were examined and shown in Table 4.7. The mean and SEM of the silhouette lengths and several gait parameters are depicted in Figure 4.8. In addition, the p-values of the multiple comparison tests are depicted by heat-maps [Timo 18a] in Figure 4.9. The color blue in the heat maps represents lower parameter value of the transgenic rodents compared to their corresponding wild-type rodents, whereas the color red in the heat maps represents higher parameter value of the transgenic rodents compared to their corresponding wild-type rodents.

As shown in Table 4.7, all non-scaled gait parameters (stride lengths and speed-related gait parameters) and silhouette parameters showed significant effects of age ($p < 0.05$). In rats, the silhouette-length-based scaled gait parameters did not show any significant effect of age. Whereas in mice, reduced age effects were observed in the scaled gait parameters. No interaction between age and genotype in any gait parameter was observed. The genotype effects shown by the scaled gait parameters were lower compared with their corresponding non-scaled gait parameters. Besides the silhouette parameters, significant differences between genotypes were observed in the scaled front stride length, scaled hind stride length, and scaled hind swing speed.

Significant genotype-related differences in the scaled front stride length were observed in 42-week-old rats. The scaled hind stride length showed significant differences between genotypes in the young rats until they were 42 weeks old. Furthermore, the scaled hind swing speed showed significant genotype-related differences for 10-week-old and 26-week-old rats. In mice, significant difference of the scaled gait parameters was only shown in the scaled hind swing speed at 32 weeks of age.

Table 4.7: The effect of age, the genotype-age interaction, and the effect of genotype on the silhouette parameters and gait parameters: mixed ANOVA and multiple comparison tests by Bonferroni correction (p-values with lower bound adjustment)

Parameters	Rats			Mice		
	Age	Interaction	Genotype	Age	Interaction	Genotype
Stride Lengths:						
Front-Paw Stride Length (cm)	<0.0001	0.46	0.01	0.005	0.25	0.03
Hind-Paw Stride Length (cm)	<0.0001	0.54	<0.01	0.004	0.24	0.03
Scaled Front-Paw Stride Length*	0.60	0.58	0.046	0.013	0.17	0.90
Scaled Hind-Paw Stride Length*	0.53	0.67	0.02	0.01	0.17	0.94
Speed Parameters:						
Body Speed (cm/s)	0.01	0.55	0.26	0.004	0.25	0.03
Front-Paw Swing Speed (cm/s)	<0.001	0.43	0.35	0.004	0.43	<0.01
Hind-Paw Swing Speed (cm/s)	<0.001	0.59	<0.01	0.003	0.47	<0.001
Scaled Body Speed (1/s)*	0.16	0.51	0.47	0.007	0.25	0.18
Scaled Front-Paw Swing Speed (1/s)*	0.13	0.41	0.65	0.007	0.45	0.11
Scaled Hind-Paw Swing Speed (1/s)*	0.11	0.60	0.01	0.007	0.47	<0.01
Body Parameters:						
Silhouette Length (mm)	<0.0001	0.23	0.03	0.012	0.10	<0.0001
Silhouette Area without Tail (mm^2)	<0.0001	0.15	<0.001	<0.001	0.26	<0.0001

Continued on next page

Table 4.7 – continued from previous page

Parameters	**Rats**			**Mice**		
	Age	Interaction	Genotype	Age	Interaction	Genotype
Silhouette Area with Tail (mm^2)	<0.0001	0.26	<0.01	<0.01	0.14	<0.0001
Body Weight (g)	<0.0001	0.20	0.03	<0.0001	0.35	<0.0001
Weight Sil.-Length Index (g/cm^2)	<0.0001	0.17	0.29	<0.001	0.55	<0.001

*scaled based on the silhouette length (scaling method: $\hat{p}_g = p_g / l_{sil}$)
Sil.: Silhouette

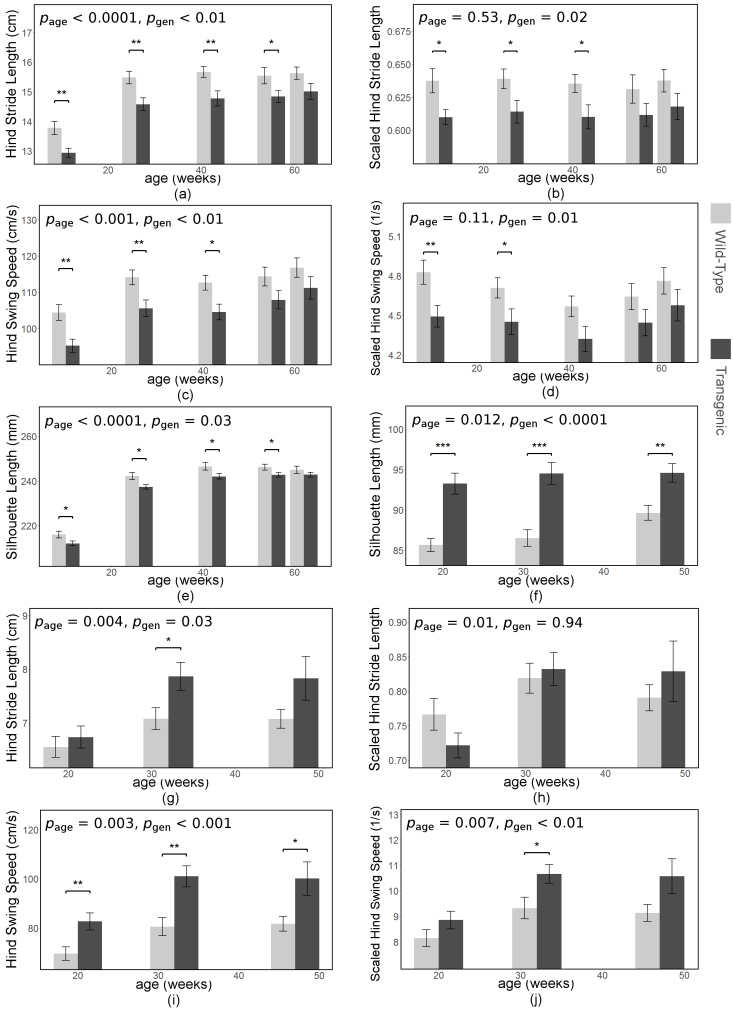

Figure 4.8: Genotype-related differences in the unscaled and scaled hind stride length, the unscaled and scaled hind swing speed, as well as the silhouette lengths along the age: (a)–(e) α-Syn rats, (f)–(j) BACHD mice. Each data point represents mean $\pm$ SEM. The p-values were calculated from the multiple comparison tests by Bonferroni correction: *$p < 0.05$, **$p < 0.01$, ***$p < 0.001$. This image was reproduced from [Timo19b] with permission.

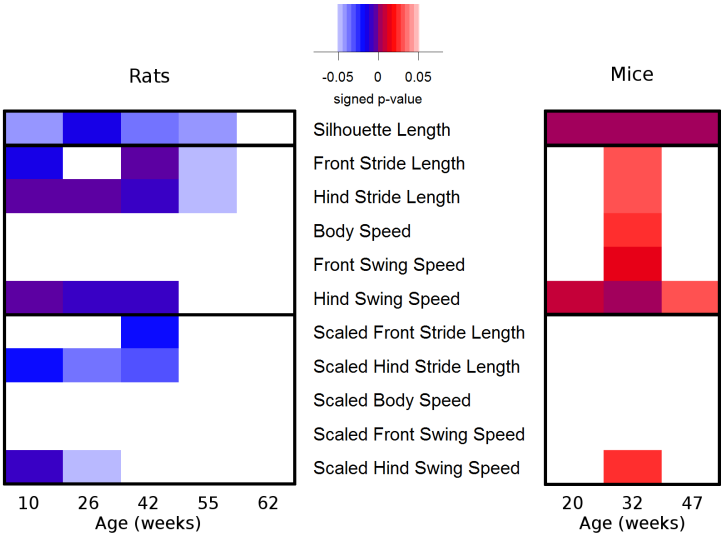

Figure 4.9: Differences between the wild-type and transgenic animal models observed by their unscaled and scaled gait parameters individually by the multiple comparison tests and reported in heat maps. The use of heat maps is described in Chapter 5. This image was reproduced from [Timo 19b] with permission.

4.4 Discussion

As in humans, several rodent gait parameters are correlated with their body size. This study presents a body silhouette length computation method for rodents based on the recorded CatWalk videos. A correlational study was performed to investigate the relationship between the computed silhouette length and several CatWalk gait parameters. Accordingly, a silhouette-length-based scaling method on stride lengths and speed-related gait parameters is presented, which is able to reduce their correlation with the body size. This silhouette-length-based scaling method cannot be directly replaced by silhouette-area-, body-weight-, or age-based scaling methods. As proof of concept, two rodent models of neurodegenerative disorders were investigated based on their scaled gait parameters. The results show smaller genotype-related

differences compared with the non-scaled gait parameters due to the genotype-related body size difference.

The computed silhouette parameters, stride lengths, and speed-related gait parameters were found to change with advancing age. Significant effects of age on the silhouette length and silhouette area, both with and without tail area, were observed in both rats and mice. Correlations between the body silhouette length and stride lengths were significant for both rats and mice. The silhouette-length-based scaling/normalization reduced this correlation. The effect of age on the stride lengths was significant in rats, but not in mice. However, in both species, the scaled parameters gave higher p-values in the repeated measures ANOVA compared with the non-scaled parameters. The effect of age on the silhouette and gait parameters, as well as the effect of scaling on the gait parameters, was more visible in rats compared with mice since the rats' age range was broader than the mice'. There was no significant effect of age on the scaled stride lengths. This suggests that the scaled stride lengths were better tools for a longitudinal study compared with the non-scaled stride lengths.

Significant correlations between the silhouette length and speed (or velocity) parameters were observed in rats, but not in mice. Nevertheless, in rats and mice, both scaling methods the gave scaled speed parameters higher p-values compared with the non-scaled version. The first scaling method, in accordance with Equation 4.7, was more suitable for the scaling of the speed-related gait parameters. As speed is proportional to length and is inversely proportional to time, along with considering the non-significant correlation of the duration-related gait parameter to the silhouette length, it is reasonable that the scaling method of the length-related gait parameters was also suitable for the speed-related gait parameters. The walking speed is a gait parameter that is affected by many factors [Batk14]. Therefore, it is reasonable that the correlations of silhouette length to the speed-related gait parameters were not as strong as to the length-related gait parameters.

No significant correlation was found in the gait parameters relating to duration. The silhouette length scaling on the duration-related gait parameters produces scaled gait parameters, which are more correlated with the silhouette length as compared to the non-scaled version. This suggests that no silhouette-length-based scaling is needed for the duration-related gait parameters.

In human gait analysis, gait parameters are typically evaluated by presenting data in the form of non-dimensional numbers [Hof 96] [Zijl 96]. The scaling method suggested for human's gait is not relevant to the practice in rodents. The silhouette-length-based scaling is recommended in rodent's stride lengths and speed parameters, but not in the duration-related gait parameters since the duration-related gait parameters in rodents do not significantly correlate with the silhouette length.

The measured body lengths of anesthetized rats showed significant correlation with the silhouette lengths. The measured body lengths were similar to the silhouette lengths with an absolute difference of 0.49 ± 0.39 cm (mean $\pm$ SD). Most of the measured body lengths were higher compared to the silhouette length. This difference occurred most likely because of the different body curve while lying on the plain surface versus walking.

Since the silhouette length, silhouette area, and body weight are all related to the body size, they were all correlated to each other. However, replacing the silhouette length with the silhouette area for scaling is not recommended since the silhouette-area-based-scaled stride lengths and speed parameters were significantly correlated with the silhouette area. The same can also be noticed in the body-weight-based gait parameter scaling. The duration-related gait parameters did not display significant correlation with the silhouette length or body weight.

Even though body size changes with advancing age of the animal, the silhouette-length-based gait parameter scaling should not be replaced by the age-based parameter scaling. This due to the fact that the age-based scaled gait parameters have significant correlations with age, that in all likelihood happened because the animals grow faster in their early life [Lui 11]. Therefore, the age and body size do not have a linear correlation.

Because rodents do not grow linearly [Lui 11], the wild-type rats in this study grew over the months and reached the greatest silhouette length by the age of 10 months. Afterward, their silhouette length decreased slightly, possibly due to postural changes (hunched-back). The wild-type mice showed an increase in silhouette length with advancing age.

In the animal models with genotype-related body size differences, gait parameters can be directly and indirectly (through body size) related to the genotype. In the analysis of the genotype-related differences as described in Subsection 4.3.3, the effect of age was observed on all body parameters and the non-scaled gait parameters. The geno-

type and age of the animals had lower effects on the scaled gait parameters compared to the non-scaled gait parameters for rodent models with genotype-related body size differences. No significant genotype-age interaction was observed. Considering the results shown in Figure 4.8 and Figure 4.9, significant genotype-driven silhouette-length differences were observed. Additionally, less genotype-related differences were detected by the scaled gait parameters. Gait analysis in preclinical studies is mostly aimed at the development of new treatment strategies for specific diseases. Observing the effect of diseases and treatments on gait is often more important than observing the effect of body size on gait. Therefore, gait parameters used in the analysis of gait should have minimal relation with body size. Accordingly, the results in Figure 4.8 and Figure 4.9 depict an analytic value improvement, as the scaling/normalizing approach reduces the effect of the body size. Therefore, it can be confirmed that the gait-parameter scaling is recommended in a study involving rodent models with significant genotype-related silhouette length differences.

Significant genotype-related differences in the α-Syn rat model were detected on the scaled stride lengths, scaled hind-paw swing speed, silhouette length, silhouette area, and body weight. By observing the silhouette length, area, and body weight, the α-Syn rats were smaller as compared to their wild-type littermates. Genotype-related differences in the α-Syn rat model were more pronounced in young animals than in the geriatric animals.

In the BACHD mouse model, a genotype-related difference was observed on the scaled hind-paw swing speed, specifically in 32-weeks-old mice. The body parameters show that the BACHD mice were bigger as compared to their wild-type mates.

In summary, a method of calculating body silhouette length is described in this chapter. This silhouette length information is beneficial for the scaling of stride lengths and speed-related gait parameters. This gait parameter scaling is suggested to be an important tool for augmenting the reliability of motor function analyses in rodent models, especially in studies involving young animals or rodent models with genotype-related silhouette length differences, as well as in longitudinal studies.

5 Systematic Initial Gait Data Analysis by Heat Mapping

This chapter presents a systematic initial data analysis (IDA) for CatWalk gait parameters. The material, methods, results, and discussion of this chapter are closely based on the manuscript published in the Journal of Neuroscience Methods [Timo 19a] and the proceeding of the Measuring Behavior Conference 2018 [Timo 18a], which were written by the author of this dissertation jointly with the coauthors of the manuscripts.

The CatWalk data used in this chapter were collected primarily by the coauthors: Fabio Canneva, Georgia Minakaki, Sandra Moceri, and Anne-Christine Plank. The author of this dissertation subsequently uses the data to exemplify a systematic IDA. The PD-relevant mouse models were involved in a study published in the journal Behavioral Brain Research [Mina 19], where the author of this dissertation is a coauthor of the publication. Additionally, these PD-relevant mouse models were used in a study reported in Chapter 3, which was published in the Journal of Neuroscience Methods [Timo 18b] and the journal Data in Brief [Timo 18c]. The PD-relevant rat model and HD-relevant mouse model were involved in the study described in Chapter 4 and published in the eNeuro journal [Timo 19b]. The data from the PD-relevant rat model were also involved in a study presented in the AAT-AD/PD Conference 2018 [Moce 18], where the author of this dissertation is a coauthor of the presented poster.

The fundamentals relating to this chapter are given in Section 2.5.1 (PD), Section 2.5.2 (HD), and Section 2.4 (CatWalk gait parameters).

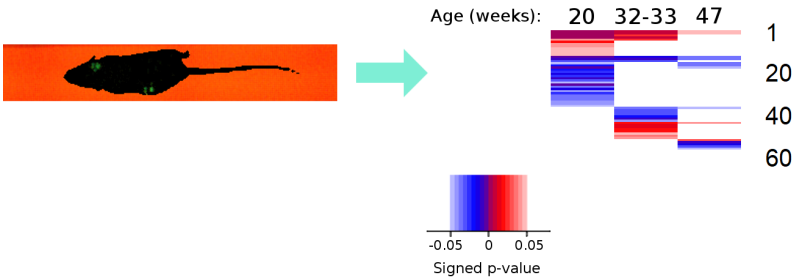

Figure 5.1: Graphical overview: Systematic initial gait data analysis by heat mapping. This image was reproduced from [Timo 19a] with permission.

5.1 Overview

The CatWalk system computes an extensive number of gait parameters that needs to be analyzed by experts and needs to be reported accordingly. The number of parameters often raises complication, which leads to a premature parameter selection and an elimination of reporting negative results.

An initial data analysis (IDA), including a visualization of all gait parameters, will enable researchers to initially explore gait parameters. In addition, the visualization will prevent the practice of p-hacking (manipulatively selecting reported parameters [Head 15]) and help researchers to report negative results, which are also essential to be reported [Earp 17] [Kann 14a] [Mast 16]. This chapter presents a systematic approach of IDA using a clustered heat map for data visualization. This IDA is exemplified in an intervention study of PD-relevant transgenic mouse models, as well as longitudinal studies of a PD-relevant transgenic rat model and a HD-relevant transgenic mouse model. An overview of the use of the approach in a longitudinal study involving a transgenic mouse model is depicted in Figure 5.1. The resulting heat map from an IDA is able to report clustered gait parameter differences in one single chart, which is advantageous especially for exploring gait parameters.

5.2 Material and Methods

5.2.1 Animals and Data Acquisition

In this work, the assessment of gait was performed on several neurodegenerative-disease-relevant rodent models. For all disease models, each rodent can explore and walk freely above the walkway without any rewards. Typically, an experimental session lasts for 5-15 minutes. No dedicated session for habituation to the CatWalk apparatus was performed.

All of the animals were kept under standard laboratory conditions under specific-pathogen-free (SPF) conditions throughout all testing phases, on a 12h:12h light:dark cycle, as well as food and water were available *ad libitum*. All procedures were approved by the local animal welfare and ethics committee of Bavaria, Germany (RegUFr#55.2-2532-2-218, RegUFr#55.2-2532.1-37/13, and RegUFr#54-2532.1-49/ 12) and performed according to the international guidelines.

Alpha-synuclein (α-Syn) transgenic mice with relevance for PD

Adult male mice (C57BL/6N background) which were wild type ("WT"), or transgenic knock-outs for the murine endogenous α-Syn ("KO Syn" or "KO") ([Abel 00]), or exclusively expressing human α-Syn ("huWT Syn" or "HU") using a bacterial artificial chromosome (BAC) ([Kohl 16] [Nube 13] [Wass 18]) were included at 7–8 months of age. The mouse models are described in detail in [Mina 19].

The CatWalk data acquisition was performed before (T0; baseline) and after 4-weeks of treadmill intervention (T1; final) (paradigm described in [Mina 19]). Approximately 10-15 videos (trials) were recorded per animal at each time point with the aim of collecting three compliant runs, defined as runs during which the mouse completed an unforced and uninterrupted walk along the full length of the walkway. The mean and SD of collected compliant runs were 2.9 ± 0.7 for each animal at each time point. Specifically, at T0, CatWalk data from 12 WT (34 runs), 14 KO (34 runs), and 8 HU (23 runs) were collected. Following T0 recording, mice were randomly assigned to treated and non-treated cohorts. The number of animals involved in data acquisition at T1 are 8 non-treated WT ("WN", 24 runs), 4 treated WT ("WE", 16 runs), 6 non-treated KO Syn ("KN", 17 runs), 7 treated KO Syn ("KE", 25 runs), 4 non-treated huWT Syn ("HN", 11 runs), and 5 treated huWT Syn ("HE",

16 runs). The different number of animals at T0 and T1 are attributed to the reluctance of performing a voluntary traversal along the CatWalk walkway at either time point.

Human alpha-synuclein (α-Syn) overexpressing rats with relevance to PD

A total of 27 wild-type rats ("WT rats") and 32 BAC-(α-Syn) transgenic rats ("TG rats") ([Kohl 16] [Nube 13] [Moce 18]) were included in this study. The CatWalk data were collected at five different age points, i.e. 10–12 weeks, 26–29 weeks, 42–45 weeks, 55–56 weeks, and 62–64 weeks. At these age points, the number of animals (and the number of runs) included in the data acquisition are respectively 22 rats (170 runs), 27 rats (152 runs), 18 rats (120 runs), 17 rats (110 runs), 16 rats (126 runs) for WT and 24 rats (171 runs), 32 rats (193 runs), 22 rats (160 runs), 19 rats (138 runs), 19 rats (146 runs) for TG. A mean and SD of 6.9 ± 2.7 compliant runs were recorded for each animal at each time point.

Transgenic mice expressing mutant human huntingtin modeling HD

A longitudinal study in an HD-relevant mouse model was included here. BACHD transgenic mice ("BACHD-TG") ([Gray 08]), backcrossed on the C57BL/6N background, as well as their wild-type littermates ("BACHD-WT") were included. The CatWalk data were collected at three age-points, i.e. 20 weeks (11 BACHD-TG mice and 13 BACHD-WT mice), 32-33 weeks (10 BACHD-TG mice and 13 BACHD-WT mice), and 47 weeks (9 BACHD-TG mice and 12 BACHD-WT mice). A mean and SD of 2.7 ± 0.7 compliant runs were recorded for each animal at each time point.

5.2.2 Initial Data Analysis (IDA) of CatWalk Gait Parameters

The data cleaning in IDA [Demp 71] [Broe 05] is performed to identify inconsistencies and faulty data. The data cleaning of CatWalk gait data is carried out by first selecting the videos with a compliant run from all recording videos. This compliance examination is performed automatically by the CatWalk software according to the duration of the run and the variation of the speed [Hame 01] [Nold 12]. An experienced

observer should subsequently clean the data by discarding runs containing non-walking behaviors, such as rearing, sniffing, exploring, grooming, sitting, stopping, and turning. Since the intention of performing CatWalk test is to analyze gait, the data cleaning should only be used to exclude non-walking or interrupted-walking recording and should not be used to manipulate the end results nor to practice p-hacking [Head 15] [Raj 17].

The data screening in IDA aims to describe data. Data screening of CatWalk data is performed by analyzing differences between cohorts. Here, several computations of the differences can be applied, including:

1. Significance tests, e.g. p-value of a t-test, which compares two group means [Mcdo 08].

2. Between-group effect size, which computes the magnitude of between-group difference [Ferg 09] [Sull 12], e.g. f-value, which depends on the between-group and within-group variability [Arms 00] [Fish 21], D-value, which is the mean difference and SD ratio [Fest 02], estimated arithmetic means, which depends on the groups' means and SD [Timo 13a] [Timo 13b].

The computation of the difference can be chosen based on the following formal data analysis. A signed computation of difference might be applied when the change direction information is essential. To decide if a parameter is different, a threshold T_h needs to be determined.

The data reporting of CatWalk parameters is visualized by heat maps. Since the CatWalk gait test often aims to study the differences between cohorts, the colors in the heat maps should also represent these differences. To make the heat map understandable, clustering the rows and columns is important [Gehl 12]. In generating the heat map, all gait parameters showing no between-cohort differences or negative results can be clustered together.

5.2.3 Study Designs

The CatWalk gait acquisitions were conducted in three study designs as described below, involving mice and rats transgenic for α-Syn (models with relevance for PD) as well as mice transgenic for mutant HTT (model with relevance for HD). All animals were repeatedly recruited to the CatWalk gait analysis. The acquired CatWalk data runs were averaged for each animal at each time point.

α-Syn transgenic mice with relevance for PD

The gait parameter were screened individually based on the signed f-values (with a threshold $T_h = 4.5$) of (a) the parameters for characterizing the disorder observed at To (KO vs. WT and HU vs. WT) (b) the parameters which at T1 had improved by the four-week treadmill treatment compared to To (KE vs. KO and HE vs. HU) (c) the parameters which improved naturally without any treatment (KN vs KO and HN vs. HU) (d) the parameters at T1 which specifically improved due to the treadmill treatment (KE vs. KN and HE vs. HN).

Human α-Syn overexpressing rats with relevance to PD

From the longitudinal CatWalk data, the first appearance of gait parameter differences between wild-type and transgenic rats was screened. The data screening was conducted based on the p-value of a t-test (with a threshold of $T_h = 0.05$).

Transgenic mice expressing mutant human huntingtin modeling HD

Similar to the longitudinal study in PD-relevant rats, the first appearance of gait parameter differences between the BACHD-TG and their wild-type littermates (BACHD-WT) was screened. The screening was based on the p-value of a t-test (with a threshold of $T_h = 0.05$).

5.3 Results and Discussion: Study Designs

The columns in heat maps were organized according to the study designs described in Section 5.2.3. The shaded color red in the heat map depicts an increase, whereas the shaded color blue depicts a decrease. Additionally, the color white represents a non-observable difference. The heat maps are accompanied by tables of the essential parameter names.

5.3.1 Heat map illustrating differences in PD-relevant mice

To avoid complication, the gait parameters in the heat map were first categorized. Then, the gait parameters were arranged according to the research main interests, such as group-wise comparisons. Here, the gait

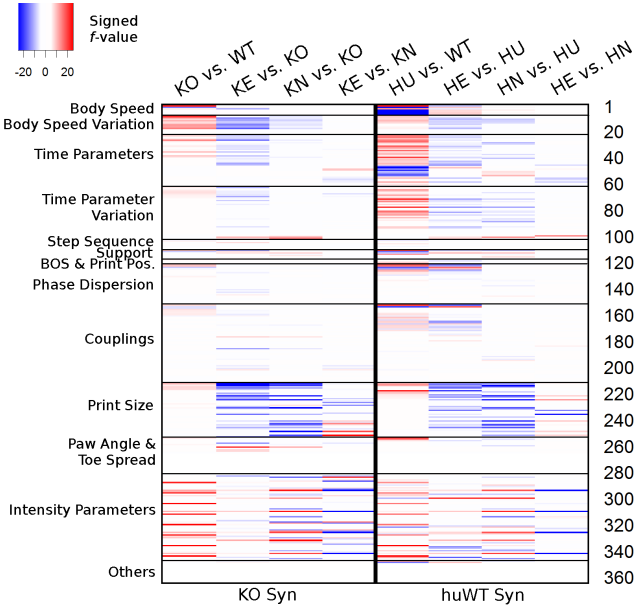

Figure 5.2: The heat map for reporting CatWalk gait parameters from a before-after intervention study in the PD-relevant mouse models. The gait parameters were clustered and arranged according to the researcher's main interests. This image was reproduced from [Timo 19a] with permission.

parameters relating to speed, time, regularity (or step sequence), number of paws supporting the body, base of support, and print positions (total of 121 parameters) were placed on the top of the heat map. All gait parameters, which show no differences between cohorts, were clustered together. Some gait parameters depend on the intensity and software setting, i.e. print size, paw angle, toe spread, intensity parameter, and others. Therefore, they serve as additional information and were placed in the lower part of the heat map. The resulting heat map is shown in Figure 5.2. The parameter names that showed differences between the cohorts at T0, and showed differences between the treated and non-treated group at T1 for both models, are listed in Table 5.1.

Table 5.1: The gait parameters, which indicate differences between the cohorts at To (38 gait parameters in the KO cohort and 84 gait parameters in the HU cohort) and show differences between the treated and non-treated cohort at T1 in the PD-relevant mouse models.

No.	Parameter names	Signed f-value
	KO cohort (KE vs. KN)	
34	LH Step Cycle (s) Mean	-4.66
68	RH Swing (s) SD	-6.95
70	LF Swing (s) SD	-4.55
	HU cohort (HE vs. HN)	
46	LH Stand Index Mean	-7.49
49	RH Swing Speed (cm/s) Mean	4.75
56	LF Swing (s) Mean	-8.64
59	RF Single Stance (s) Mean	-8.83

Discussion: PD-relevant mice

In this before-after intervention study, the aim is to screen the influential gait parameters in the study. As shown in Figure 5.2, from the first 121 parameters, a total of 38 parameters showed differences (f-value > 4.5) at To for KO Syn (KO vs. WT, the first column in the heat map in Figure 5.2). For the huWT Syn at To (HU vs. WT, the fifth column in the heat map in Figure 5.2), a total of 84 parameters showed differences (f-value > 4.5). From the 38 gait parameters that showed significant differences at To in the KO cohort, there were more parameters that improved in the treated group (the second column in the heat map on Figure 5.2) compared to the non-treated group (the third column in the heat map on Figure 5.2). The same can be concluded from the 84 gait parameters in the HU cohort by comparing the sixth and the seventh columns in the heat map in Figure 5.2.

In the KO Syn cohort, not all body speed parameters depicted differences at To. Specifically, several body speed parameters calculated from the body silhouette showed group differences, whereas the body speed parameters calculated from the labeled paw positions did not show any significant between-group differences. Overall, this suggests that there was no significant difference in body speed in the selected range of walkway of the KO Syn cohort. In the huWT Syn cohort, all body speed parameters depicted significant group differences at To. This suggests

that a significant difference in body speed was observed in the huWT Syn cohort. Especially in time-related parameters, the differences at To were more obvious in the huWT Syn than the KO Syn cohort.

The treadmill treatment in the intervention study affected a few gait parameters as listed in Table 5.1, i.e. three gait parameters in the KO Syn cohort (related to step cycle time and swing variation: the fourth column in the heat map on Figure 5.2) and four parameters in the huWT Syn cohort (related to stand index, swing speed, swing time, and single stand time: the eighth column in the heat map on Figure 5.2). Note that there were several gait parameters showing significant differences between the treated and non-treated cohort, but did not show any significant difference between cohorts at To.

5.3.2 Heat map illustrating differences in a rat model with relevance to PD

In this study, the gait parameters which are directly connected to intensity, were placed in the lower part of the heat map due to their dependency on the software setting. The other 288 gait parameters were placed according to their first appearance of significant differences between the transgenic rats and their wild-type mates ($p < 0.05$). The resulting heat map is shown in Figure 5.3, and part of the corresponding parameters is listed in Table 5.2.

Discussion: PD-relevant rats

Some gait parameter differences appeared in the early stage of the disease. At 10–12 weeks of age, 28 gait parameters showed significant differences. These include parameters related to stride length, swing speed, swing time, body speed variation, hind body of support (BOS), and print size. According to the number of gait parameters that showed significant differences, the differences between the old transgenic rats and old wild-type rats were not as obvious as at their young age.

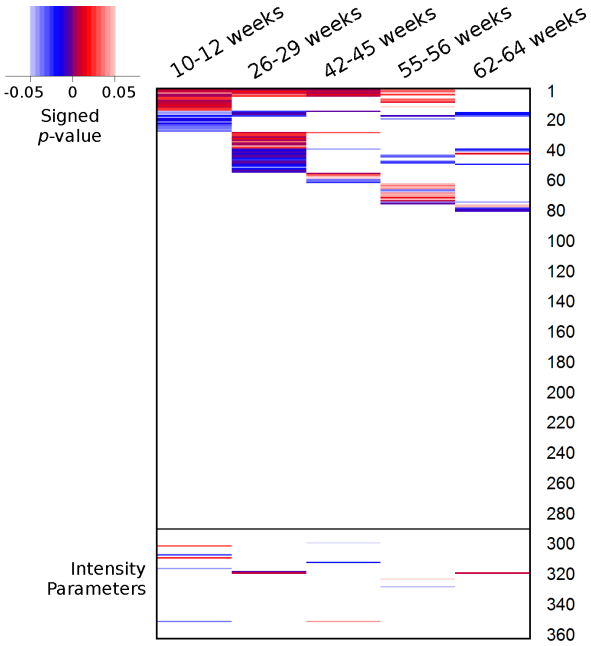

Figure 5.3: The heat map for reporting CatWalk gait parameters from the longitudinal study in PD-relevant rat model. The gait parameters were arranged according to the appearance of differences. This image was reproduced from [Timo 19a] with permission.

Table 5.2: Part of gait parameters together with their first appearance of differences between the PD-relevant transgenic rats and their wild-type littermates

No.	Parameter names	First appearance (weeks)	Starting p-value
⋮	⋮	⋮	⋮
10	RH Body Speed Variation (%) SD	10–12	< 0.01
11	LH Body Speed (cm/s) SD	10–12	0.01
12	BOS Hind Paws Mean (cm)	10–12	< 0.01
13	RH Stand Index SD	10–12	0.03
14	LF Print Length (cm) Mean	10–12	0.03
⋮	⋮	⋮	⋮
38	Step Sequence CA (%)	26–29	0.02
39	RF Initial Dual Stance (s) Mean	26–29	< 0.01
40	LF Terminal Dual Stance (s) Mean	26–29	0.01
41	RF Duty Cycle (%) Mean	26–29	< 0.01
⋮	⋮	⋮	⋮
55	RF Stride Length (cm) Mean	42–45	< 0.01
56	RF Swing Speed (cm/s) Mean	42–45	0.02
⋮	⋮	⋮	⋮
72	LF Swing (s) Mean	55–56	0.04
73	RF Swing (s) SD	55–56	< 0.01
⋮	⋮	⋮	⋮
79	Couplings RF $\rightarrow$ LF Mean	62–64	< 0.01
80	Couplings RF $\rightarrow$ LF CCStat Mean	62–64	< 0.01

5.3.3 Heat map illustrating differences in an HD-relevant mouse model

Similar to the PD-relevant rat model, the intensity-related gait parameters in the HD-relevant mouse model were placed at the lower part of the heat map. The other 288 gait parameters were ordered according to their appearance of significant differences ($p < 0.05$). The resulting heat

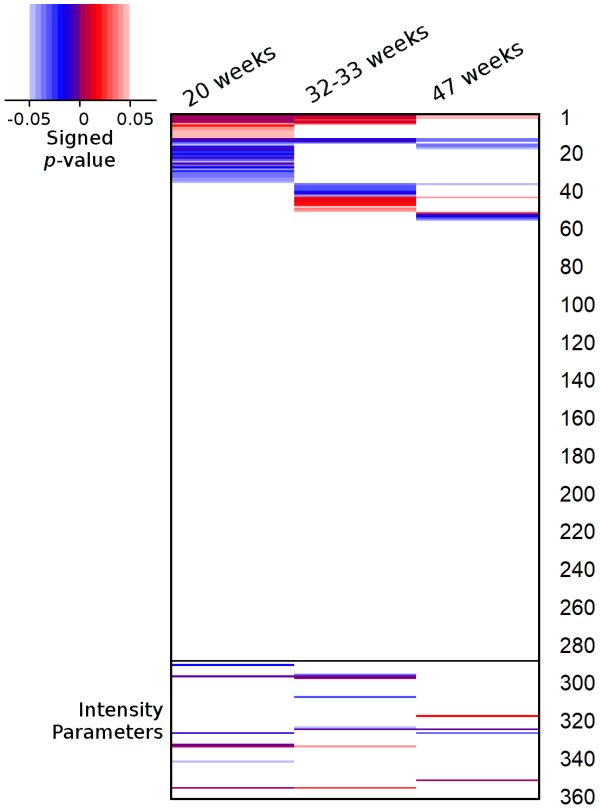

Figure 5.4: The heat map for reporting CatWalk gait parameter differences from the longitudinal study in the HD-relevant mouse model. The gait parameters were ordered according to their appearance of significant differences. This image was reproduced from [Timo 19a] with permission.

map is depicted in Figure 5.4, and part of the corresponding parameter names are listed in Table 5.3.

Table 5.3: Part of the gait parameters, which show differences between the BACHD-TG mice and BACHD-WT mice, as well as their first appearance

No.	Parameter names	First appearance (weeks)	Starting p-value
1	Left Hind Single Stance (s) Mean	20	< 0.01
2	Right Hind Single Stance (s) Mean	20	< 0.01
3	Right Hind Swing (s) Mean	20	< 0.01
4	Left Hind Swing (s) Mean	20	< 0.01
5	Left Front Swing (s) Mean	20	0.04
⋮	⋮	⋮	⋮
37	Left Front Swing Speed (cm/s) Mean	32 - 33	0.03
38	Left Front Swing Speed (cm/s) SD	32 - 33	0.03
39	Right Front Swing Speed (cm/s) Mean	32 - 33	0.02
40	Right Hind Swing Speed (cm/s) SD	32 - 33	0.03
41	Left Front Stand Index SD	32 - 33	0.02
⋮	⋮	⋮	⋮
52	Step Sequence Regularity Index (%)	47	0.03
53	Left Hind Duty Cycle (%) SD	47	< 0.01
54	Left Front Body Speed (cm/s) SD	47	0.01
55	Right Hind Body Speed (cm/s) SD	47	0.03
56	Left Front Print Width (cm) Mean	47	0.047

Discussion: HD-relevant mice

In this longitudinal study in the HD-relevant mouse model, 36 gait parameters showed significant differences between the BACHD-TG and BACHD-WT. There were more gait parameters showing significant differences in early age (20 weeks) than at older age points (47 weeks). The gait parameters that significantly differ between the HD mouse model and their wild-type littermates were, among others, related to single stance time, swing time, swing speed, swing speed variation, hind body of support (BOS), and footprint size.

5.4 Discussion: Heat Maps in IDA

This study introduces the utilization of clustered heat maps in a systematic initial gait parameter analysis. The approach is exemplified to an intervention study in a PD-relevant mouse models, a longitudinal study of a PD-relevant rat model and a longitudinal study of a HD-relevant mouse model. It is demonstrated that this systematic IDA is applicable to avoid purely hypothesis-driven parameter selection. Hence, presenting gait parameters in heat maps is advantageous for data mining, since the comprehensive visualization of all parameters in a visually clear way is innovative and includes presentation of negative findings as a part of an initial screening process.

By using a heat map, CatWalk parameter differences, together with the negative results, can be reported in a single chart with many rows and columns. For ease of understanding, heat maps need to be designed according to the aim of the studies and the gait parameter similarities.

Applying heat-mapping to the intervention study in the PD-relevant mice demonstrated that categorization and arrangement according to group-wise comparisons represent a meaningful approach: the IDA requirements for ease of understanding and comprehensive display of all data were met.

In both of the longitudinal studies of the PD-relevant rat model and the HD-relevant mouse model, the aim is to observe the occurrence of gait parameter differences between the disease models compared to their wild-type littermates. Therefore, it is apparent to cluster gait parameters according to the time-points of the appearance of differences. Thus, the heat-mapping approach presented here appears to be excellently suitable for depicting time-dependent differences.

The reporting of negative results in the heat map was performed by grouping the gait parameters, which show no difference between cohorts. Therefore, heat-mapping approach in IDA is able to display both positive and negative results.

In previous studies involving α-Syn transgenic mice, a limited number of CatWalk gait parameters were reported (Table 5.4). In the initial analysis of the treadmill intervention study in α-Syn transgenic mice, 38 gait parameters in the KO cohort and 84 gait parameters in the HU cohort showed differences compared with the wild-type mice at To.

In previous studies involving PD-relevant (6-OHDA) rats, various CatWalk gait parameters were reported (Table 5.4), mostly include stride

length, stand time, swing time, and swing speed. In the initial observation of the CatWalk parameter generated from the PD-relevant (α-Syn overexpression) rats used in this chapter, 80 gait parameters showed differences in at least one age-point.

Previously, in a study involving HD-relevant mice [Abad 13], several CatWalk gait parameters were evaluated (5.4). From these gait parameters, significant differences between the transgenic and wild-type animals (aged between 9–10 months) were observed in CA-, CB-, and AB- sequences, forelimb BOS, hindlimb max contact at (%), phase dispersion for RH-LH and LF-LH phases. In the initial observation of the CatWalk parameters recorded from the HD-relevant mice used in this chapter, differences between cohorts (aged 47 weeks) appeared in different set of gait parameters, including LH-, RH-, and RF- single stance (s) mean, LH-, RH-, and LF- swing speed (cm/s) mean, LH swing speed SD, LH duty cycle SD, body speed SD, LF print area mean, as well as regularity index (RI).

Preceding studies reported a variety of CatWalk gait parameter sets. This variety is reasonable since gait characteristic differences might occur due to animal gender [Datt 16], strain/breed [Koop 07], or disease model. This variety also suggests the importance of being cautious in using a parameter set from other studies and emphasizes the importance of observing all CatWalk gait parameters. The use of heat-mapping in IDA is, therefore, valuable to report both the possible gait differences and the negative results.

The described IDA is designed to initially explore gait parameters, it should be followed by a formal statistical analysis. Though it only served as initial analysis, it is useful for avoiding premature parameter selection. Moreover, the heat map reporting helps researchers to depict the gait parameter differences and the negative results in a single chart.

Table 5.4: The reported CatWalk gait parameters in previous studies of α-Syn transgenic mice, PD-relevant (6-OHDA) rats, and HD-relevant mice

Rodent model	**Study**	**Reported CatWalk Gait Parameters**
α-Syn transgenic mice	[Casa 14]	number of steps, stand time.
	[Rote 14]	*stride length*, mean intensity, print length.
	[Tate 16]	*stride length*, average speed, swing speed, print area, print position, regularity index (RI).
	[Frah 18]	*front paw stride length*
PD-relevant (6-OHDA) rats	[Vlam 07]	*stride length, stand time, swing time, swing speed,* run duration, base of support (BOS), cruciate sequences (CA, CB), alternate sequences (AA, AB), rotary sequences (RA, RB), regularity index (RI), maximum contact area, maximum paw intensity, phase dispersion/lag (girdle, diagonal, ipsilateral), phase dispersion/lag variability.
	[Vand 10]	*stand time, swing time, swing speed,* stand index, intensity.
	[West 12]	*stride length, stand time, swing time, swing speed,* step cycle, duty cycle, base of support (BOS), print position, regularity index (RI).
	[Zhou 15]	*stride length, stand time, swing speed,* step cycle, duty cycle, base of support (BOS), max contact area, mean intensity, terminal dual stance.

Continued on next page

Table 5.4 – continued from previous page

Rodent model	Study	Reported CatWalk Gait Parameters
	[Boix 18]	*stride length, stand time, swing time,* average speed, step cycle, cadence, stand index, print position, print length, print area, initial dual stance, phase dispersion.
HD-relevant mice	[Abad 13]	*stride length, stand time, swing time,* walking speed, cruciate sequence (CA, CB), alternate sequence (AB), regularity index (RI), base of support (BOS), print position, max contact at (%), intensity, phase dispersion.

The most reported parameters, shown in the listed previous studies, are written in italics

6 Gait Parameter Combination in Spinal Cord Injured Rats

This chapter presents a computational method of combining CatWalk gait parameters for predicting gait alteration in rat spinal cord injury (SCI) models. The material, method, datasets, and results of this chapter are closely based on a manuscript prepared for submission to a journal [Timo 19c], written by the author of this dissertation in collaboration with the coauthors of the manuscript. The CatWalk data collection was primarily done by the coauthors: Radhika Puttagunta, Beatrice Sandner, Daniel Garcia-Ovejero, Lara Bieler, and Veronica Estrada. Subsequently, the author of this dissertation developed the computational method for combining parameters and applied it to the collected CatWalk data.

The method of linear discriminant analysis (LDA) was used to form this gait parameter combination relating to spinal cord injury (SCI). The fundamentals relating to this chapter are given in Section 2.5.3 (SCI), Section 2.3.1 (BBB) and Section 2.8 (LDA).

6.1 Overview

A long term assessment of gait is essential for evaluating and developing new treatments in SCI. The most common approach used for evaluating gait in middle/lower rat thoracic SCI models is based on a non-parametric 21-point scale, named the BBB Locomotor Rating Scale [Bass 95]. As described in Section 2.3.1, this BBB scoring system depends on how often specific gait characteristics occurred [Bhim 17]. A paw-position-based gait analysis system for rodents, namely the CatWalk system [Hame 01] [Hame 06], generates gait parameters objectively. Therefore, this system is valuable in providing further gait information for the studies of SCI.

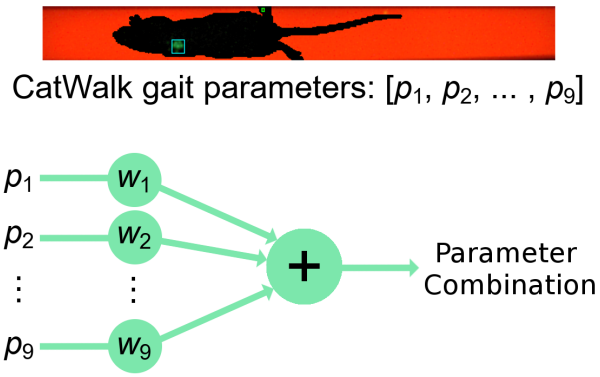

Figure 6.1: Graphical overview: Gait parameter combination in spinal cord injured rats.

Although the CatWalk system generates hundreds of gait parameters, many pre-clinical studies in SCI (as listed in Table 1.1 and explained in Section 1.2.5) observed the CatWalk parameter individually. No single CatWalk gait parameter is enough in representing the whole gait movement of an injured animal. Similarly, the need of observing several gait characteristics is also reflected in the BBB scale, which is determined by observing several gait characteristics simultaneously.

For this reason, this chapter describes a method to combine CatWalk gait parameters into a single gait score, which aims to represent the gait recovery progression of rat SCI models and give an alternative to the non-parametric (observation-based) locomotion score for rat thoracic SCI models (BBB score). The most distinctive CatWalk parameters between the uninjured and the severely spinal cord injured animals were chosen to be included for developing the parameter combination. Subsequently, the parameter linear combination was developed based on LDA and was applied to assess several SCI studies: three thoracic contusion studies, a thoracic dorsal hemisection study, and a cervical dorsal column lesion study. An overview of the use of this parameter combination method is depicted in Figure 6.1. Using this parameter combination, gait recovery progression can be represented in the thoracic contusion lesions and the thoracic dorsal hemisection lesions, including in cases when differences were not detectable by the BBB score.

6.2 Material and Methods

6.2.1 Animals and Data Acquisition

The gait recovery progression assessment method was applied to three rat Th8/9 contusion SCI studies, one rat Th8/9 dorsal hemisection transection SCI study, and one rat C_4 bilateral dorsal column transection SCI study, which are summarized in Table 6.1. The studies were conducted using two different versions of CatWalk system, which have different camera frame rate (50 fps for CatWalk 7.1 and 100 fps for CatWalk XT).

Study 1

This study was performed as published previously [Sand18] and briefly explained here. Experiments were carried out in accordance with the European Union Directive (2010/63/EU) and institutional guidelines.

Th8/9 contusion SCI model: Adult female Fischer rats weighing 160–180 g were used. For all surgical procedures, rats were anesthetized. The rats received a spinal cord contusion injury at mid-thoracic level Th9 using the Infinite Horizon (IH) Impactor SCI device with an impact force of 150 kDyn without any additional dwell time as previously described [Sche03]. Rats received either intraperitoneal (i.p.) injections of Epothilone (Epo) D (Abcam, Cambridge, UK, cat. no.: ab143616) (1.5 mg/kg body-weight) dissolved in dimethylsulfoxid (DMSO) (3 mg/ml) and diluted 1:1 with pre-warmed saline immediately prior to injections (Epo D group) or vehicle (1:1 mixture of DMSO and saline, control group) on day 1 and 15 post-injury (at an equivalent time of the day as the SCI surgery was performed) by a blinded unbiased experimenter. A rat in each cohort was excluded due to inadequate force impact curves upon spinal cord contusion. Based on the variability in spinal cord displacement, rats were divided into 2 groups dependent upon the injury-induced spinal displacement prior to Epo D administration and any functional testing. A threshold at a displacement value of 1000 μm allowing for equal distribution of rats into 2 cohorts (moderate; Mod.< 1000 μm and moderate severe; Mod-Sev. > 1000 μm) was chosen. These rats were then assigned to receive either vehicle or Epo D treatment.

Table 6.1: The rat SCI studies included in this chapter

	Study 1	**Study 2**	**Study 3**	**Study 4**	**Study 5**
Rats	Female Fischer	Male Wistar	Female Fischer	Female Wistar	Female Fischer
SCI	Th8/9 contusion Mod & Mod.Sev. (150 kDyn)	Th8 contusion Mod.Sev. (200 kDyn)	Th8 contusion Mod.Sev. (200 kDyn)	Th8/9 dorsal hemisection Scouten wire-knife transection	C_4 bilateral dorsal column tungsen wire-knife transection
Time-points of gait assessment	UI, 60 dpi	UI, 7, 30, 60 dpi	UI, 15, 22, 29, 36, 43 dpi	UI, 30, 60 dpi	UI, 30 dpi
CatWalk	CatWalk XT	CatWalk 7.1.	CatWalk XT	CatWalk XT	CatWalk XT
Groups	UI Veh.Mod. Veh.Mod.-Sev. Exp.Mod. Exp.Mod.-Sev.	UI SCI + Veh. SCI + Prog	Young SCI Old SCI	UI SCI Veh.	UI SCI Veh.

UI: Uninjured; dpi: days post injury; Mod.: Moderate; Sev.: Severe; Veh.: Vehicle; Exp.: Experiment

Behavioral testing: At 60 dpi, CatWalk test and BBB test [Bass 95] were performed. The number of rats and CatWalk runs collected in this study are listed in Table 6.2. The BBB scores ranged from 10 to 19.

Table 6.2: Number of Rats and CatWalk Runs of Study 1

Study 1		# Rats	# Runs
Uninjured		6	27
Vehicle*	Mod.	8	31
	Mod–Sev.	7	30
Experiment*	Mod.	8	38
	Mod–Sev.	9	39

*60 days post injury (dpi)
Mod.: Moderate; Sev.: Severe

Study 2

This study was performed as published previously [Garc 14] and briefly explained here. Experiments were carried out in accordance with the European Union Directive (2010/63/EU) and institutional guidelines.

Th8 contusion SCI model: Young adult male Wistar rats (300–335 g, 12 weeks of age) were submitted to a moderate-severe contusive SCI. Briefly, rats were anesthetized for all surgical procedures. After removing Th8 vertebra, spinal cord contusion was performed with the IH Impactor SCI device, applying a force of 200 kDyn. Injured rats received daily subcutaneous injections of either natural progesterone (16 mg/kg/day, Sigma Aldrich, SCI+Prog group) or vehicle (Castor oil, Sigma Aldrich, SCI+Vehicle group) for 60 days until the sacrifice day. First injection was given to awake rats 1 hour after injury.

Behavioral testing: Gait data were collected using CatWalk 7.1. The BBB scores [Bass 95] were additionally scored for coordination with the CatWalk regularity index [Koop 05]. The rats with BBB-score of 9 or higher were further examined weekly by CatWalk system. The number of rats and CatWalk runs included in the data collection are listed in Table 6.3.

Table 6.3: Number of Rats and CatWalk Runs of Study 2

Study 2		# Rats	# Runs
Uninjured		5	18
SCI + Vehicle	7 dpi	4	16
	30 dpi	7	32
	60 dpi	7	32
Experiment (SCI + Prog)	7 dpi	7	27
	30 dpi	8	29
	60 dpi	7	27

Study 3

Th8 contusion SCI model: In this study, motor recovery after traumatic mid-thoracic SCI of 3-month old female Fischer rats (160.1 $\pm$ 7.1 g) was compared to rats of 20–24 months of age (273.7 $\pm$ 23.7 g). Rats underwent a laminectomy at Th8 vertebral level followed by a contusion with 200 kDyn using the IH Impactor SCI device without additional dwell time. For surgical purposes rats were under general inhalative anesthesia. All of the described procedures were authorized by the ethical committee of the "Land Salzburg" (20910-TVG-79/17-2014) according to the European Directive 2010/63/EU for the use of rats in research.

Behavioral testing: BBB tests [Bass 95] were performed on days 1, 4, and 7 post injury followed by weekly evaluation. The rats with BBB scores of 11 or higher were further examined weekly by Catwalk XT analyses. For the Catwalk XT analyses, rats were trained on the Catwalk device for at least two weeks (two times per week) prior to surgery and a baseline (uninjured) was created. Rats did not receive food rewards during the testing. The experiment ended after 49 days for the young and after 35 days for the aged group. The number of rats and CatWalk runs in this study are shown in Table 6.4.

Table 6.4: Number of Rats and CatWalk Runs of Study 3

Study 3		# Rats	# Runs
Young: injury at 3 months	0 dpi (Uninjured)	19	91
	15 dpi	2	7
	22 dpi	6	29
	29 dpi	6	28
	36 dpi	6	25
	43 dpi	7	28
Old: injury at 20–24 months	0 dpi (Uninjured)	12	131
	15 dpi	3	37
	22 dpi	6	40
	29 dpi	6	33

Study 4

Th9 Dorsal hemisection Scouten wire-knife transection model: Adult female Wistar rats weighing 220–250 g at the time of operation were anaesthetized. Following laminectomy at Th8/9 the dura mater was opened at Th8/9 with a longitudinal cut and a dorsal hemisection injury was performed with a Scouten wire knife. All surgical interventions as well as the pre- and post-surgical rat care were provided in compliance with the German Animal Protection law (State Office, Environmental and Consumer Protection of North Rhine-Westphalia, LANUV NRW, AZ 8.87-50.10.34.08.061) and the institutional guidelines for rat's safety and comfort. Experimental animals were housed in groups under standard conditions. Water and food were available *ad libitum*.

Behavioral testing: Four weeks prior to surgery all rats were familiarized and pre-trained in the behavioral tests. The overall hindlimb function was assessed in an open field using the BBB test [Bass 95] by two blinded examiners at 30 and 60 days post-lesion. Differences in gait were investigated using the CatWalk XT System. The number of rats and runs involved in the CatWalk test are shown in Table 6.5.

Exclusion criteria: Some rats showed signs of automutilation. In the case of severe automutilation the respective rat was sacrificed prematurely. If only minimal signs of automutilation were detected, the respective rat was not included in the behavioral tests at individual test time points.

Table 6.5: Number of Rats and CatWalk Runs of Study 4

Study 4	# Rats	# Runs
0 dpi (Baseline/Uninjured)	19	63
30 dpi	16	42
60 dpi	12	36

Study 5

This study was performed as published previously [Biel 18] and briefly explained here. Experiments were performed in accordance with the Directive 2010/63/EU of the European Parliament and of the Council and were approved by the local animal health commission (20901-TVG-65/8-2013).

C4 bilateral dorsal column tungsten wire-knife transection SCI model: This study was carried out on female Fischer rats (body weight 169 $\pm$ 8 g). The lesion rat group underwent a bilateral transection of the dorsal column at the fourth cervical segment. Prior to surgery, rats were deeply anaesthetized. The dorsal spine of the rat was exposed and a laminectomy at C4 was performed to expose the spinal cord. Using a blunt tungsten wire-knife device (M122, David Kopf Instruments), the dorsal column was precisely transected bilaterally (2.5 mm width, 1.1 mm depth) as described in [Biel 18] [Sand 13] [Weid 99] [Weid 01].

Behavioral testing: Differences in gait parameters were investigated using the Catwalk XT. In the two weeks prior to injury, rats were familiarized with the device and testing conditions. Rats crossed the Catwalk walkway voluntarily without the use of food rewards. After injury rats were tested at 30 days post injury. The number of rats and CatWalk runs involved in this study are shown in Table 6.6.

Table 6.6: Number of Rats and CatWalk Runs of Study 5

Study 5	# Rats	# Runs
0 dpi (Uninjured)	6	36
30 dpi	6	36

6.2.2 Establishment of the CatWalk Parameter Linear Combination

The parameter linear combination was developed based on the gait parameters, which were extracted by the CatWalk software based on the recorded videos. Only the gait parameters, which are available in both the CatWalk 7.1. and CatWalk XT, were utilized in this study. In developing the parameter combination, gait parameters related to mean values of paw statistics, step sequence, base of support, print position, and number of paws supporting the walk were included. The parameters, which are directly related to intensity, were not utilized as they are often too sensitive to the experiment setting. Because of their similarity, all gait parameters were averaged from the right and left paws except for body speed, which was averaged from all four paws.

In order to develop a combination parameter which would efficiently examine the gait recovery differences between experimental and vehicle samples, the gait parameters, which are the most representative of SCI rat, were first designated. To do this, uninjured rats from Study 1 and Study 2 were grouped together as the controls. Additionally, the vehicle moderate-severe SCI rats from Study 1 along with the vehicle SCI rats (60 dpi) from Study 2 were combined to form the SCI group. This was continued by running t-tests (without assuming equal variances) between these two groups for all the individual gait parameters. To perform this t-test, parameters from all the runs of each rat were first averaged. All gait parameters having $p < 0.01$ from the t-test were then used in developing the linear combination of CatWalk parameters.

The linear combination of CatWalk parameters p_{LDA} can be expressed as Eq. 6.1, where p_i is the i-th Catwalk gait parameter, $w_{1,i}$ is the corresponding parameter-weight, and N_p is the number of gait parameters.

$$p_{LDA} = \mathbf{w}_1 \cdot \mathbf{p} = \sum_{i=1}^{N_p} w_{1,i} p_i \tag{6.1}$$

The parameter-weights $w_{1,i}$ of the linear combination were computed here based on LDA, which aims to maximize the between-class scatter and minimize the within-class scatter. Here, the LDA utilized gait parameter values from all of the runs and was performed according to the description in Section 2.8.

6.2.3 Analysis

The differences between groups in each study were analyzed based on the resulting parameter combination p_{LDA}. These parameter combinations p_{LDA} were calculated for all of the run data and the analysis was performed based on the average of each rat. For comparison, an analysis of the thoracic SCI rats' BBB score was also performed.

Analysis using two-way ANOVA for unbalanced design was performed for the examination of groups with longitudinal data within a study. The statistical analysis between two groups were performed by t-tests without assuming equal variances. The differences between three or more groups were investigated by ANOVA [Arms 00] [Fish 21], [Mull 09] and multiple comparison tests by Bonferroni correction provided in Matlab R2015a (8.5.0). Groups were considered significant different when the p-values were below $p < 0.05$.

6.3 Results

The purpose of this chapter was to examine if a combination parameter for CatWalk could be designed to be more predictive of gait recovery after spinal cord injury than single Catwalk parameter reporting alone or the BBB score. The resulting CatWalk parameter combination p_{LDA} is reported in Section 6.3.1. This combination was applied in the assessment of gait recovery in the studies described in Subsection 6.2.1.

6.3.1 CatWalk Parameter Linear Combination

The gait parameters having $p < 0.01$ from the t-test (without assuming equal variances) as well as the values of the first eigen-vector $\mathbf{w}_1$ are listed in Table 6.7. Although developed from injuries directly affecting hind limb function, the list consists several front-paw-related gait parameters. This suggests that the front paws play an important role in supporting body weight during impaired walking following a SCI directed to the hind limbs [Ghos 10] [Wilc 17]. Their combination as described in Eq. 6.1 was then used to assess gait recovery progression in the studies described in Subsection 6.2.1.

Table 6.7: List of gait parameters p_i ($N_p = 9$) and their corresponding parameter-weight $w_{1,i}$ for the linear combination of parameters

$w_{1,i}$	p_i
1	Front paw swing time (s)
0.0015	Front paw stride length (cm)
0.0005	Front paw duty cycle (%)
-0.0103	Hind paw base of support/BOS (cm)
0.00002	Regularity index/RI (%)
0.001	Body speed (cm/s)
-0.0001	AB sequence (%)
-0.0015	Front paw max contact at (%)
-0.0017	Hind paw stride length (cm)

6.3.2 Testing of the CatWalk Parameter Linear Combination in Distinguished Contusion Lesion Severities (Study 1)

By applying the gait parameter combination to the CatWalk data in Study 1, the ability of the p_{LDA} in distinguishing differing lesion severity as well as experimental treatment groups was tested. The uninjured rats showed significantly higher values of p_{LDA} compared to the injured rats (60 dpi), as shown in Figure 6.2a. Furthermore, significant gait performance difference can be distinguished between the moderate and moderate-severe injured rats. No significant gait improvement due to the treatment can be observed by p_{LDA}, as shown in Figure 6.2b and 6.2c. Similar results are shown by the BBB scores (Figure 6.2d, 6.2e, and 6.2f). The mean and SD of the p_{LDA} values and nine CatWalk parameters of vehicle moderate and vehicle moderate-severe groups are given in Table 6.8, as well as their p-values calculated from the t-test without assuming equal variances. Table 6.8 illustrates that most of the single CatWalk parameters did not display significant differences, while the combination of those parameters p_{LDA} was able to detect gait difference.

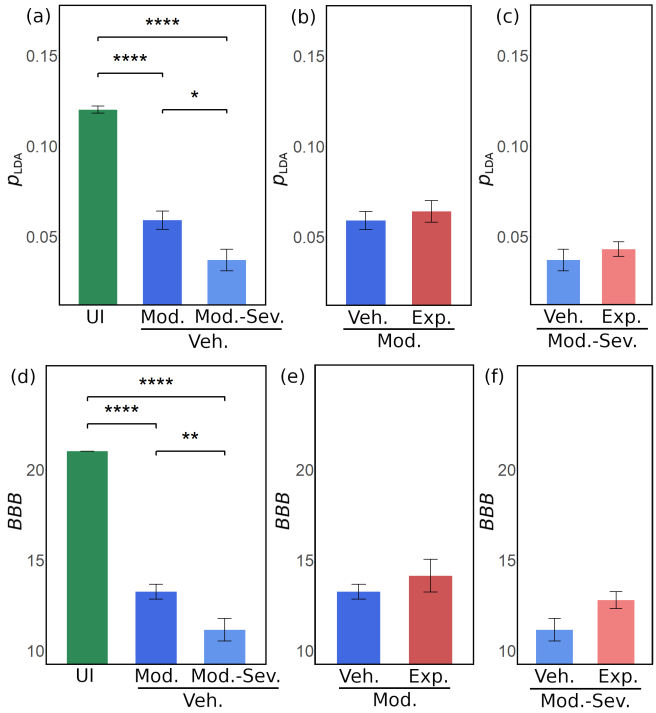

Figure 6.2: The combinations of gait parameters (p_{LDA}) and BBB scores for each group in Study 1 (Mean $\pm$ SEM). UI = Uninjured; Veh.Mod. = Vehicle Moderate SCI; Veh.Mod.-Sev. = Vehicle Moderate-Severe SCI; Exp.Mod. = Experimental Moderate SCI; Exp.Mod.-Sev. = Experimental Moderate-Severe SCI. $^{*}p < 0.05$; $^{**}p < 0.01$; $^{***}p < 0.001$; $^{****}p < 0.0001$.

Table 6.8: The mean and SD of the p_{LDA} and several CatWalk parameters from the vehicle moderate SCI and vehicle moderate-severe SCI models in Study 1 at 60 dpi and their p-values as shown in Figure 6.2a. *p<0.05

Study 1	Veh.Mod. Mean ± SD	Veh.Mod-Sev. Mean ± SD	p-value
p_{LDA}	0.059 ± 0.015	0.037 ± 0.016	0.018*
Front paw swing time (s)	0.11 ± 0.01	0.11 ± 0.01	1
Front paw stride length (cm)	10.5 ± 1.2	9.6 ± 0.8	0.21
Front paw duty cycle (%)	64.7 ± 5.0	68.3 ± 3.4	0.25
Hind paw base of support (cm)	3.6 ± 0.3	4.1 ± 0.7	0.15
Regularity index (%)	93.8 ± 2.6	5.9 ± 10.5	0.077
Body speed (cm/s)	32.9 ± 6.5	27.5 ± 3.5	0.23
AB sequence (%)	64.1 ± 22.9	62.4 ± 16.8	1
Front paw max contact at (%)	48.0 ± 3.9	52.9 ± 3.2	0.037*
Hind paw stride length (cm)	12.2 ± 1.0	11.7 ± 1.6	1

6.3.3 Examination of the CatWalk Parameter Linear Combination Across Various Studies with Similar Lesion Type and Severity (Study 2 & Study 3)

Here, published data (Study 2, [Garc 14]) of a similar lesion type with Study 1 were examined as a confirmation of validity across studies for the p_{LDA}. Study 2 [Garc 14] already demonstrated differences with experimental treatment with single Catwalk parameters (hind paw swing time (s), hind paw duty cycle (%), hindpaw BOS (cm), phase dispersion, and regularity index (%)) as well as regularity-index-controlled BBB score. In addition, unpublished data (Study 3), that did not exhibit significant differences in recovery by the BBB score or over half of the single Catwalk parameters selected here, were examined.

Examining using the p_{LDA}, vehicle SCI rats in Study 2 (male Wistar rats) and Study 3 (female Fischer rats) showed similar gait performance (Figure 6.3a) after a Th8 200 kDyn contusion injury. Correspondingly, the BBB scores (Figure 6.3d) between the vehicle SCI rats in these two studies show that they were equally injured and did not recover over 60 days (Study 2) and over 43 days (Study 3). It should be noted that different CatWalk systems (CatWalk 7.1 and CatWalk XT, respectively) between the two studies did not influence the results we observed here.

By observing both the p_{LDA} and regularity-index-controlled BBB scores in Study 2 (Figure 6.3b and 6.3e), the treatment with natural progesterone improved the gait performance as reported in the publication [Garc 14]. Significant differences of gait performance between the vehicle and the treated rats were observed at 60 dpi with the p_{LDA} and at 30 and 60 dpi by the regularity-index-controlled BBB score. The mean and SD of p_{LDA} and nine single CatWalk parameters of the SCI+Vehicle and SCI+Prog at 60 dpi are shown in Table 6.9, as well as their p-value calculated from the t-tests without assuming equal variances.

In Study 3, a gait severity difference assessed by the p_{LDA} was observed between the rats undergoing injury at a young age (3 months) and at an old age (20–24 months) as shown in Figure 6.3c. This difference was not shown by the result of the BBB tests as shown in Figure 6.3f. The mean and SD of the p_{LDA} and nine single CatWalk parameters of the young and old groups at 29 dpi are shown in Table 6.10, as well as their p-value calculated from the t-tests without assuming equal variances.

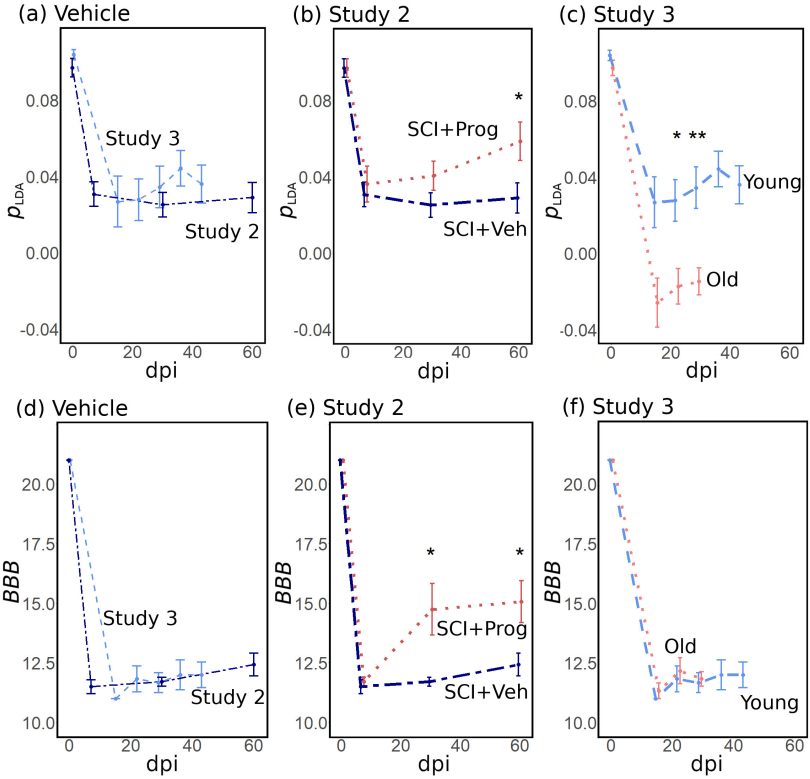

Figure 6.3: The combinations of gait parameters (p_{LDA}) and BBB scores for each group in Study 2 and Study 3 (Mean ± SEM). The two-way ANOVA in Study 2 shows significant effects on p_{LDA} of both groups (p = 0.037) and time (p < 0.00001), without significant interaction. In the regularity-index controlled BBB score (Study 2), significant effects of both groups (p = 0.003) and time (p < 0.00001) were observed, as well as significant interaction (p = 0.049). The two-way ANOVA in Study 3 shows significant effect on p_{LDA} of both group (p < 0.00001) and time (p < 0.00001), with significant interaction (p < 0.001). In the BBB (Study 3) score, significant effect of time (p < 0.00001) was observed, but no significant effect of group and interaction. *$p < 0.05$; **$p < 0.01$.

Table 6.9: The mean and SD of the p_{LDA} and several CatWalk parameters from the SCI+Veh. and SCI+Prog models in Study 2 at 60 dpi and their p-value as shown in Figure 6.3b. *$p < 0.05$

Study 2	SCI+Veh. Mean ± SD	SCI+Prog Mean ± SD	p-value
p_{LDA}	0.029 ± 0.021	0.059 ± 0.027	0.040*
Front paw swing time (s)	0.09 ± 0.01	0.12 ± 0.02	0.040*
Front paw stride length (cm)	9.0 ± 1.5	10.4 ± 1.6	0.103
Front paw duty cycle (%)	72.2 ± 3.2	67.6 ± 2.0	0.010*
Hind paw base of support (cm)	5.1 ± 0.8	4.6 ± 0.8	0.28
Regularity index (%)	89.8 ± 7.3	97.8 ± 2.4	0.027*
Body speed (cm/s)	27.9 ± 6.7	30.5 ± 8.1	0.52
AB sequence (%)	55.6 ± 15.4	66.3 ± 19.5	0.28
Front paw max contact at (%)	43.5 ± 3.9	43.9 ± 1.7	0.79
Hind paw stride length (cm)	11.6 ± 1.9	12.1 ± 1.2	0.60

Table 6.10: The mean and SD of the p_{LDA} and several CatWalk parameters from the young and old SCI models in Study 3 at 29 dpi and their p-value as shown in Figure 6.3c. *$p < 0.05$; **$p < 0.01$

Study 3	Young Mean ± SD	Old Mean ± SD	p-value
p_{LDA}	0.034 ± 0.027	-0.015 ± 0.018	0.0049**
Front paw swing time (s)	0.10 ± 0.01	0.088 ± 0.009	0.21
Front paw stride length (cm)	11.0 ± 2.1	9.1 ± 1.1	0.079
Front paw duty cycle (%)	67.4 ± 6.6	74.0 ± 3.1	0.061
Hind paw base of support (cm)	4.9 ± 0.8	6.4 ± 0.7	0.0036**
Regularity index (%)	87.0 ± 14.7	85.5 ± 5.4	0.82
Body speed (cm/s)	37.2 ± 9.7	26.4 ± 5.0	0.043*
AB sequence (%)	56.8 ± 20.3	43.1 ± 12.4	0.20
Front paw max contact at (%)	48.6 ± 5.9	60.8 ± 4.4	0.0028**
Hind paw stride length (cm)	13.5 ± 2.6	12.3 ± 1.1	0.33

6.3.4 Examination of the CatWalk Parameter Linear Combination of Distinct SCI Lesion Models (Study 2, Study 4, and Study 5)

The combination of gait parameters p_{LDA} was used to distinguish various SCI lesion models such as a bilateral dorsal column transection (Study 5) and a dorsal hemisection model (Study 4) in comparison to the previous contusion model (Study 2).

Figure 6.4a shows results from the uninjured rats and vehicle SCI rats at 30 dpi in Study 2 (Th8 contusion), Study 4 (Th8/9 dorsal hemisection), and Study 5 (C4 bilateral dorsal column lesion). In the rat thoracic contusion and dorsal hemisection studies (Study 2 and 4), the p_{LDA} was able to distinguish the gait differences between uninjured and injured rats. It also observed motor differences between the varying lesion models at 30 dpi. The mean and SD of the p_{LDA} and nine single CatWalk parameters of the vehicle SCI rats from Study 2 and 4 at 30 dpi are shown in Table 6.11, as well as their p-value calculated from the ANOVA and multiple comparison test by Bonferroni correction. The mean and SD of the p_{LDA} and nine single CatWalk parameters of the uninjured rat and injured rat (30 dpi) from Study 5 are shown in Table 6.12. The CatWalk single parameters depicted a different gait characteristic of C4 bilateral dorsal column lesion rats (Study 5) compared with the Th8/9 dorsal hemisection (Study 4) or contusion rats (Study 2). For example, the injured rats in Study 5 showed significantly longer front paw stride lengths compared with the uninjured rats, while the injured rats in Study 1 – 4 mostly showed shorter front paw stride lengths compared with the uninjured rats. Consequently, this parameter combination p_{LDA} can not reflect a reasonable gait recovery progression in C4 bilateral dorsal column lesion rats.

To compare gait recovery progression in distinct lesion models of the same spinal level, direct comparison between Study 2 (Th8 contusion) and Study 4 (Th8 dorsal hemisection) were performed and are reported in Figure 6.4b (p_{LDA}) and 6.4c (BBB-score). Although the BBB scores were not found to be statistically different between the lesion types, the p_{LDA} did observe significant gait differences, displaying its enhanced sensitivity in differentiation. Noteworthy, regardless that Study 2 and 4 utilized male and female Wistar rats, respectively, their p_{LDA} prior to surgery were nearly identical irrespective of body weight and gender differences. It should be noted here that Study 4's dorsal hemisection

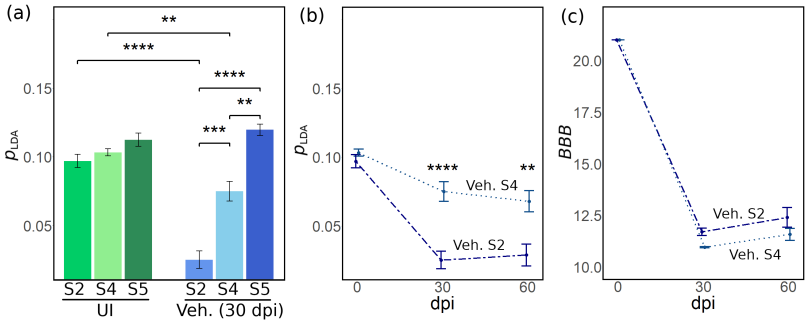

Figure 6.4: (a) The combinations of gait parameters (p_{LDA}) of uninjured rats and vehicle SCI rats in Study 2 (S2: Th8 contusion), Study 4 (S4: Th8/9 dorsal hemisection), and Study 5 (S5: C4 bilateral dorsal column lesion), UI: Uninjured; (b) The combinations of gait parameters (p_{LDA}) of vehicle SCI rats in Study 2 and Study 4; (c) The BBB scores of vehicle SCI rats in Study 2 and 4; Mean $\pm$ SEM, *$p < 0.05$; **$p < 0.01$; ***$p < 0.001$; ****$p < 0.0001$.

did produce longer hind paw stride lengths like that of Study 5's bilateral dorsal column lesion.

Table 6.11: The mean and SD of the p_{LDA} and several CatWalk parameters from the vehicle rats in Study 2 and Study 4 at 30 dpi and their p-values (ANOVA and multiple comparison tests by Bonferroni correction) shown in Figure 6.4a. *$p < 0.05$; **$p < 0.01$; ***$p < 0.001$; ****$p < 0.0001$

30 dpi	**Study 2** Mean ± SD	**Study 4** Mean ± SD	p-value
p_{LDA}	0.025 ± 0.017	0.075 ± 0.029	< 0.001***
Front paw swing time (s)	0.09 ± 0.01	0.11 ± 0.02	0.006**
Front paw stride length (cm)	9.2 ± 0.8	13.3 ± 2.9	0.001**
Front paw duty cycle (%)	72.8 ± 3.1	58.8 ± 7.6	< 0.0001****
Hind paw base of support (cm)	5.0 ± 0.7	3.6 ± 0.9	0.003**
Regularity index (%)	91.2 ± 2.8	78.8 ± 29.4	0.69
Body speed (cm/s)	29.3 ± 5.9	42.8 ± 10.6	0.007**
AB sequence (%)	44.2 ± 11.1	62.9 ± 28.9	0.26
Front paw max contact at (%)	44.3 ± 5.7	41.3 ± 6.5	0.80
Hind paw stride length (cm)	12.0 ± 1.7	16.8 ± 2.3	< 0.0001****

Table 6.12: The mean and SD of the p_{LDA} and several CatWalk parameters from Study 5 and their p-values (t-test without assuming equal variances) shown in Figure 6.4a. *$p < 0.05$; **$p < 0.01$

Study 5	**Uninjured C4** Mean ± SD	**C4, 30 dpi** Mean ± SD	p**-value**
p_{LDA}	0.112 ± 0.012	0.120 ± 0.010	0.28
Front paw swing time (s)	0.14 ± 0.01	0.14 ± 0.01	0.55
Front paw stride length (cm)	13.1 ± 1.4	15.2 ± 0.6	0.01*
Front paw duty cycle (%)	61.3 ± 4.1	57.9 ± 1.2	0.10
Hind paw base of support (cm)	2.1 ± 0.1	2.0 ± 0.5	0.78
Regularity index (%)	98.2 ± 1.6	99.4 ± 1.4	0.18
Body speed (cm/s)	32.6 ± 8.7	41.5 ± 3.9	0.06
AB sequence (%)	93.1 ± 11.1	83.3 ± 9.1	0.13
Front paw max contact at (%)	43.1 ± 3.0	40.6 ± 2.9	0.18
Hind paw stride length (cm)	12.9 ± 1.3	15.1 ± 0.6	0.08**

6.4 Discussion

To understand the effectiveness of potential clinical interventions in preclinical work performed in the field of SCI, sensitive gait recovery progression analysis of either spontaneous recovery or treatment-induced recovery is necessary. However, the current reliance on observer-based open field locomotor scoring, the BBB score, is not always sensitive to distinguish between lesion types and severity or treatment regimes. Here, an unbiased combination of SCI specific gait parameters, obtained by the automated CatWalk system, was developed based upon LDA (p_{LDA}). It is noteworthy that the use of this parameter combination in five studies from various international laboratories, performed on different rat strains and genders, by diverse experimenters using distinctive lesion types and levels makes it a one of kind application in the field of SCI. Furthermore, it demonstrates its practicality to assess the gait recovery progression of rat SCI models that cause damage to a region greater than that of the dorsal column. Therefore, the p_{LDA} indicates damage to tracts involved in overground locomotor control by displaying a significant lowering of the overall value. This distinction between lesion severities and types was not always correspondingly observed by the BBB score. By combining nine SCI-related CatWalk static and dynamic gait parameters simultaneously, the p_{LDA} is sensitive to differences that may not be detected by analyzing each individual gait parameter separately or the BBB score alone. Thus, this p_{LDA} can better represents the fluid motion of gait than the individual CatWalk parameters.

To determine the CatWalk parameters to be combined in the p_{LDA}, data from two different studies (Study 1 and Study 2) were combined increasing overall numbers, as well as mixing strain and gender. Specifically the thoracic contusion injuries with the greatest severity of lesion were used to establish the widest difference between the uninjured and injured animals. Interestingly, half of the parameters showing the greatest difference between the uninjured and injured animals resulted in many front paw parameters. This front paw significance from an injury to the thoracic cord is not novel as was shown previously by other studies [Ghos 10] [Wilc 17].

In Study 1, gait assessments using both the p_{LDA} and BBB-score showed a significant difference in motor impairment between the moderate and moderate-severe vehicle groups. Both gait assessments also showed no significant effect of the treatment to the motor recovery

during walking. In this study, one force of 150 kDyn with the IH impactor produced two groups with varying displacements, thus severity. For this reason the number of animals may have been less than what is necessary for analysis of significance. However, in Study 2 an equal number of animals were used and significance was observed. The more likely possibility is that the drug of choice in Study 1 is not relevant for recovery of overground locomotion/gait but is for fine motor control as was observed by the uneven horizontal ladder test [Sand 18]. In Study 1, the results show an agreement between the objective assessment method using the p_{LDA} and the subjective assessment method using the BBB score. In line with the publication [Sand 18], single CatWalk parameters except for one did not show significant differences between the two lesion models (Table 6.8). However, when combined, the p_{LDA} shows a strong significant difference between the two groups. Therefore, it is the whole representation of the gait parameters in unison that is more relevant than the individual components of movement.

The selection of the parameters for the p_{LDA} also came from the vehicle SCI animals in Study 2, therefore the p_{LDA} was applied here to examine if the gait recovery progression treatment effect exhibited in the publication would likewise be observed. Indeed, the treatment brings motor recovery, which was detected by both the p_{LDA} and BBB score. The p_{LDA} shows an increased progression of gait recovery with treatment over time. In Study 2, BBB score was integrated with the CatWalk regularity index parameter which may give a different representation than the BBB-score alone. Some of the same parameters presented individually in the publication [Garc 14] (hind paw BOS and stride length) are covered in p_{LDA}. However, other parameters presented here are for front paw rather than hind paw (swing time and duty cycle). Interestingly, the publication [Garc 14] reported that front paw parameters were not significantly different, although here the front paws showed significant differences in individual parameter analysis. This is likely due to the difference in statistical analysis performed. All in all the p_{LDA} appears to be better at observing gait recovery progression over time with treatment.

The p_{LDA} was subsequently tested on a similar model, Study 3. The vehicle group of Study 2 showed similar gait recovery progression to the injury-at-young group of Study 3, assessed by both the p_{LDA} and BBB score. This established that there is a similar injury severity induced and

natural recovery happening between the two studies regardless of strain and gender.

In Study 3, the p_{LDA} could detect the difference of motor impairment affected by injuries performed at different ages, which was not detectable by the BBB test. This result shows the gait difference sensitivity of the p_{LDA}. It should be noted that even though the rats were different ages when the injury was performed their pre-injury scores for both the p_{LDA} and the BBB score were similar so age was not observed to alter gait by this analysis method. The reason why the BBB score did not detect gait differences might be related to the fact that the BBB scale is based on a set of descriptive gait characteristics, where the characteristic difference between each score is pre-defined and not equal. Therefore, if a gait difference happens not according to the BBB description sequence, it will not be detected by the BBB scoring system. For example, for SCI rats to reach a BBB score of 14, they need to show consistent FL-HL coordination. Improvement in other gait characteristics will not give a higher BBB score if the coordination is not yet consistent. On the other hand, any changes in one of the nine parameters in the p_{LDA} can easily affect its value. No sequence of gait characteristic is considered in the assessment using the p_{LDA}.

Subsequently, lesions of distinct regions of the spinal cord were examined. In Figure 6.4a, a wire-knife lesion severing the entire dorsal half of the spinal cord at Th8/9 (Study 4) shows a reasonable gait recovery progression with the gait parameter combination p_{LDA}. Comparable to the contusion work, the uninjured rats have a higher value of p_{LDA} compared with the injured rats. While comparing directly the Th8 contusion (Study 2) to the Th8/9 hemisection (Study 4), the p_{LDA} showed a difference (Figure 6.4b) similar to that of Study 1 with differing contusion severity (Figure 6.2a). It suggests that the depth of the lesion and specifically which nerve tracts are disrupted play a role in overground locomotion. The gait parameter combination p_{LDA} failed to reflect a reasonable gait recovery progression in a wire-knife model that only disrupted the dorsal column (Study 5, Figure 6.4a). It should be noted that this was the only cervical lesion examined and that should be taken into consideration regarding the comparison of lesion models.

The gait parameter combination p_{LDA} provides a more sensitive parametric score compared to the common non-parametric BBB score. The p_{LDA} can find similarity between thoracic contusion models of similar severity and differences between varying severity (Study 1, Study 2, and Study 3). It can also reflect gait recovery progression in thoracic dorsal hemisection wire-knife transaction model (Study 4). However, it failed to reflect a reasonable gait recovery progression in a C4 dorsal column wire-knife transaction model (Study 5).

7 Summary, Discussion and Outlook

In this chapter, the scientific contributions of the dissertation are summarized and discussed. Successively, the possible directions of future research are outlined. The chapter is finalized with the conclusions of this dissertation.

7.1 Summary and Discussion

Several computational methods for extracting additional information obtained from the CatWalk gait analysis system, with a possibility to be applied to other gait analysis systems, are presented in this dissertation. The contributions are summarized in four main groups: clinically relevant gait characteristic quantification, gait parameter scaling/normalization, initial data analysis, and multiple gait parameter analysis.

7.1.1 Gait Characteristic Quantification

Three computational methods for quantifying locomotion sway were presented in Chapter 3. The three methods were developed based on signal-processing approaches: (i) FFT-based sway parameter (ii) FFT-based intensity sway parameter (iii) LPF-based sway parameter or sway index. These methods were applied to the CatWalk dynamic paw position information recorded from all paws as well as from the front/hind-paws separately. In total nine sway-related parameters were generated to assess the difference between two PD-relevant mouse models and their wild-type littermates. The PD-relevant mice displayed higher locomotion sway compared with their wild-type littermates. Furthermore, one of the PD-relevant mouse models (i.e. the huWT/KO) revealed significantly higher locomotion sway compared by the wild-type littermates observed by eight of the nine sway-relevant parameters. The

presented gait parameters lead to the identification of locomotion-sway-related gait characteristic in rodents model of PD.

The computational methods described here were applied only on C57BL/6N mouse models with a mean of 3.60 step/sec for the wild-type mice. Every rodent strain/breed has different walking characteristics [Koop 07] [Webb 03], and probably also different sway characteristic. Therefore, the proposed methods should be further investigated for other types of rodents and other types of diseases.

7.1.2 Gait Parameter Scaling/Normalization

A method for scaling/normalizing rodent's gait parameters based on the rodent's silhouette length was presented in Chapter 4. The study relating this scaling method was supported by a body-silhouette-length computation method based on image processing approaches, a correlation study between the body silhouette length and several gait parameters, a comparison study between the silhouette-length-based scaling and the silhouette-area-, body-weight-, and age-based scaling methods, as well as the application of the silhouette-length-based scaling method in longitudinal data obtained from two rodent models of neurodegenerative diseases.

The computed intra-assay body silhouette length is correlated to the rodent's stride lengths and speed-related parameters even in wild-type mice and rats. The silhouette-length-based scaling lowers this correlation and performed better compared with other normalization factors such as the silhouette-area, body-weight, and age. The application of this scaling method to transgenic PD-relevant rats and HD-relevant mice reveals smaller genotype-related gait parameter differences. This demonstrates that this silhouette-length-based scaling method improves the reliability of the gait analysis in rodents by normalizing stride lengths, body speed, and swing speed by the individual body-size. In addition, this shows the importance of silhouette-length-based gait parameter scaling in rodent gait analysis, especially in preclinical studies involving young animals, rodent models with genotype-related silhouette length differences, as well as in longitudinal studies.

7.1.3 Initial Data Analysis (IDA)

An approach of IDA using heat mapping for data visualization was presented in Chapter 5. The approach was exemplified in an intervention

study of PD-relevant mouse models, as well as longitudinal studies of PD-relevant rat model and HD-relevant mouse model.

The CatWalk-IDA approach helps the researchers to capture group differences, to condense information, to report negative results, and to avoid premature parameter selection. Of note, this IDA approach should be followed by a formal statistical analysis.

7.1.4 Multiple Parameter Analysis

A method for assessing gait using the combination of CatWalk parameters in rat SCI models was presented in Chapter 6. The method was developed based on LDA and it was applied to assess gait recovery of five different rat SCI studies conducted in various international laboratories: three thoracic contusion SCI studies, a thoracic dorsal hemisection SCI study, and a cervical dorsal column lesion SCI study. Using this gait parameter combination, reasonable gait recovery progression was observed in thoracic contusion lesions and thoracic dorsal hemisection lesions, including in cases when differences were not detectable by the BBB score.

When rats have not regain hindlimb weight support (BBB score ≥ 9), their hind paw positions can not be detected by the CatWalk system. Therefore, even though the CatWalk gait parameter combination is more sensitive to the BBB-score, the use of this parameter combination is limited to a range of SCI severity.

In addition to the types and severity of the lesions, other aspects can influence the calculated gait parameters in rodents, such as the strain/breed and locomotion speed [Hegl 74] [Koop 07] [Neck 13] [Neck 15] [Tayl 78] [Webb 03], the gender [Datt 16], and the body size [Hegl 74] [Mach 15] [Tayl 78]. In using the described parameter combination researches should take this influence into consideration.

7.2 Outlook

Generally, computational methods are able to support the effort of quantifying behavior, which is needed in a variety of study fields [Berm 18] [Robi 17] [Calh 17] [Roia 16] [Ande 14] [Mart 93]. Therefore, future research on developing computational methods in behavioral studies (not limited to the study of gait) will be important and valuable. To make this possible, tight and ongoing collaborations between biologists

and computer scientists are necessary [Roia 16]. Alternatively, a new generation of interdisciplinary scientists needs to be trained or recruited [Ande 14].

This section is continued by discussing the challenges and possible future development specifically in gait characteristic quantification, parameter scaling, initial data analysis, and multiple parameter analysis of CatWalk-based recorded data.

Gait Characteristic Quantification

In the future, it will be interesting to adapt the locomotion sway assessment methods for different strains/breeds of rodents, diseases, and gait analysis tests. In addition, further development of other gait parameters for rodents and further development of gait analysis tests can give new insight into preclinical studies.

Gait Parameter Scaling/Normalization

The body silhouette length is not exactly the same as the body length (nose–tip–to–anus or nose-tip–to–tail-base), because the body silhouettes recorded by the CatWalk system are the projection of the rodent's body to the walkway. Therefore, a further comparison study between the body-silhouette-length- and body-length-based gait parameter scaling can give new insight, even though anesthesia would be needed. Moreover, further studies on the normalization of other gait parameters by the individual body size (silhouette length, silhouette area, body weight, or age) are recommended. These other gait parameters include the print position (distance between the position of the hind paw and the position of the previously placed front paw on the same side of the body) and footprint dimensions (footprint length, width, and area), because body weight has been proven to be correlated with footprint dimensions [Zimp 18]. Additionally, a similar study on the relation between body size and treadmill-based gait parameters [Spar 17] will be valuable for the field of preclinical gait analysis. Furthermore, since body size is not the only factor associated with rodent's gait parameters [Koop 07] [Neck 13] [Neck 15] [Mach 15] [Tayl 78] [Webb 03] [Hegl 74] [Datt 16], further studies in developing gait parameter normalization methods need to be conducted. In addition, the line representing the silhouette length has the potential to develop 2D Eshkol Wachmann Notation (EWN) [Eila 88] and body coordinate frame [Neck 15].

Initial Data Analysis (IDA)

The approach of IDA using heat mapping is one possible approach to answer the poor consensus on how CatWalk data can be fairly investigated and reported. The approach of investigating this large amount of gait parameters to best describe a complex gait movement should continually be discussed in the scientific community.

Multiple Parameter Analysis

The study of the LDA-based gait parameter combination presents the prospect of using the combination of CatWalk parameters to assess gait recovery progression in rat SCI models. Further comparison studies using other computational methods (such as generalized discriminant analysis, GDA [Mika 99]) in developing CatWalk gait parameter combination could be valuable. Moreover, research should be further conducted to generate gait parameter combinations for different types and severity of injuries (by observing the affected nerve tracts), as well as on different animal species (such as mice).

Additionally, it will be interesting to use the scaled gait parameters described in Chapter 4 to develop a gait parameter combination similar to the method described in Chapter 6. This gives the possibility to create a silhouette-length-scaled gait parameter combination.

7.3 Conclusion

Overall, this dissertation presents several contributions in developing computational methods in analyzing rodent's gait based on the data recorded from a markerless gait analysis system. The contributions can be clustered into four groups, i.e. gait characteristic quantification, parameter scaling or normalization, initial data analysis, and multiple parameter analysis.

By using the presented locomotion-sway assessment methods, new gait information from PD-relevant mouse models based on a markerless gait analysis test can be extracted and identified. These locomotion sway quantification methods are valuable for the investigation of diseases in preclinical studies.

By establishing a silhouette-length computation method, a silhouette-length-based gait parameter scaling was developed, which is important for the analysis of the stride length, body speed, and swing speed in

preclinical studies. Furthermore, by applying the silhouette-length-based scaling method in two rodent models for neurodegenerative disorders, the genotype-related alterations for the stride length, body speed, and swing speed became smaller. This reflects the importance of applying this silhouette-length-based parameter scaling for gait analysis in rodents, especially in studies involving young rodents, in longitudinal studies, and in preclinical studies with genotype-related body size differences.

By using heat mapping in an approach of IDA of gait parameters, between-group differences can be visualized in a single comprehensive map. The approach is useful for avoiding premature parameter selection. Additionally, the resulting heat map can be used to initially report all gait parameters including the one displaying negative results. This is useful especially for initially investigating gait abnormality in rodent models of diseases.

By using LDA, a method for combining the CatWalk gait parameters was developed, which gives a reasonable parametric score related to the gait recovery progression as shown in rat thoracic contusion SCI studies and the rat thoracic dorsal hemisection SCI study. This linear combination of CatWalk gait parameters gives an alternative to the non-parametric gait assessment scaling, BBB locomotion scale [Bass 95].

Generally, by using the presented computational methods, additional and more reliable information can be extracted from the CatWalk gait analysis system. This additional information (sway-related gait parameters, silhouette-length-scaled gait parameters, initial gait parameter visualization, and the combination of gait parameters) is valuable for analyzing gait in preclinical studies.

List of Figures

List of Tables

Bibliography

[Aart 15] E. Aarts, G. Maroteaux, M. Loos, B. Koopmans, J. Kovačeví, A. B. Smit, M. Verhage, and S. Van Der Sluis. "The light spot test: measuring anxiety in mice in an automated home-cage environment". *Behavioural Brain Research*, Vol. 294, No. 294, pp. 123–130, 2015.

[Abad 13] Y.-s. K. Abada, R. Schreiber, and B. Ellenbroek. "Motor, emotional and cognitive deficits in adult BACHD mice: a model for Huntington's disease". *Behavioural Brain Research*, Vol. 238, pp. 243–251, 2013.

[Abel 00] A. Abeliovich, Y. Schmitz, I. Fariñas, D. Choi-Lundberg, W.-H. Ho, P. E. Castillo, N. Shinsky, J. M. G. Verdugo, M. Armanini, A. Ryan, M. Hynes, H. Phillips, D. Sulzer, and A. Rosenthal. "Mice lacking alpha-synuclein display functional deficits in the nigrostriatal dopamine system". *Neuron*, Vol. 25, pp. 239–252, 2000.

[Adae 14] S. Adães, M. Mendonça, T. N. Santos, J. M. Castro-Lopes, J. Ferreira-Gomes, and F. L. Neto. "Intra-articular injection of collagenase in the knee of rats as an alternative model to study nociception associated with osteoarthritis". *Arthritis Research & Therapy*, Vol. 16, No. R10, 2014.

[Adae 15] S. Adães, J. Ferreira-Gomes, M. Mendonça, L. Almeida, J. Castro-Lopes, and F. Neto. "Injury of primary afferent neurons may contribute to osteoarthritis induced pain: an experimental study using the collagenase

model in rats". *Osteoarthritis and Cartilage*, Vol. 23, pp. 914–924, 2015.

[Ahuj 17] C. S. Ahuja, J. R. Wilson, S. Nori, M. R. Kotter, C. Druschel, A. Curt, and M. G. Fehlings. "Traumatic spinal cord injury". *Nature Reviews Disease Primers*, Vol. 3, No. 17018, 2017.

[Alle 09] K. D. Allen, T. M. Griffin, R. M. Rodriguiz, W. C. Wetsel, V. B. Kraus, J. L. Huebner, L. M. Boyd, and L. A. Setton. "Decreased physical function and increased pain sensitivity in mice deficient for type IX collagen". *Arthritis and Rheumatism*, Vol. 60, No. 9, pp. 2684–2693, 2009.

[Alle 11] K. D. Allen, S. Adams Jr., B. Mata, M. Shamji, E. Gouze, L. Jing, D. Nettles, L. Latt, and L. Setton. "Gait and behavior in an IL-1 beta-mediated model of rat knee arthritis and effects of an IL1 antagonist". *Journal of Orthopaedic Research*, Vol. 29, No. 5, pp. 694–703, 2011.

[Alle 12] K. D. Allen, B. A. Mata, M. A. Gabr, J. L. Huebner, S. B. Adams, V. B. Kraus, D. O. Schmitt, and L. A. Setton. "Kinematic and dynamic gait compensations resulting from knee instability in a rat model of osteoarthritis". *Arthritis Research & Therapy*, Vol. 14, No. R78, 2012.

[Alve 16] J. A. Alves, B. C. Boerner, and D. A. Laplagne. "Flexible coupling of respiration and vocalizations with locomotion and head movements in the freely behaving rat". *Neural Plasticity*, Vol. 2016, 2016.

[Ande 09] K. D. Anderson, K. G. Sharp, M. Hofstadter, K.-A. Irvine, M. Murray, and O. Steward. "Forelimb locomotor assessment scale (FLAS): novel assessment of forelimb dysfunction after cervical spinal cord injury". *Experimental Neurology*, Vol. 220, pp. 23–33, 2009.

[Ande 14] D. J. Anderson and P. Perona. "Toward a science of computational ethology". *Neuron*, Vol. 84, No. 1, pp. 18–31, 2014.

[Ange 12] K. Ängeby Möller, S. Kinert, R. Størkson, and O.-G. Berge. "Gait analysis in rats with single joint inflammation: influence of experimental factors". *PLoS ONE*, Vol. 7, No. 10, p. 46129, 2012.

[Anto 11] P. M. A. Antony, N. J. Diederich, and R. Balling. "Parkinson's disease mouse models in translational research". *Mammalian genome*, Vol. 22, pp. 401–419, 2011.

[Arac 19] A. Arac, P. Zhao, B. H. Dobkin, S. T. Carmichael, and P. Golshani. "Deepbehavior: a deep learning toolbox for automated analysis of animal and human behavior imaging data". *Frontiers in Systems Neuroscience*, Vol. 13, pp. 1–12, 2019.

[Arms 00] R. A. Armstrong, S. V. Slade, and F. Eperjesi. "An introduction to analysis of variance (ANOVA) with special reference to data from clinical experiments in optometry". *Ophthalmic & Physiological Optics*, Vol. 20, No. 3, pp. 235–241, 2000.

[Bail 09] K. R. Bailey and J. N. Crawley. "Anxiety-related behaviors in mice". In: J. Buccafusco, Ed., *Methods of Behavior Analysis in Neuroscience*, CRC Press/Taylor & Francis, 2009.

[Bake 07] R. Baker. "The history of gait analysis before the advent of modern computers". *Gait and Posture*, Vol. 26, No. 3, pp. 331–342, 2007.

[Bass 06] D. M. Basso, L. C. Fisher, A. J. Anderson, L. B. Jakeman, D. M. Mctigue, and P. G. Popovich. "Basso mouse scale for locomotion detects differences in recovery after spinal cord injury in five common mouse strains". *Journal of Neurotrauma*, Vol. 23, No. 5, pp. 635–659, 2006.

[Bass 95] D. M. Basso, M. S. Beattie, and J. C. Bresnahan. "A sensitive and reliable locomotor rating scale for open field testing in rats". *Journal of Neurotrauma*, Vol. 12, No. 1, pp. 1–21, 1995.

[Bass 96] D. M. Basso, M. S. Beattie, J. C. Bresnahan, D. K. Anderson, A. I. Faden, J. A. Grüner, T. R. Holford, C. Y. Hsu, L. J. Noble, R. Nockels, P. L. Perot, S. K. Salzman, and W. Young. "MASCIS evaluation of open field locomotor scores: effects of experience and teamwork on reliability". *Journal of Neurotrauma*, Vol. 13, No. 7, 1996.

[Bate 05] G. P. Bates. "The molecular genetics of Huntington disease - a history". *Nature Reviews Genetics*, Vol. 6, pp. 766–773, 2005.

[Batk 14] R. J. Batka, T. J. Brown, K. P. Mcmillan, R. M. Meadows, K. J. Jones, and M. M. Haulcomb. "The need for speed in rodent locomotion analyses". *Anatomical Record*, Vol. 297, No. 10, pp. 1839–1864, 2014.

[Beit 14] J. Beitz. "Parkinson's disease: a review". *Frontiers in Bioscience*, Vol. S6, pp. 65–74, 2014.

[Bell 18] E. Bello-Arroyo, H. Roque, A. Marcos, J. Orihuel, A. Higuera-Matas, M. Desco, V. R. Caiolfa, E. Ambrosio, E. Lara-Pezzi, and M. V. Gómez-Gaviro. "MouBeAT: a new and open toolbox for guided analysis of behavioral tests in mice". *Frontiers in Behavioral Neuroscience*, Vol. 12, No. September, pp. 1–12, 2018.

[Belz 99] C. Belzung. "Measuring rodent exploratory behavior". In: W. Crusio and R. Gerlai, Eds., *Handbook of Molecular-Genetic Techniques for Brain and Behavior Research (Techniques in the Behavioral and Neural Sciences)*, pp. 738–749, Elsevier Science BV, 1999.

[Ben 17] Y. Ben-Shaul. "OptiMouse: a comprehensive open source program for reliable detection and analysis of mouse body and nose positions". *BMC Biology*, Vol. 15, No. 41, 2017.

[Berm 18] G. J. Berman. "Measuring behavior across scales". *BMC Biology*, Vol. 16, No. 23, 2018.

[Bern 17] D. Bernardes, A. Leite, and R. Oliveira. "Comprehensive catwalk gait analysis in a chronic model of multiple sclerosis subjected to treadmill exercise training". *BMC Neurology*, Vol. 17, p. 160, 2017.

[Bhim 17] A. D. Bhimani, P. Kheirkhah, G. D. Arnone, C. R. Nahhas, P. Kumar, M. Wonais, H. Hidrogo, E. Aguilar, D. Spalinski, M. Gopalka, S. Roth, and A. I. Mehta. "Functional gait analysis in a spinal contusion rat model". *Neuroscience and Biobehavioral Reviews*, Vol. 83, No. September, pp. 540–546, 2017.

[Biel 18] L. Bieler, L. Grassner, P. Zaunmair, C. Kreutzer, L. Lampe, E. Trinka, J. Marschallinger, L. Aigner, and S. Couillard-Despres. "Motor deficits following dorsal corticospinal tract transection in rats: voluntary versus skilled locomotion readouts". *Heliyon*, Vol. 4, p. 540, 2018.

[Blac 58] R. Blackman and J. Tukey. *The measurement of power spectra*. Dover Publication, New York, 1958.

[Boix 18] J. Boix, D. von Hieber, and B. Connor. "Gait analysis for early detection of motor symptoms in the 6-OHDA rat model of Parkinson's disease". *Frontiers in Behavioral Neuroscience*, Vol. 12, No. March, pp. 1–15, 2018.

[Bove 12] J. Bové and C. Perier. "Neurotoxin-based models of Parkinson's disease". *Neuroscience*, Vol. 211, pp. 51–76, 2012.

[Brod 95] J. Brodkin and J. F. Nash. "A novel apparatus for measuring rat locomotor behavior". *Journal of Neuroscience Methods*, Vol. 57, No. 2, pp. 171–176, 1995.

[Broe 05] J. van den Broeck, S. Argeseanu Cunningham, R. Eeckels, and K. Herbst. "Data cleaning: detecting, diagnosing, and editing data abnormalities". *PLoS Medicine*, Vol. 2, No. 10, p. e267, 2005.

[Broo 09] S. P. Brooks and S. B. Dunnett. "Tests to assess motor phenotype in mice: a user's guide". *Nature Reviews Neuroscience*, Vol. 10, No. 7, pp. 519–529, 2009.

[Brow 18] A. E. Brown and B. de Bivort. "Ethology as a physical science". *Nature Physics*, Vol. 14, pp. 653–657, 2018.

[Caba 17] E. Caballero-Garrido, J. Pena-Philippides, Z. Galochkina, E. Erhardt, and T. Roitbak. "Characterization of long-term gait deficits in mouse dMCAO, using the CatWalk system". *Behavioural Brain Research*, Vol. 331, pp. 282–296, 2017.

[Calh 17] A. J. Calhoun and M. Murthy. "Quantifying behavior to solve sensorimotor transformations: advances from worms and flies". *Current Opinion in Neurobiology*, Vol. 46, pp. 90–98, 2017.

[Cao 08] Y. Cao, J. S. Shumsky, M. A. Sabol, R. A. Kushner, S. Strittmatter, F. P. T. Hamers, D. H. S. Lee, S. A. Rabacchi, and M. Murray. "Nogo-66 receptor antagonist peptide (NEP1-40) administration promotes functional recovery and axonal growth after lateral funiculus injury in the adult rat". *Neurorehabilitation and Neural Repair*, Vol. 22, No. 3, pp. 262–278, 2008.

[Casa 14] N. Casadei, A.-M. Pöhler, C. Tomás-Zapico, J. Torres-Peraza, I. Schwedhelm, A. Witz, I. Zamolo, R. De Heer, B. Spruijt, L. P. J. J. Noldus, J. Klucken, J. J. Lucas, P. J. Kahle, R. Krüger, O. Riess, and S. Nuber. "Overexpression of synphilin-1 promotes clearance of soluble and misfolded alpha-synuclein without restoring the motor phenotype in aged A30P transgenic mice". *Human Molecular Genetics*, Vol. 23, No. 3, pp. 767–781, 2014.

[Chak 17] R. Chakraborty, H. N. Park, C. C. Tan, P. Weiss, M. C. Prunt, and M. T. Pardue. "Association of body length with ocular parameters in mice". *Optometry and Vision Science*, Vol. 94, No. 3, pp. 387–394, 2017.

[Chen 14] Y.-J. Chen, F.-C. Cheng, M.-L. Sheu, H.-L. Su, C.-J. Chen, J. Sheehan, and H.-C. Pan. "Detection of subtle neurological alterations by the Catwalk XT gait analysis system". *Journal of NeuroEngineering and Rehabilitation*, Vol. 11, No. 62, 2014.

[Chen 17] H. Chen, J. Du, Y. Zhang, K. Barnes, and X. Jia. "Establishing a reliable gait evaluation method for rodent studies". *Journal of Neuroscience Methods*, Vol. 283, pp. 92–100, 2017.

[Chen 97] H. Cheng, S. Almström, L. Giménez-Llort, R. Chang, S. Ove Ögren, B. Hoffer, and L. Olson. "Gait analysis of adult paraplegic rats after spinal cord repair". *Experimental Neurology*, Vol. 148, No. 2, pp. 544–557, 1997.

[Cher 14] T. Cheriyan, D. J. Ryan, J. H. Weinreb, J. Cheriyan, J. C. Paul, V. Lafage, T. Kirsch, and T. J. Errico. "Spinal cord injury models: a review". *Spinal Cord*, Vol. 52, No. 8, pp. 588–595, 2014.

[Chia 14] C.-Y. Chiang, M.-L. Sheu, F.-C. Cheng, C.-J. Chen, H.-L. Su, J. Sheehan, and C. Pan. "Comprehensive analysis of neurobehavior associated with histomorphological alterations in a chronic constrictive nerve injury model through use of the CatWalk XT system Laboratory investigation". *J Neurosurg*, Vol. 120, No. 120, pp. 250–262, 2014.

[Clar 86] K. A. Clarke and A. J. Parker. "A quantitative study of normal locomotion in the rat". *Physiology & Behavior*, Vol. 38, pp. 345–351, 1986.

[Clar 91] K. A. Clarke. "Swing time changes contribute to stride time adjustment in the walking rat". *Physiology & Behavior*, Vol. 50, pp. 1261–1262, 1991.

[Clar 95] K. A. Clarke. "Differential fore-and hindpaw force transmission in the walking rat". *Physiology & Behavior*, Vol. 58, No. 3, pp. 415–419, 1995.

[Clar 99] K. A. Clarke and J. Still. "Gait analysis in the mouse". *Physiology & Behavior*, Vol. 66, No. 5, pp. 723–729, 1999.

[Clem 17] E. K. H. Clemensson, L. E. Clemensson, B. Fabry, O. Riess, and H. P. Nguyen. "Further investigation of phenotypes and confounding factors of progressive ratio performance and feeding behavior in the

BACHD rat model of Huntington disease". *PLoS ONE*, Vol. 12, No. 3, p. e0173232, 2017.

[Coll 68] R. L. Collins. "On the Inheritance of Handedness. I. Laterality in inbred mice". *Journal of Heredity*, Vol. 59, No. 1, pp. 9–12, 1968.

[Cool 65] J. Cooley and J. Tukey. "An algorithm for the machine computation of the complex fourier series". *Mathematics of Computation*, Vol. 19, pp. 297–301, 1965.

[Cost 10] K. E. Costello, F. Guilak, L. A. Setton, and T. M. Griffin. "Locomotor activity and gait in aged mice deficient for type IX collagen". *Journal of Applied Physiology*, Vol. 109, pp. 211–218, 2010.

[Coul 02] P. Coulthard, B. J. Pleuvry, M. Brewster, K. L. Wilson, and T. V. Macfarlane. "Gait analysis as an objective measure in a chronic pain model". *Journal of Neuroscience Methods*, Vol. 116, pp. 197–213, 2002.

[Cour 09] G. Courtine, Y. Gerasimenko, R. Van Den Brand, A. Yew, P. Musienko, H. Zhong, B. Song, Y. Ao, R. M. Ichiyama, I. Lavrov, R. R. Roy, M. V. Sofroniew, and V. Reggie Edgerton. "Transformation of nonfunctional spinal circuits into functional states after the loss of brain input". *Nature Neuroscience*, Vol. 12, No. 10, pp. 1333–1343, 2009.

[Cout 99] F. Coutts. "Gait analysis in the therapeutic environment". *Manual Therapy*, Vol. 4, No. 1, pp. 2–10, 1999.

[Crow 18] S. T. Crowley, K. Kataoka, and K. Itaka. "Combined CatWalk Index: An improved method to measure mouse motor function using the automated gait analysis system". *BMC Research Notes*, Vol. 11, No. 263, pp. 1–8, 2018.

[Dano 14] M. Danoudis and R. Iansek. "Gait in Huntington's disease and the stride length-cadence relationship". *BMC Neurology*, Vol. 14, No. 161, 2014.

[Datt 15] J. P. Datto, J. C. Bastidas, N. L. Miller, A. K. Shah, K. L. Arheart, A. E. Marcillo, W. D. Dietrich, and D. D. Pearse. "Female rats demonstrate improved locomotor recovery and greater preservation of white and gray matter after traumatic spinal cord injury compared to males". *Journal of Neurotrauma*, Vol. 32, No. 15, pp. 1146–1157, 2015.

[Datt 16] J. P. Datto, A. K. Shah, J. C. Bastidas, K. L. Arheart, A. E. Marcillo, W. D. Dietrich, and D. D. Pearse. "Use of the CatWalk gait device to assess differences in locomotion between genders in rats inherently and following spinal cord injury". *Dataset Papers in Science*, Vol. 2016, pp. 1–11, 2016.

[Demp 71] A. P. Dempster. "An overview of multivariate data analysis". *Journal of Multivariate Analysis*, Vol. 1, pp. 316–346, 1971.

[Derr 16] B. Derrick, D. Toher, and P. White. "Why Welch's test is Type I error robust". *The Quantitative Methods for Psychology*, Vol. 12, No. 1, pp. 30–38, 2016.

[Duha 90] P. Duhamel and M. Vetterli. "Fast fourier transforms: a tutorial review and a state of the art". *Signal Processing*, Vol. 19, No. 4, pp. 259–299, 1990.

[Dunn 09] G. A. Dunn and T. L. Bale. "Maternal high-fat diet promotes body length increases and insulin insensitivity in second-generation mice.". *Endocrinology*, Vol. 150, No. 11, pp. 4999–5009, 2009.

[Dupl 18] M. Dupleichs, M. Masson, O. Gauthier, M. Dutilleul, J. M. Bouler, E. Verron, and P. Janvier. "Pain management after bone reconstruction surgery using an analgesic bone cement: a functional noninvasive in vivo study using gait analysis". *Journal of Pain*, Vol. 19, No. 10, pp. 1169–1180, 2018.

[Dutt 16] S. Dutta and P. Sengupta. "Men and mice: relating their ages". *Life Sciences*, Vol. 152, pp. 244–248, 2016.

[Earp 17] B. D. Earp. "The need for reporting negative results — a 90 year update". *Journal of Clinical and Translational Research*, Vol. 3, No. S2, pp. 1–4, 2017.

[Eila 88] D. Eilam and I. Golani. "The ontogeny of exploratory behavior in the house rat (Rattus rattus): The mobility gradient". *Developmental Psychobiology*, Vol. 21, No. 7, pp. 679–710, 1988.

[Eric 13] A. C. Ericsson, M. J. Crim, and C. L. Franklin. "A brief history of animal modeling". *Missouri Medicine*, Vol. 110, No. 3, pp. 201–205, 2013.

[Fago 16] N. D. Fagoe, C. L. Attwell, R. Eggers, L. Tuinenbreijer, D. Kouwenhoven, J. Verhaagen, and M. R. Mason. "Evaluation of five tests for sensitivity to functional deficits following cervical or thoracic dorsal column transection in the rat". *PLoS ONE*, Vol. 11, No. 3, pp. 1–20, 2016.

[Ferg 09] C. J. Ferguson. "An effect size primer: a guide for clinicians and researchers". *Professional Psychology: Research and Practice*, Vol. 40, No. 5, pp. 532–538, 2009.

[Ferl 11] C. E. Ferland, S. Laverty, F. Beaudry, and P. Vachon. "Gait analysis and pain response of two rodent models of osteoarthritis". *Pharmacology Biochemistry and Behavior*, Vol. 97, No. 3, pp. 603–610, 2011.

[Ferr 12] J. Ferreira-Gomes, S. Adães, M. Mendonça, and J. M. Castro-Lopes. "Analgesic effects of lidocaine, morphine and diclofenac on movement-induced nociception, as assessed by the Knee-Bend and CatWalk tests in a rat model of osteoarthritis". *Pharmacology Biochemistry and Behavior*, Vol. 101, No. 4, pp. 617–624, 2012.

[Fest 02] M. F. W. Festing and D. G. Altman. "Guidelines for the design and statistical analysis of experiments using laboratory animals". *ILAR Journal*, Vol. 43, No. 4, pp. 244–258, 2002.

[Fish 21] R. A. Fisher. "Studies in crop variation. I. An examination of the yield of dressed grain from broadbalk". *Journal of Agricultural Science*, Vol. 11, pp. 107–135, 1921.

[Fish 36] R. Fisher. "The use of multiple measurements in taxonomic problems". *Annals of Eugenics*, Vol. 7, pp. 179–188, 1936.

[Forg 14] N. Forgione, S. K. Karadimas, W. D. Foltz, K. Satkunendrarajah, A. Lip, and M. G. Fehlings. "Bilateral contusion-compression model of incomplete traumatic cervical spinal cord injury". *Journal of Neurotrauma*, Vol. 31, No. 21, pp. 1776–1788, 2014.

[Frah 18] S. Frahm, V. Melis, D. Horsley, J. E. Rickard, G. Riedel, P. Fadda, M. Scherma, C. R. Harrington, C. M. Wischik, F. Theuring, and K. Schwab. "Alpha-synuclein transgenic mice, h-alpha-synL62, display alpha-Syn aggregation and a dopaminergic phenotype reminiscent of Parkinson's disease". *Behavioural Brain Research*, Vol. 339, No. November 2017, pp. 153–168, 2018.

[Froh 18] H. Fröhlich, K. Claes, C. De Wolf, X. Van Damme, and A. Michel. "A machine learning approach to automated gait analysis for the Noldus Catwalk system". *IEEE Transactions on Biomedical Engineering*, Vol. 65, No. 5, pp. 1133–1139, 2018.

[Gago 15] M. F. Gago, V. Fernandes, J. Ferreira, H. Silva, M. L. Rodrigues, L. Rocha, E. Bicho, and N. Sousa. "The effect of levodopa on postural stability evaluated by wearable inertial measurement units for idiopathic and vascular Parkinson's disease". *Gait and Posture*, Vol. 41, No. 2, pp. 459–464, 2015.

[Garc 14] D. Garcia-Ovejero, S. González, B. Paniagua-Torija, A. Lima, E. Molina-Holgado, A. F. De Nicola, and F. Labombarda. "Progesterone reduces secondary damage, preserves white matter, and improves locomotor outcome after spinal cord contusion". *Journal of Neurotrauma*, Vol. 31, No. 9, pp. 857–871, 2014.

[Gehl 12] N. Gehlenborg and B. Wong. "Heat maps". *Nature Methods*, Vol. 9, No. 3, p. 213, 2012.

[Geld 15] W. J. Geldenhuys, T. L. Guseman, I. S. Pienaar, D. E. Dluzen, and J. W. Young. "A novel biomechanical analysis of gait changes in the MPTP mouse model of Parkinson's disease". *PeerJ*, Vol. 3, p. e1175, 2015.

[Ghos 10] A. Ghosh, F. Haiss, E. Sydekum, R. Schneider, M. Gullo, M. T. Wyss, T. Mueggler, C. Baltes, M. Rudin, B. Weber, and M. E. Schwab. "Rewiring of hindlimb corticospinal neurons after spinal cord injury". *Nature Neuroscience*, Vol. 13, No. 1, pp. 97–104, 2010.

[Goet 03] C. G. Goetz, W. Poewe, O. Rascol, C. Sampaio, and G. T. Stebbins. "The Unified Parkinson's Disease Rating Scale (UPDRS): status and recommendations". *Movement Disorders*, Vol. 18, No. 7, pp. 738 –750, 2003.

[Gonz 08] R. C. Gonzalez and R. E. Woods. *Digital image processing*. Prentice-Hall, New Jersey, 3rd Ed., 2008.

[Gorp 14] S. van Gorp, M. Leerink, S. Nguyen, O. Platoshyn, M. Marsala, and E. A. Joosten. "Translation of the rat thoracic contusion model; Part 2-forward versus backward locomotion testing". *Spinal Cord*, Vol. 52, No. 7, pp. 529–535, 2014.

[Gray 08] M. Gray, D. I. Shirasaki, C. Cepeda, V. M. Andre, B. Wilburn, X.-H. Lu, J. Tao, I. Yamazaki, S.-H. Li, Y. E. Sun, X.-J. Li, M. S. Levine, and X. W. Yang. "Full-length human mutant huntingtin with a stable polyglutamine repeat can elicit progressive and selective neuropathogenesis in BACHD Mice". *Journal of Neuroscience*, Vol. 28, No. 24, pp. 6182–6195, 2008.

[Gris 17] K. Gris, J. Coutu, and D. Gris. "Supervised and unsupervised learning technology in the study of rodent behavior". *Frontiers in Behavioral Neuroscience*, Vol. 11, p. 141, 2017.

[Guil 08] T. S. Guillot, S. A. Asress, J. R. Richardson, J. D. Glass, and G. W. Miller. "Treadmill gait analysis does not

detect motor deficits in animal models of Parkinson's disease or amyotrophic lateral sclerosis.". *Journal of Motor Behavior*, Vol. 40, No. 6, pp. 568–77, 2008.

[Haas 16] R. de Haas, F. G. Russel, and J. A. Smeitink. "Gait analysis in a mouse model resembling Leigh disease". *Behavioural Brain Research*, Vol. 296, pp. 191–198, 2016.

[Hame 01] F. P. T. Hamers, A. J. Lankhorst, T. Jan, V. Laar, W. B. Veldhuis, and W. H. Gispen. "Automated quantitative gait analysis during overground locomotion in the rat: Its application to spinal cord contusion and transection injuries". *Journal of Neurotrauma*, Vol. 18, No. 2, pp. 187–201, 2001.

[Hame 06] F. P. Hamers, G. C. Koopmans, and E. A. Joosten. "CatWalk-assisted gait analysis in the assessment of spinal cord injury". *Journal of Neurotrauma*, Vol. 23, No. 3/4, pp. 537–548, 2006.

[Harv 08] B. K. Harvey, Y. Wang, and B. J. Hoffer. "Transgenic rodent models of Parkinson's disease". *Acta Neurochirurgica Supplement*, Vol. 101, pp. 89–92, 2008.

[Haus 18] R. A. Hauser. "Help cure Parkinson's disease: please don't waste the Golden Year". *npj Parkinson's Disease*, Vol. 4, No. 1, p. 29, 2018.

[Haya 15] K. Hayakawa, S. Uchida, T. Ogata, S. Tanaka, K. Kataoka, and K. Itaka. "Intrathecal injection of a therapeutic gene-containing polyplex to treat spinal cord injury". *Journal of Controlled Release*, Vol. 197, pp. 1–9, 2015.

[Hays 13] S. A. Hays, N. Khodaparast, A. M. Sloan, D. R. Hulsey, M. Pantoja, A. D. Ruiz, M. P. Kilgard, and R. L. Rennaker. "The isometric pull task: A novel automated method for quantifying forelimb force generation in rats". *Journal of Neuroscience Methods*, Vol. 212, No. 2, pp. 329–337, 2013.

[Head 15] M. L. Head, L. Holman, R. Lanfear, A. T. Kahn, and M. D. Jennions. "The extent and consequences of P-

Hacking in science". *PLoS Biology*, Vol. 13, No. 3, pp. 1–15, 2015.

[Hegl 74] N. C. Heglund, R. C. Taylor, and T. A. McMahon. "Scaling stride frequency and gait to animal size: mice to horses". *Science*, Vol. 186, No. 4169, pp. 1112–1113, 1974.

[Heik 15a] T. Heikkinen, T. Bragge, O. Kontkanen, T. Parkkari, I. Munoz-Sanjuan, and L. C. Park. "Fine motor kinematic analysis in R6 / 2 mouse model of Huntington's disease: capturing dyskinesia-like movement as a component of progressive motor deficits". In: *45th annual meeting of the Society for Neuroscience (Neuroscience 2015)*, 2015.

[Heik 15b] T. Heikkinen, T. Bragge, A. Nurmi, and R. Hodgson. "Use of high precision kinematic analysis to assess pharmacologically - induced motor impairment in mice". In: *45th annual meeting of the Society for Neuroscience (Neuroscience 2015)*, 2015.

[Hend 06] W. T. J. Hendriks, R. Eggers, M. J. Ruitenberg, B. Blits, F. P. T. Hamers, J. Verhaagen, and G. J. Boer. "Profound differences in spontaneous long-term functional recovery after defined spinal tract lesions in the rat". *Journal of Neurotrauma*, Vol. 23, No. 1, pp. 18–35, 2006.

[Hero 16] S. Herold, P. Kumar, K. Jung, I. Graf, H. Menkhoff, X. Schulz, M. Bähr, and K. Hein. "CatWalk gait analysis in a rat model of multiple sclerosis". *BMC Neuroscience*, Vol. 17, No. 78, 2016.

[Hetz 12] S. Hetze, C. Römer, C. Teufelhart, A. Meisel, and O. Engel. "Gait analysis as a method for assessing neurological outcome in a mouse model of stroke". *Journal of Neuroscience Methods*, Vol. 206, No. 1, pp. 7–14, 2012.

[Hild 89] M. Hildebrand. "The quadrupedal gaits of vertebrates". *BioScience*, Vol. 39, No. 11, pp. 766–775, 1989.

[Hill 12] C. E. Hill, D. M. Brodak, and M. Bartlett Bunge. "Dissociated predegenerated peripheral nerve transplants for spinal cord injury repair: a comprehensive assessment of their effects on regeneration and functional recovery compared to Schwann cell transplants". *Journal of Neurotrauma*, Vol. 29, No. 12, pp. 2226–2243, 2012.

[Hodg 15] V. L. Hodgkinson, J. M. Dale, M. L. Garcia, G. A. Weisman, J. Lee, J. D. Gitlin, and M. J. Petris. "X-linked spinal muscular atrophy in mice caused by autonomous loss of ATP7A in the motor neuron". *The Journal of Pathology*, Vol. 236, No. 2, pp. 241–50, 2015.

[Hof 96] A. L. Hof. "Scaling gait data to body size". *Gait & Posture*, Vol. 4, pp. 222–223, 1996.

[Hong 15] W. Hong, A. Kennedy, X. P. Burgos-Artizzu, M. Zelikowsky, S. G. Navonne, P. Perona, and D. J. Anderson. "Automated measurement of mouse social behaviors using depth sensing, video tracking, and machine learning". *Proceedings of the National Academy of Sciences*, Vol. 112, No. 38, pp. E5351–E5360, 2015.

[Hors 03] S. von Hörsten, I. Schmitt, H. P. Nguyen, C. Holzmann, T. Schmidt, T. Walther, M. Bader, R. Pabst, P. Kobbe, J. Krotova, D. Stiller, A. Kask, A. Vaarmann, S. Rathke-Hartlieb, J. B. Schulz, U. Grasshoff, I. Bauer, A. M. M. Vieira-Saecker, M. Paul, L. Jones, K. S. Lindenberg, B. Landwehrmeyer, A. Bauer, X. J. Li, and O. Riess. "Transgenic rat model of Huntington's disease". *Human Molecular Genetics*, Vol. 12, No. 6, pp. 617–624, 2003.

[Hueb 16] M. Huebner, W. Vach, and S. Le Cessie. "A systematic approach to initial data analysis is good research practice". *The Journal of Thoracic and Cardiovascular Surgery*, Vol. 151, No. 1, pp. 25–27, 2016.

[Humb 99] T. Humby, F. M. Laird, W. Davies, and L. S. Wilkinson. "Visuospatial attentional functioning In mice: Interactions between cholinergic manipulations and

genotype". *European Journal of Neuroscience*, Vol. 11, No. 8, pp. 2813–2823, 1999.

[Huna 13] A. S. Hunanyan, H. A. Petrosyan, V. Alessi, and V. L. Arvanian. "Combination of chondroitinase ABC and AAV-NT3 promotes neural plasticity at descending spinal pathways after thoracic contusion in rats". *Journal of Neurophysiology*, Vol. 110, No. 8, pp. 1782–1792, 2013.

[Hunt 96] Huntington Study Group. "The unified Huntington's disease rating scale: reliability and consistency". *Movement Disorders*, Vol. 11, No. 2, pp. 136–142, 1996.

[Hutc 07] D. Hutchinson, V. Ho, M. Dodd, H. N. Dawson, A. C. Zumwalt, D. Schmitt, and C. A. Colton. "Quantitative measurement of postural sway in mouse models of human neurodegenerative disease". *Neuroscience*, Vol. 148, No. 4, pp. 825–832, 2007.

[Ishi 14] G. Ishikawa, Y. Nagakura, N. Takeshita, and Y. Shimizu. "Efficacy of drugs with different mechanisms of action in relieving spontaneous pain at rest and during movement in a rat model of osteoarthritis". *European Journal of Pharmacology*, Vol. 738, pp. 111–117, 2014.

[Jack 12] V. Jackson-Lewis, J. Blesa, and S. Przedborski. "Animal models of Parkinson's disease". *Parkinsonism and Related Disorders*, Vol. 18, No. 1, pp. S183–S185, 2012.

[Jaco 14] B. Y. Jacobs, H. E. Kloefkorn, and K. D. Allen. "Gait analysis methods for rodent models of osteoarthritis". *Current Pain Headache Reports*, Vol. 18, No. 10, 2014.

[Jaco 17] B. Y. Jacobs, K. Dunnigan, M. Pires-Fernandes, and K. D. Allen. "Unique spatiotemporal and dynamic gait compensations in the rat monoiodoacetate injection and medial meniscus transection models of knee osteoarthritis". *Osteoarthritis and Cartilage*, Vol. 25, No. 5, pp. 750–758, 2017.

[Jaco 18] B. Y. Jacobs, E. H. Lakes, A. J. Reiter, S. P. Lake, T. R. Ham, N. D. Leipzig, S. L. Porvasnik, C. E. Schmidt, R. A. Wachs, and K. D. Allen. "The open source GAITOR suite for rodent gait analysis". *Scientific Reports*, Vol. 8, No. 1, pp. 1–14, 2018.

[Jaen 74] R. Jaenisch and B. Mintz. "Simian virus 40 DNA sequences in DNA of healthy adult mice derived from preimplantation blastocysts injected with Viral DNA (blastocyst microinjection in vitro/development/DNA reassociation kinetics of simian virus 40)". *Proceedings of the National Academy of Sciences of the United States of America*, Vol. 71, No. 4, pp. 1250–1254, 1974.

[Jala 17] D. Jalan, N. Saini, M. Zaidi, A. Pallottie, S. Elkabes, and R. F. Heary. "Effects of early surgical decompression on functional and histological outcomes after severe experimental thoracic spinal cord injury". *Journal of Neurosurgery Spine*, Vol. 26, No. 1, pp. 62–75, 2017.

[Jank 08] J. Jankovic. "Parkinson's disease: clinical features and diagnosis". *Journal of Neurology, Neurosurgery & Psychiatry*, Vol. 79, No. 4, pp. 368–376, 2008.

[Kali 15] L. V. Kalia and A. E. Lang. "Parkinson's disease". *The Lancet*, Vol. 386, pp. 896–912, 2015.

[Kame 17] T. Kameda, Y. Kaneuchi, M. Sekiguchi, and S.-i. Konno. "Measurement of mechanical withdrawal thresholds and gait analysis using the CatWalk method in a nucleus pulposus-applied rodent model". *Journal of Experimental Orthopaedics*, Vol. 4, No. 31, 2017.

[Kann 14a] S. Kannan and S. Gowri. "Contradicting/negative results in clinical research: why (do we get these)? why not (get these published)? where (to publish)?". *Perspectives in Clinical Research*, Vol. 5, No. 4, pp. 151–153, 2014.

[Kann 14b] H. Kanno, Y. Pressman, A. Moody, R. Berg, E. M. Muir, J. H. Rogers, H. Ozawa, E. Itoi, D. D. Pearse, and

M. B. Bunge. "Combination of engineered Schwann cell grafts to Secrete neurotrophin and chondroitinase promotes axonal regeneration and locomotion after spinal cord injury". *Journal of Neuroscience*, Vol. 34, No. 5, pp. 1838–1855, 2014.

[Kapp 17] E. A. Kappos, P. K. Sieber, P. E. Engels, A. V. Mariolo, S. D'Arpa, D. J. Schaefer, and D. F. Kalbermatten. "Validity and reliability of the CatWalk system as a static and dynamic gait analysis tool for the assessment of functional nerve recovery in small animal models". *Brain and Behavior*, Vol. 7, No. 7, pp. 1–12, 2017.

[Karw 01] Z. Karwacki, P. Kowiański, and J. Moryś. "General anaesthesia in rats undergoing experiments on the central nervous system". *Folia Morphologica*, Vol. 60, No. 4, pp. 235–242, 2001.

[Kas 11] M. J. Kas, I. Golani, Y. Benjamini, E. Fonio, and O. Stiedl. "Longitudinal assessment of deliberate mouse behavior in the home cage and attached environments: relevance to anxiety and mood disorders". *Neuromethods*, Vol. 2, pp. 1–20, 2011.

[Kjel 16] J. Kjell and L. Olson. "Rat models of spinal cord injury: from pathology to potential therapies". *Disease Models & Mechanisms*, Vol. 9, pp. 1125–1137, 2016.

[Kloe 15] H. E. Kloefkorn, B. Y. Jacobs, A. M. Loye, and K. D. Allen. "Spatiotemporal gait compensations following medial collateral ligament and medial meniscus injury in the rat: Correlating gait patterns to joint damage". *Arthritis Research and Therapy*, Vol. 17, No. 287, 2015.

[Kloe 17] H. E. Kloefkorn, T. R. Pettengill, S. M. F. Turner, K. A. Streeter, E. J. Gonzalez-Rothi, D. D. Fuller, and K. D. Allen. "Automated gait analysis through hues and areas (AGATHA): a method to characterize the spatiotemporal pattern of rat gait". *Annals of Biomedical Engineering*, Vol. 45, No. 3, pp. 711–725, 2017.

[Kloo 05] A. Kloos, L. Fisher, M. Detloff, D. Hassenzahl, and D. Basso. "Stepwise motor and all-or-none sensory recovery is associated with nonlinear sparing after incremental spinal cord injury in rats". *Experimental Neurology*, Vol. 191, No. 2, pp. 251–265, 2005.

[Kluc 12] J. Klucken, A.-M. Poehler, D. Ebrahimi-Fakhari, J. Schneider, S. Nuber, E. Rockenstein, U. Schlötzer-Schrehardt, B. T. Hyman, P. J. McLean, E. Masliah, and J. Winkler. "Alpha-synuclein aggregation involves a bafilomycin A1-sensitive autophagy pathway". *Autophagy*, Vol. 8, No. 5, pp. 754–766, 2012.

[Kluc 13] J. Klucken, J. Barth, P. Kugler, J. Schlachetzki, T. Henze, F. Marxreiter, Z. Kohl, R. Steidl, J. Hornegger, B. Eskofier, and J. Winkler. "Unbiased and mobile gait analysis detects motor impairment in Parkinson's disease". *PLoS ONE*, Vol. 8, No. 2, p. e56956, 2013.

[Kohl 16] Z. Kohl, N. Abdallah, J. Vogelgsang, L. Tischer, J. Deusser, D. Amato, S. Anderson, C. P. Müller, O. Riess, E. Masliah, S. Nuber, and J. Winkler. "Severely impaired hippocampal neurogenesis associates with an early serotonergic deficit in a BAC α-synuclein transgenic rat model of Parkinson's disease". *Neurobiology of Disease*, Vol. 85, pp. 206–217, 2016.

[Koop 05] G. C. Koopmans, R. Deumens, W. M. M. Honig, F. P. T. Hamers, H. W. M. Steinbusch, and E. A. J. Joosten. "The assessment of locomotor function in spinal cord injured rats: the importance of objective analysis of coordination". *Journal of Neurotrauma*, Vol. 22, No. 2, pp. 214–225, 2005.

[Koop 07] G. C. Koopmans, R. Deumens, G. Brook, J. Gerver, W. M. M. Honig, F. P. T. Hamers, and E. A. J. Joosten. "Strain and locomotor speed affect over-ground locomotion in intact rats". *Physiology and Behavior*, Vol. 92, No. 5, pp. 993–1001, 2007.

[Krak 17] J. W. Krakauer, A. A. Ghazanfar, A. Gomez-Marin, M. A. MacIver, and D. Poeppel. "Neuroscience needs

behavior: correcting a reductionist bias". *Neuron*, Vol. 93, No. 3, pp. 480–490, 2017.

[Krem 10] A. E. Kremer, J. J. Martens, W. Kulik, F. Rueff, E. M. Kuiper, H. R. Van Buuren, K. J. Van Erpecum, J. Kondrackiene, J. Prieto, C. Rust, V. L. Geenes, C. Williamson, W. H. Moolenaar, U. Beuers, and R. P. Oude Elferink. "Lysophosphatidic acid is a potential mediator of cholestatic pruritus". *Gastroenterology*, Vol. 139, No. 3, pp. 1008–1018, 2010.

[Lake 16] E. Lakes and K. Allen. "Gait analysis methods for rodent models of arthritic disorders: reviews and recommendations". *Osteoarthritis and Cartilage*, Vol. 24, No. 11, pp. 1837–1849, 2016.

[Lang 05] D. H. Lang, N. A. Sharkey, A. Lionikas, H. A. Mack, L. Larsson, G. P. Vogler, D. J. Vandenbergh, D. A. Blizard, J. T. Stout, J. P. Stitt, and G. E. McClearn. "Adjusting data to body size: a comparison of methods as applied to quantitative trait loci analysis of musculoskeletal phenotypes". *Journal of Bone and Mineral Research*, Vol. 20, No. 5, pp. 748–57, 2005.

[Lees 09] A. J. Lees, J. Hardy, and T. Revesz. "Parkinson's disease". *The Lancet*, Vol. 373, pp. 2055–2066, 2009.

[Leza 17] K. R. Lezak, G. Missig, and W. A. Carlezon. "Behavioral methods to study anxiety in rodents". *Dialogues Clinical Neuroscience*, Vol. 19, No. 2, pp. 181–191, 2017.

[Li 05] M. Li and B. Yuan. "2D-LDA: a statistical linear discriminant analysis for image matrix". *Pattern Recognition Letters*, Vol. 26, No. 5, pp. 527–532, 2005.

[Lind 06] J. Lindsey and H. Baker. "Historical foundation". In: M. Suckow, C. Franklin, and S. Weisbroth, Eds., *The Laboratory Rat*, Chap. 1, Elsevier Inc., 2006.

[Liu 13] Y. Liu, L. J. Ao, G. Lu, E. Leong, Q. Liu, X. H. Wang, X. L. Zhu, T. F. D. Sun, Z. Fei, T. Jiu, X. Hu, and W. S.

Poon. "Quantitative gait analysis of long-term locomotion deficits in classical unilateral striatal intracerebral hemorrhage rat model". *Behavioural Brain Research*, Vol. 257, pp. 166–177, 2013.

[Lope 10] I. C. López, P. J. G. Ruiz, S. V. F. del Pozo, and V. S. Bernardos. "Motor complications in Parkinson's disease: Ten year follow-up study". *Movement Disorders*, Vol. 25, No. 16, pp. 2735–2739, 2010.

[Loua 73] T. Loua. *Atlas statistique de la population de Paris*. J. Dejey, Paris, 1873.

[Luga 11] V. Lugade, V. Lin, and L.-S. Chou. "Center of mass and base of support interaction during gait". *Gait & Posture*, Vol. 33, No. 3, pp. 406–411, 2011.

[Lui 11] J. C. Lui and J. Baron. "Mechanisms limiting body growth in mammals". *Endocrine Reviews*, Vol. 32, No. 3, pp. 422–440, 2011.

[Lund 04] M. Lundblad, B. Picconi, H. Lindgren, and M. A. Cenci. "A model of L-DOPA-induced dyskinesia in 6-hydroxydopamine lesioned mice: Relation to motor and cellular parameters of nigrostriatal function". *Neurobiology of Disease*, Vol. 16, No. 1, pp. 110–123, 2004.

[Mach 15] A. S. Machado, D. M. Darmohray, J. Fayad, H. G. Marques, and M. R. Carey. "A quantitative framework for whole-body coordination reveals specific deficits in freely walking ataxic mice". *eLife*, Vol. 4, No. e07892, pp. 1–22, 2015.

[Macp 01] G. J. Macphee and D. A. Stewart. "Parkinson's disease". *Reviews in Clinical Gerontology*, Vol. 11, pp. 33–49, 2001.

[Madi 14] A. Madinier, M. J. Quattromani, C. Sjölund, K. Ruscher, and T. Wieloch. "Enriched housing enhances recovery of limb placement ability and reduces

aggrecan-containing perineuronal nets in the rat somatosensory cortex after experimental stroke". *PLoS ONE*, Vol. 9, No. 3, p. e93121, 2014.

[Mage 10] I. Magen and M.-F. Chesselet. "Genetic mouse models of Parkinson's disease: the state of the art". *Progress in Brain Research*, Vol. Volume 184, pp. 53–87, 2010.

[Magh 15] O. H. Maghsoudi, A. V. Tabrizi, B. Robertson, P. Shamble, and A. Spence. "A novel automatic method to track the body and paws of running mice in high speed video". In: *2015 IEEE Signal Processing in Medicine and Biology Symposium*, IEEE, 2015.

[Magh 16] O. H. Maghsoudi, A. V. Tabrizi, B. Robertson, P. Shamble, and A. Spence. "A rodent paw tracker using support vector machine". In: *2016 IEEE Signal Processing in Medicine and Biology Symposium, SPMB 2016*, IEEE, 2016.

[Maim 18] R. Maimon, A. Ionescu, A. Bonnie, S. Sweetat, S. Wald-Altman, S. Inbar, T. Gradus, D. Trotti, M. Weil, O. Behar, and E. Perlson. "miR126-5p down-regulation facilitates axon degeneration and NMJ disruption via a non-cell-autonomous mechanism in ALS". *Journal of Neuroscience*, 2018.

[Manc 12a] M. Mancini, P. Carlson-Kuhta, C. Zampieri, J. G. Nutt, L. Chiari, and F. B. Horak. "Postural sway as a marker of progression in Parkinson's disease: a pilot longitudinal study". *Gait & Posture*, Vol. 36, No. 3, pp. 471–476, 2012.

[Manc 12b] M. Mancini, A. Salarian, P. Carlson-Kuhta, C. Zampieri, L. King, L. Chiari, and F. B. Horak. "ISway: a sensitive, valid and reliable measure of postural control". *Journal of NeuroEngineering and Rehabilitation*, Vol. 9, No. 1, p. 59, 2012.

[Manf 17] G. Manfré, E. K. H. Clemensson, E. I. Kyriakou, L. E. Clemensson, J. E. Van Der Harst, J. R. Homberg, H. P. Nguyen, N. Sousa, X.-J. Li, and X. Xifró. "The BACHD

rat model of Huntington disease shows specific deficits in a test battery of motor function". *Frontiers in Behavioral Neuroscience*, Vol. 11, pp. 1–13, 2017.

[Mang 96] L. Mangiarini, K. Sathasivam, M. Seller, B. Cozens, A. Harper, C. Hetherington, M. Lawton, Y. Trottier, H. Lehrach, S. W. Davies, and G. P. Bates. "Exon 1 of the HD Gene with an Expanded CAG Repeat Is Sufficient to Cause a Progressive Neurological Phenotype in Transgenic Mice The onset of symptoms is generally in midlife although". *Cell*, Vol. 87, pp. 493–506, 1996.

[Mart 01] A. M. Martínez and A. C. Kak. "PCA versus LDA". *IEEE Transactions on Pattern Analysis and Machine Intelligence*, Vol. 23, No. 2, pp. 228–233, 2001.

[Mart 93] P. Martin and P. Bateson. *Measuring behaviour: an introductory guide*. Cambridge University Press, Cambridge, 1993.

[Mast 16] T. Mastracci. "Scientific methods and the reporting of negative results: critically important to patient safety". *European Journal of Vascular & Endovascular Surgery*, Vol. 51, pp. 165–166, 2016.

[Mati 07] M. Matinolli, J. T. Korpelainen, R. Korpelainen, K. A. Sotaniemi, M. Virranniemi, and V. V. Myllylä. "Postural sway and falls in Parkinson's disease: a regression approach". *Movement Disorders*, Vol. 22, No. 13, pp. 1927–1935, 2007.

[Mazu 11] M. Mazur-Milecka and A. Nowakowski. "Comparison of tracking methods in respect of automation of an animal behavioral test". *Metrology and Measurement Systems*, Vol. 18, No. 1, pp. 91–104, 2011.

[Mcca 14] H. Mccann, C. H. Stevens, H. Cartwright, and G. M. Halliday. "α-Synucleinopathy phenotypes". *Parkinsonism and Related Disorders*, Vol. 20, pp. S62–S67, 2014.

[McCo 18] P. McColgan and S. J. Tabrizi. "Huntington's disease: a clinical review". *European Journal of Neurology*, Vol. 25, No. 1, pp. 24–34, 2018.

[Mcdo 08] J. H. Mcdonald. *Handbook of Biological Statistics*. Sparky House, Baltimore, Maryland, 2008.

[Meka 09] K. Mekada, K. Abe, A. Murakami, S. Nakamura, H. Nakata, K. Moriwaki, Y. Obata, and A. Yoshiki. "Genetic differences among C57BL/6 substrains". *Experimental Animals*, Vol. 58, No. 2, pp. 141–149, 2009.

[Mend 13] C. S. Mendes, I. Bartos, T. Akay, S. Márka, and R. S. Mann. "Quantification of gait parameters in freely walking wild type and sensory deprived Drosophila melanogaster". *eLife*, Vol. 2013, No. 2, pp. 1–24, 2013.

[Mend 15] C. S. Mendes, I. Bartos, Z. Márka, T. Akay, S. Márka, and R. S. Mann. "Quantification of gait parameters in freely walking rodents.". *BMC Biology*, Vol. 13, p. 50, 2015.

[Mett 04] P. Metten, K. L. Best, A. J. Cameron, A. B. Saultz, J. M. Zuraw, C.-H. Yu, D. Wahlsten, and J. C. Crabbe. "Observer-rated ataxia: rating scales for assessment of genetic differences in ethanol-induced intoxication in mice". *J Appl Physiol*, Vol. 97, pp. 360–368, 2004.

[Metz 02] G. A. Metz and I. Q. Whishaw. "Cortical and subcortical lesions impair skilled walking in the ladder rung walking test: a new task to evaluate fore-and hindlimb stepping, placing, and co-ordination". *Journal of Neuroscience Methods*, Vol. 115, No. 2, pp. 167–179, 2002.

[Meye 18] A. F. Meyer, J. Poort, J. O'Keefe, M. Sahani, and J. F. Linden. "A head-mounted camera system integrates detailed behavioral monitoring with multichannel electrophysiology in freely moving mice". *Neuron*, Vol. 100, pp. 46–60, 2018.

[Mika 99] S. Mika, G. Rätsch, J. Weston, B. Schölkopf, and K.-R. Müller. "Fisher discriminant analysis with kernels". In: *Neural Networks for Signal Processing IX: Proceedings of the 1999 IEEE Signal Processing Society Workshop*, pp. 41–48, IEEE, Madison, WI, USA, 1999.

[Mina 19] G. Minakaki, F. Canneva, F. Chevessier, F. Bode, S. Menges, I. K. Timotius, L. S. Kalinichenko, H. Meixner, C. P. Müller, B. M. Eskofier, N. Casadei, O. Riess, R. Schröder, J. Winkler, W. Xiang, S. von Hörsten, and J. Klucken. "Treadmill exercise intervention improves gait and postural control in alpha-synuclein mouse models without inducing cerebral autophagy". *Behavioural Brain Research*, Vol. 363, pp. 199–215, 2019.

[Miya 11] M. Miyagi, T. Ishikawa, H. Kamoda, S. Orita, K. Kuniyoshi, N. Ochiai, S. Kishida, J. Nakamura, Y. Eguchi, G. Arai, M. Suzuki, Y. Aoki, T. Toyone, K. Takahashi, G. Inoue, and S. Ohtori. "Assessment of gait in a rat model of myofascial inflammation using the CatWalk system". *Spine*, Vol. 36, No. 21, pp. 1760–1764, 2011.

[Miya 13] M. Miyagi, T. Ishikawa, H. Kamoda, M. Suzuki, Y. Sakuma, S. Orita, Y. Oikawa, Y. Aoki, T. Toyone, K. Takahashi, G. Inoue, and S. Ohtori. "Assessment of pain behavior in a rat model of intervertebral disc injury using the Catwalk gait analysis system". *Spine*, Vol. 38, No. 17, pp. 1459–1465, 2013.

[Moce 18] S. Moceri, F. Canneva, J. Habermeyer, J. Dobner, A. Schulze-Krebs, M. Puchades, J. G. Bjaalie, Z. Kohl, J. Winkler, I. K. Timotius, B. Eskofier, S. Schilling, H.-u. Demuth, M. Hartlage-Rübsamen, S. Rossner, N. Casadei, O. Riess, and S. von Hörsten. "Association of early phenotypic behavioral alterations in human α-synuclein overexpressing transgenic rats with α-synuclein/ huntingtin/ amyloid-β protein cross-seeding". In: *Advances in Alzheimer's and Parkinson's Therapies an AAT-AD/PD Focus Meeting*, Torino, Italy, 2018.

[Mond 15] S. E. Mondello, M. D. Sunshine, A. E. Fischedick, C. T. Moritz, and P. J. Horner. "A cervical hemi-contusion spinal dord injury model for the investigation of novel therapeutics targeting proximal and distal forelimb functional recovery". *Journal of Neurotrauma*, Vol. 32, No. 24, pp. 1994–2007, 2015.

[Morr 01] M. E. Morris, F. Huxham, J. McGinley, K. Dodd, and R. Iansek. "The biomechanics and motor control of gait in Parkinson disease". *Clinical Biomechanics*, Vol. 16, No. 6, pp. 459–470, 2001.

[Morr 08] S. Morrison, G. Kerr, K. M. Newell, and P. A. Silburn. "Differential time- and frequency-dependent structure of postural sway and finger tremor in Parkinson's disease". *Neuroscience Letters*, Vol. 443, No. 3, pp. 123–128, 2008.

[Morr 84] R. Morris. "Developments of a water-maze procedure for studying spatial learning in the rat". *Journal of Neuroscience Methods*, Vol. 11, No. 1, pp. 47–60, 1984.

[Mull 09] K. Muller. "Analysis of variance concepts and computations". *WIREs Computational Statistics*, Vol. 1, pp. 271–282, 2009.

[Mura 14] Y. Muramatsu, T. Sasho, M. Saito Yz, S. Yamaguchi, R. Akagi, S. Mukoyama, Y. Akatsu, J. Katsuragi, T. Fukawa, J. Endo, H. Hoshi, Y. Yamamoto, and K. Takahashi. "Preventive effects of hyaluronan from deterioration of gait parameters in surgically induced mice osteoarthritic knee model". *Osteoarthritis and Cartilage*, Vol. 22, pp. 831–835, 2014.

[Muyb 99] E. Muybridge. *Animals in Motion*. Chapman & Hall, London, 1899.

[Nage 91] N. Nagelkerke. "A note on a general definition of the coefficient of determination". *Biometrika*, Vol. 78, No. 3, pp. 691–692, 1991.

[Naka 15] A. Nakamura, H. Funaya, N. Uezono, K. Nakashima, Y. Ishida, T. Suzuki, S. Wakana, and T. Shibata. "Low-cost three-dimensional gait analysis system for mice with an infrared depth sensor". *Neuroscience Research*, Vol. 100, pp. 55–62, 2015.

[Nati 19] National SCI Statistical Center. "Spinal cord injury facts and figures at a glance". Tech. Rep., National SCI Statistical Center, Birmingham, 2019.

[Neck 13] N. D. Neckel, H. Dai, and B. S. Bregman. "Quantifying changes following spinal cord injury with velocity dependent locomotor measures". *Journal of Neuroscience Methods*, Vol. 214, pp. 27–36, 2013.

[Neck 15] N. D. Neckel. "Methods to quantify the velocity dependence of common gait measurements from automated rodent gait analysis devices". *Journal of Neuroscience Methods*, Vol. 253, pp. 244–253, 2015.

[Niew 16] W. Niewiadomski, E. Palasz, M. Skupinska, M. Zylinski, M. Steczkowska, A. Gasiorowska, G. Niewiadomska, and G. Riedel. "TracMouse: a computer aided movement analysis script for the mouse inverted horizontal grid test". *Scientific Reports*, Vol. 6, No. December, pp. 1–15, 2016.

[Nold 01] L. P. J. J. Noldus, A. J. Spink, and R. A. J. Tegelenbosch. "EthoVision: a versatile video tracking system for automation of behavioral experiments". *Behavior Research Methods, Instruments, & Computers*, Vol. 33, No. 3, pp. 398–414, 2001.

[Nold 12] Noldus Information Technology b.v. *CatWalk XT version 10.0. reference manual*. Noldus Information Technology b.v., Wageningen, The Netherlands, 2012.

[Nold 91] L. Noldus. "The observer: a software system for collection and analysis of observational data". *Research Methods, Instruments & Computers*, Vol. 23, No. 3, pp. 415–429, 1991.

[Nove 07] E. L. B. Novelli, Y. S. Diniz, C. M. Galhardi, G. M. X. Ebaid, H. G. Rodrigues, F. Mani, A. A. H. Fernandes, A. C. Cicogna, and J. L. V. B. Novelli Filho. "Anthropometrical parameters and markers of obesity in rats". *Laboratory Animals*, Vol. 41, No. 1, pp. 111–119, 2007.

[Nube 13] S. Nuber, F. Harmuth, Z. Kohl, A. Adame, M. Trejo, K. Schö, F. Zimmermann, C. Bauer, N. Casadei, C. Giel, C. Calaminus, B. J. Pichler, P. H. Jensen, C. P. Mü, D. Amato, J. Kornhuber, J. Winkler, E. Masliah,

and O. Riess. "A progressive dopaminergic phenotype associated with neurotoxic conversion of a-synuclein in BAC-transgenic rats". *Brain*, Vol. 136, pp. 412–432, 2013.

[Nurm 15] A. Nurmi, L. Tolppanen, T. Heikkinen, R. Hodgson, and A.-m. Zainana. "Assessment of gait deficiencies to provide a functional endpoint in the spinal nerve ligation model and spared nerve injury model in rats". *45th annual meeting of the Society for Neuroscience (Neuroscience 2015)*, 2015.

[Nyqu 28] H. Nyquist. "Certain topics in telegraph transmission theory". *Transactions of the American Institute of Electrical Engineers*, Vol. 47, No. 2, pp. 617–644, 1928.

[Oppe 14] A. Oppenheim and R. Schafer. *Discrete-time signal processing*. Pearson New International Edition, Harlow, 3rd Ed., 2014.

[Oppe 96] A. Oppenheim, A. Willsky, and S. H. Nawab. *Signals and Systems*. Prentice-Hall Signal Processing Series, New Jersey, 2nd Ed., 1996.

[Pajo 10] A. Pajoohesh-Ganji, K. R. Byrnes, G. Fatemi, and A. I. Faden. "A combined scoring method to assess behavioral recovery after mouse spinal cord injury". *Neuroscience Research*, Vol. 67, No. 2, pp. 117–25, 2010.

[Park 02] J. Parkinson. "An essay on the shaking palsy. 1817". *The Journal of Neuropsychiatry and Clinical Neurosciences*, Vol. 14, No. 2, pp. 223–236, 2002.

[Parv 13] S. S. Parvathy and W. Masocha. "Gait analysis of C57BL/6 mice with complete Freund's adjuvant-induced arthritis using the CatWalk system". *BMC Musculoskeletal Disorder*, Vol. 14, No. 14, 2013.

[Pear 95] K. Pearson. "Note on regression and inheritance in the case of two parents". *Proceedings of the Royal Society of London*, Vol. 58, pp. 240–242, 1895.

[Pere 14] A. Pérez-Escudero, J. Vicente-Page, R. C. Hinz, S. Arganda, and G. G. de Polavieja. "idTracker: tracking individuals in a group by automatic identification of unmarked animals". *Nature Methods*, Vol. 11, No. 7, pp. 743–748, 2014.

[Pete 07] L. L. Peters, R. F. Robledo, C. J. Bult, G. A. Churchill, B. J. Paigen, and K. L. Svenson. "The mouse as a model for human biology: a resource guide for complex trait analysis". *Nature Reviews Genetics*, Vol. 8, No. 1, pp. 58–69, 2007.

[Piel 14] M. J. Piel, J. S. Kroin, A. J. Van Wijnen, R. Kc, and H. J. Im. "Pain assessment in animal models of osteoarthritis". *Gene*, Vol. 537, No. 2, pp. 184–188, 2014.

[Pluc 14] K. Plucińska, B. Crouch, D. Koss, L. Robinson, M. Siebrecht, G. Riedel, and B. Platt. "Knock-in of human BACE1 cleaves murine APP and teiterates Alzheimer-like phenotypes". *Journal of Neuroscience*, Vol. 34, No. 32, pp. 10710–10728, 2014.

[Poul 13] M. A. Pouladi, A. Jennifer Morton, and M. R. Hayden. "Choosing an animal model for the study of Huntington's disease". *Nature Reviews Neuroscience*, Vol. 14, pp. 708–721, 2013.

[Puri 18] I. Puri and D. D. Cox. "A system for accurate tracking and video recordings of rodent eye movements using convolutional neural networks for biomedical image segmentation". In: *Proceedings of the Annual International Conference of the IEEE Engineering in Medicine and Biology Society, EMBS*, pp. 3590–3593, 2018.

[Qin 14a] J. Qin, S.-H. Chow, A. Guo, W.-N. Wong, K.-S. Leung, and W.-H. Cheung. "Low magnitude high frequency vibration accelerated cartilage degeneration but improved epiphyseal bone formation in anterior cruciate ligament transect induced osteoarthritis rat model". *Osteoarthritis and Cartilage*, Vol. 22, No. 7, pp. 1061–1067, 2014.

[Qin 14b] L. Qin, D. Jing, S. Parauda, J. Carmel, R. R. Ratan, F. S. Lee, and S. Cho. "An adaptive role for BDNF Val66Met polymorphism in motor recovery in chronic stroke". *Journal of Neuroscience*, Vol. 34, No. 7, pp. 2493–2502, 2014.

[Rabi 78] L. Rabiner and R. Schafer. *Digital processing of speech signals*. Prentice-Hall, Englewood Cliffs, New Jersey, 1978.

[Raj 17] A. T. Raj, S. Patil, S. Sarode, and G. Sarode. "P-hacking". *Journal of Contemporary Dental Practice*, Vol. 18, No. 8, pp. 633–634, 2017.

[Reev 16] S. L. Reeves, K. E. Fleming, L. Zhang, and A. Scimemi. "M-Track: a new software for automated detection of grooming trajectories in mice". *PLOS Computational Biology*, Vol. 12, No. 9, p. e1005115, 2016.

[Rich 15] C. A. Richardson. "The power of automated behavioural homecage technologies in characterizing disease progression in laboratory mice: A review". *Applied Animal Behaviour Science*, Vol. 163, pp. 19–27, 2015.

[Ried 94] G. Riedel, T. Seidenbecher, and K. Reymann. "LTP in hippocampal CA1 of urethane- narcotized rats requires stronger tetanization parameters". *Physiology & Behavior*, Vol. 55, No. 6, pp. 1141–1146, 1994.

[Robi 01] L. Robinson, H. Bridge, and G. Riedel. "Visual discrimination learning in the water maze: a novel test for visual acuity". *Behavioural Brain Research*, Vol. 119, pp. 77–84, 2001.

[Robi 12] L. Robinson, J. Guy, L. McKay, E. Brockett, R. C. Spike, J. Selfridge, D. De Sousa, C. Merusi, G. Riedel, A. Bird, and S. R. Cobb. "Morphological and functional reversal of phenotypes in a mouse model of Rett syndrome". *Brain*, Vol. 135, pp. 2699–2710, 2012.

[Robi 17] A. A. Robie, K. M. Seagraves, S. E. Roian Egnor, and K. Branson. "Machine vision methods for analyzing

social interactions". *Journal of Experimental Biology*, Vol. 220, pp. 25–34, 2017.

[Rocc 04] L. Rocchi, L. Chiari, and A. Cappello. "Feature selection of stabilometric parameters based on principal component analysis". *Medical & Biological Engineering & Computing*, Vol. 42, No. 1, pp. 71–79, 2004.

[Rocc 14] L. Rocchi, L. Palmerini, A. Weiss, T. Herman, and J. M. Hausdorff. "Balance testing with inertial sensors in patients with Parkinson's disease: assessment of motor subtypes". *IEEE Transactions on Neural Systems and Rehabilitation Engineering*, Vol. 22, No. 5, pp. 1064–1071, 2014.

[Roge 01] D. C. Rogers, J. Peters, J. E. Martin, S. Ball, S. J. Nicholson, A. S. Witherden, M. Hafezparast, J. Latcham, T. L. Robinson, C. A. Quilter, and E. M. C. Fisher. "SHIRPA, a protocol for behavioral assessment: validation for longitudinal study of neurological dysfunction in mice". *Neuroscience Letter*, Vol. 306, pp. 89–92, 2001.

[Roge 97] D. C. Rogers, E. M. C. Fisher, S. D. M. Brown, J. Peters, A. J. Hunter, and J. E. Martin. "Commentary behavioral and functional analysis of mouse phenotype: SHIRPA, a proposed protocol for comprehensive phenotype assessment". *Mammalian Genome*, Vol. 8, No. 10, pp. 711–713, 1997.

[Roia 16] S. E. Roian Egnor and K. Branson. "Computational analysis of behavior". *Annual Review of Neuroscience*, Vol. 39, pp. 217–236, 2016.

[Roos 10] R. A. Roos. "Huntington's disease: a clinical review". *Orphanet Journal of Rare Diseases*, Vol. 5, No. 40, 2010.

[Rose 04] E. S. Rosenzweig and J. W. McDonald. "Rodent models for treatment of spinal cord injury: research trends and progress toward useful repair". *Current Opinion in Neurology*, Vol. 17, No. 2, pp. 121–131, 2004.

[Rote 14] C. Rotermund, F. M. Truckenmüller, H. Schell, and P. J. Kahle. "Diet-induced obesity accelerates the onset of

terminal phenotypes in α-synuclein transgenic mice". *Journal of Neurochemistry*, Vol. 131, No. 6, pp. 848–858, 2014.

[Saal 15] K. A. Saal, J. C. Koch, L. Tatenhorst, É. M. Szego, V. T. Ribas, U. Michel, M. Bähr, L. Tönges, and P. Lingor. "AAV.shRNA-mediated downregulation of ROCK2 attenuates degeneration of dopaminergic neurons in toxin-induced models of Parkinson's disease in vitro and in vivo". *Neurobiology of Disease*, Vol. 73, pp. 150–162, 2015.

[Salv 14] J. Salvi, F. Bertaso, A.-L. Mausset-Bonnefont, A. Metz, C. Lemmers, F. Ango, L. Fagni, P. Lory, and A. Mezghrani. "RNAi silencing of P/Q-type calcium channels in Purkinje neurons of adult mouse leads to episodic ataxia type 2". *Neurobiology of Disease*, Vol. 68, pp. 47–56, 2014.

[Sand 13] B. Sandner, F. J. Rivera, M. Caioni, L. Nicholson, V. Eckstein, U. Bogdahn, L. Aigner, A. Blesch, and N. Weidner. "Bone morphogenetic proteins prevent bone marrow stromal cell-mediated oligodendroglial differentiation of transplanted adult neural progenitor cells in the injured spinal cord". *Stem Cell Research*, Vol. 11, No. 2, pp. 758–771, 2013.

[Sand 18] B. Sandner, R. Puttagunta, M. Motsch, F. Bradke, J. Ruschel, A. Blesch, and N. Weidner. "Systemic epothilone D improves hindlimb function after spinal cord contusion injury in rats". *Experimental Neurology*, Vol. 306, pp. 250–259, 2018.

[Sche 03] S. W. Scheff, A. G. Rabchevsky, I. Fugaccia, J. A. Main, and J. E. Lumpp. "Experimental modeling of spinal cord injury: characterization of a force-defined injury device". *Journal of Neurotrauma*, Vol. 20, No. 2, pp. 179–193, 2003.

[Sedy 08] J. Šedý, L. Urdzíková, P. Jendelová, and E. Syková. "Methods for behavioral testing of spinal cord injured

rats". *Neuroscience & Biobehavioral Reviews*, Vol. 32, No. 3, pp. 550–580, 2008.

[Shig 14] M. Shigyo, N. Tanabe, T. Kuboyama, S. H. Choi, and C. Tohda. "New reliable scoring system, Toyama mouse score, to evaluate locomotor function following spinal cord injury in mice". *BMC Research Notes*, Vol. 7, No. 332, pp. 1–4, 2014.

[Silv 14] N. A. Silva, N. Sousa, R. L. Reis, and A. J. Salgado. "From basics to clinical: a comprehensive review on spinal cord injury". *Progress in Neurobiology*, Vol. 114, No. November, pp. 25–57, 2014.

[Silv 95] L. M. Silver. *Mouse genetics*. Oxford University Press, 1995.

[Sing 14] A. Singh, L. Krisa, K. L. Frederick, H. Sandrow-Feinberg, S. Balasubramanian, S. K. Stackhouse, M. Murray, and J. S. Shumsky. "Forelimb locomotor rating scale for behavioral assessment of recovery after unilateral cervical spinal cord injury in rats". *Journal of Neuroscience Methods*, Vol. 226, pp. 124–31, 2014.

[Skin 38] B. F. Skinner. *The behavior of organisms: an experimental analysis*. Appleton-Century-Crofts, New York, 1938.

[Slus 17] W. Slusarczyk, S. Gumularz, R. Zachara, M. Hamm, H. Cholewa, D. Chlebosz, K. Duda, M. Kornaś, A. Liśkiewicz, J. Wiaderkiewicz, W. Marcol, P. Morawski, A. Właszczuk, and J. Lewin-Kowalik. "Application of novel computing technologies regarding gait analysis, such as CatWalk XT, in spinal cord regeneration, in the fields of experimental neurosurgery and neutophysiology". *Journal of Spinal Studies and Surgery*, Vol. 1, No. 1, pp. 14–18, 2017.

[Smit 15] B. J. H. Smith, L. Cullingford, and J. R. Usherwood. "Identification of mouse gaits using a novel force-sensing exercise wheel". *Journal of Applied Physiology*, Vol. 119, No. 6, pp. 704–718, 2015.

[Sous 06] N. Sousa, O. Almeida, and C. Wotjak. "A hitchhiker's guide to behavioral analysis in laboratory rodents". *Genes, Brain and Behavior*, Vol. 5, pp. 5–24, 2006.

[Spar 17] L. M. Sparrow, E. Pellatt, S. S. Yu, D. A. Raichlen, H. Pontzer, and C. Rolian. "Gait changes in a line of mice artificially selected for longer limbs". *PeerJ*, Vol. 5, No. e3008, 2017.

[Spil 97] M. G. Spillantini, M. L. Schmidt, V. M. Lee, J. Q. Trojanowski, R. Jakes, and M. Goedert. "Alpha-synuclein in Lewy bodies". *Nature*, Vol. 388, No. 6645, pp. 839–840, 1997.

[Staa 06] F. J. van der Staay. "Animal models of behavioral dysfunctions: Basic concepts and classifications, and an evaluation strategy". *Brain Research Reviews*, Vol. 52, pp. 131–159, 2006.

[Stel 15] I. van der Stelt, E. F. Hoek-van den Hil, H. J. Swarts, J. J. Vervoort, L. Hoving, L. Skaltsounis, N. Lemonakis, I. Andreadou, E. M. van Schothorst, and J. Keijer. "Nutraceutical oleuropein supplementation prevents high fat diet-induced adiposity in mice". *Journal of Functional Foods*, Vol. 14, pp. 702–715, 2015.

[Stol 04] H. Stolze, S. Klebe, C. Zechlin, C. Baecker, L. Friege, and G. Deuschl. "Falls in frequent neurological diseases". *Journal of Neurology*, Vol. 251, No. 1, pp. 79–84, 2004.

[Stow 17] J. R. Stowers, M. Hofbauer, R. Bastien, J. Griessner, P. Higgins, S. Farooqui, R. M. Fischer, K. Nowikovsky, W. Haubensak, I. D. Couzin, K. Tessmar-Raible, and A. D. Straw. "Virtual reality for freely moving animals". *Nature Methods*, Vol. 14, pp. 995–1002, 2017.

[Sull 12] G. M. Sullivan and R. Feinn. "Using effect size-or why the p value is not enough". *Journal of Graduate Medical Education*, pp. 279–282, 2012.

[Swee 15] P. J. Sweeney, T. Ahtoniemi, J. Puoliväli, K. Lehtimäki, P. Karhunen, T. Heikkinen, A. Nurmi, and D. Wells.

"Fine motor kinematic analysis in the MDX mouse model of duchenne muscular dystrophy a longitudinal study of chronically exercised VS non-exercised MDX mice". In: *45th annual meeting of the Society for Neuroscience (Neuroscience 2015)*, 2015.

[Tan 17] B.-T. Tan, L. Jiang, L. Liu, Y. Yin, Z.-R.-X. Luo, Z.-Y. Long, S. Li, L.-H. Yu, Y.-M. Wu, and Y. Liu. "Local injection of Lenti-Olig2 at lesion site promotes functional recovery of spinal cord injury in rats". *CNS Neuroscience & Therapeutics*, Vol. 23, No. 6, pp. 475–487, 2017.

[Tate 16] L. Tatenhorst, K. Eckermann, V. Dambeck, L. Fonseca-Ornelas, H. Walle, T. Lopes, D. Fonseca, J. C. Koch, S. Becker, L. Tönges, M. Bähr, T. F. Outeiro, M. Zweckstetter, and P. Lingor. "Fasudil attenuates aggregation of α-synuclein in models of Parkinson's disease". *Acta Neuropathologica Communications*, Vol. 4, No. 39, 2016.

[Tayl 78] C. R. Taylor. "Why change gaits? recruitment of muscles and muscle fibers as a function of speed and gait". *American Zoologist*, Vol. 18, pp. 153–161, 1978.

[Timo 13a] I. K. Timotius and I. Setyawan. "Using estimated arithmetic means of accuracies to select features for face-based gender classification". In: *Int. Conf. on Information Technology and Electrical Engineering (ICITEE)*, pp. 242–247, IEEE, Yogjakarta, 2013.

[Timo 13b] I. K. Timotius. "Predicting receiver operating characteristic curve, area under curve, and arithmetic means of accuracies based on the distribution of data samples". In: *Int. Conf. on Control, Systems and Industrial Informatics (ICCSII)*, pp. 60–64, Bandung, Indonesia, 2013.

[Timo 18a] I. K. Timotius, F. Canneva, G. Minakaki, S. Moceri, N. Casadei, O. Riess, J. Winkler, S. von Hörsten, B. Eskofier, and J. Klucken. "Systematic data analysis and data mining in gait analysis by heat mapping". In:

11th Int. Conf. on Methods and Techniques in Behavioral Research (Measuring Behavior 2018), pp. 43–49, Manchester, UK, 2018.

[Timo 18b] I. K. Timotius, F. Canneva, G. Minakaki, C. Pasluosta, S. Moceri, N. Casadei, O. Riess, J. Winkler, J. Klucken, S. von Hörsten, and B. Eskofier. "Dynamic footprint based locomotion sway assessment in α-synucleinopathic mice using fast Fourier transform and low pass filter". *Journal of Neuroscience Methods*, Vol. 296, pp. 1–11, 2018.

[Timo 18c] I. K. Timotius, F. Canneva, G. Minakaki, C. Pasluosta, S. Moceri, N. Casadei, O. Riess, J. Winkler, J. Klucken, S. von Hörsten, and B. Eskofier. "Dynamic footprints of α-synucleinopathic mice recorded by CatWalk gait analysis". *Data in Brief* , Vol. 17, pp. 189–193, 2018.

[Timo 18d] I. K. Timotius, S. Moceri, A. Plank, J. Habermeyer, F. Canneva, N. Casadei, O. Riess, J. Winkler, J. Klucken, B. Eskofier, and S. von Hörsten. "Rodent's stride length depends on body size: implications for CatWalk assay". In: *11th Int. Conf. on Methods and Techniques in Behavioral Research (Measuring Behavior 2018)*, pp. 50–52, Manchester, UK, 2018.

[Timo 19a] I. K. Timotius, F. Canneva, G. Minakaki, S. Moceri, A.-C. Plank, N. Casadei, O. Riess, J. Winkler, J. Klucken, B. Eskofier, and S. von Hörsten. "Systematic data analysis and data mining in CatWalk gait analysis by heat mapping exemplified in rodent models for neurodegenerative diseases". *Journal of Neuroscience Methods*, Vol. 326, 2019.

[Timo 19b] I. K. Timotius, S. Moceri, A.-C. Plank, J. Habermeyer, F. Canneva, J. Winkler, J. Klucken, N. Casadei, O. Riess, B. Eskofier, and S. von Hörsten. "Silhouette-length-scaled gait parameters for motor functional analysis in mice and rats". *eNeuro*, 2019.

[Timo 19c] I. K. Timotius, B. Sandner, V. Estrada, D. Garcia-Ovejero, L. Bieler, S. Couillard-Despres, F. Labombar-

da, H. W. Müller, J. Winkler, J. Klucken, B. Eskofier, and R. Puttagunta. "Combination of defined CatWalk gait parameters for predictive locomotion recovery in experimental thoracic spinal cord injured rat models". *in preparation*, 2019.

[Tolo 06] E. Tolosa, G. Wenning, and W. Poewe. "The diagnosis of Parkinson's disease". *The Lancet Neurology*, Vol. 5, No. 1, pp. 75–86, 2006.

[Tsik 14] E. Tsika, M. Kannan, C. S. Y. Foo, D. Dikeman, L. Glauser, S. Gellhaar, D. Galter, G. W. Knott, T. M. Dawson, V. L. Dawson, and D. J. Moore. "Conditional expression of Parkinson's disease-related R1441C LRRK2 in midbrain dopaminergic neurons of mice causes nuclear abnormalities without neurodegeneration". *Neurobiology of Disease*, Vol. 71, No. 1, pp. 345–358, 2014.

[Vale 07] D. Valente, H. Wang, P. Andrews, P. P. Mitra, S. Saar, O. Tchernichovski, I. Golani, and Y. Benjamini. "Characterizing animal behavior through audio and video signal processing". *IEEE Multimedia*, Vol. 14, No. 4, pp. 32–41, 2007.

[Vale 15] T. C. Vale and F. Cardoso. "Chorea: a journey through history". *Tremor and other Hyperkinet Movements*, Vol. 5, pp. 1–6, 2015.

[Vall 17] J. J. Valletta, C. Torney, M. Kings, A. Thornton, and J. Madden. "Applications of machine learning in animal behaviour studies". *Animal Behaviour*, Vol. 124, pp. 203–220, 2017.

[Vand 10] C. Vandeputte, J.-M. Taymans, C. Casteels, F. Coun, Y. Ni, K. van Laere, and V. Baekelandt. "Automated quantitative gait analysis in animal models of movement disorders". *BMC Neuroscience*, Vol. 11, No. 92, 2010.

[Vand 14] T. F. Vandamme. "Use of rodents as models of human diseases". *Journal of Pharmacy & Bioallied Sciences*, Vol. 6, No. 1, pp. 2–9, 2014.

[Vida 17] P. M. Vidal, S. K. Karadimas, A. Ulndreaj, A. M. Laliberte, L. Tetreault, S. Forner, J. Wang, W. D. Foltz, and M. G. Fehlings. "Delayed decompression exacerbates ischemia-reperfusion injury in cervical compressive myelopathy". *JCI Insight*, Vol. 2, No. 11, 2017.

[Vlam 07] R. Vlamings, V. Visser-Vandewalle, G. Koopmans, E. A. J. Joosten, R. Kozan, S. Kaplan, H. W. M. Steinbusch, and Y. Temel. "High frequency stimulation of the subthalamic nucleus improves speed of locomotion but impairs forelimb movement in Parkinsonian rats". *Neuroscience*, Vol. 148, No. 3, pp. 815–823, 2007.

[Wahl 11] D. Wahlsten. *Mouse behavioral testing: how to use mice in behavioral neuroscience*. Academic Press, 2011.

[Wang 12] X. H. Wang, G. Lu, X. Hu, K. S. Tsang, W. H. Kwong, F. X. Wu, H. W. Meng, S. Jiang, S. W. Liu, H. K. Ng, and W. S. Poon. "Quantitative assessment of gait and neurochemical correlation in a classical murine model of Parkinson's disease". *BMC Neuroscience*, Vol. 13, No. 142, 2012.

[Wass 18] Z. Wassouf, T. Hentrich, S. Samer, C. Rotermund, P. J. Kahle, I. Ehrlich, O. Riess, N. Casadei, and J. M. Schulze-Hentrich. "Environmental enrichment prevents transcriptional disturbances induced by alpha-synuclein overexpression". *Frontiers in Cellular Neuroscience*, Vol. 12, No. April, 2018.

[Webb 03] A. A. Webb, K. Gowribai, and G. D. Muir. "Fischer (F-344) rats have different morphology, sensorimotor and locomotor abilities compared to Lewis, Long-Evans, Sprague-Dawley and Wistar rats". *Behavioural Brain Research*, Vol. 144, No. 1-2, pp. 143–156, 2003.

[Weid 01] N. Weidner, A. Ner, N. Salimi, and M. H. Tuszynski. "Spontaneous corticospinal axonal plasticity and functional recovery after adult central nervous system injury". *Proceedings of the National Academy of Sciences of the United States of America*, Vol. 98, No. 6, pp. 3513–3518, 2001.

[Weid 99] N. Weidner, R. J. Grill, and M. H. Tuszynski. "Elimination of basal lamina and the collagen "scar" after spinal vord injury fails to augment corticospinal tract regeneration". *Experimental Neurology*, Vol. 160, pp. 40–50, 1999.

[Wein 08] J. N. Weinstein. "A postgenomic visual icon". *Science (New York, N.Y.)*, Vol. 319, No. 1, pp. 1772–1773, 2008.

[West 12] J. E. Westin, M. L. Janssen, T. N. Sager, and Y. Temel. "Automated gait analysis in bilateral Parkinsonian rats and the role of l-DOPA therapy". *Behavioural Brain Research*, Vol. 226, No. 2, pp. 519–528, 2012.

[Whit 96] M. W. Whittle. "Clinical gait analysis: a review". *Human Movement Science*, Vol. 15, pp. 369–387, 1996.

[Wilc 17] J. T. Wilcox, K. Satkunendrarajah, Y. Nasirzadeh, A. M. Laliberte, A. Lip, D. W. Cadotte, W. D. Foltz, and M. G. Fehlings. "Generating level-dependent models of cervical and thoracic spinal cord injury: Exploring the interplay of neuroanatomy, physiology, and function". *Neurobiology of Disease*, Vol. 105, pp. 194–212, 2017.

[Wile 12] J. Wiles, S. Heath, D. Ball, L. Quinn, and A. Chiba. "Rat meets iRat". In: *2012 IEEE Int. Conf. on Development and Learning and Epigenetic Robotics, ICDL 2012*, IEEE, 2012.

[Wilk 09] L. Wilkinson and M. Friendly. "The history of the cluster heat map". *The American Statistician*, Vol. 63, No. 2, pp. 179–184, 2009.

[Wilt 15] A. B. Wiltschko, M. J. Johnson, G. Iurilli, R. E. Peterson, J. M. Katon, S. L. Pashkovski, V. E. Abraira, R. P. Adams, and S. R. Datta. "Mapping sub-second structure in mouse behavior". *Neuron*, Vol. 88, No. 6, pp. 1121–1135, 2015.

[Wool 09] C. M. Wooley, S. Xing, R. W. Burgess, G. A. Cox, and K. L. Seburn. "Age, experience and genetic background influence treadmill walking in mice". *Physiology and Behavior*, Vol. 96, No. 2, pp. 350–361, 2009.

[Yoo 15] S.-W. Yoo, M. G. Motari, K. Susuki, J. Prendergast, A. Mountney, A. Hurtado, and R. L. Schnaar. "Sialylation regulates brain structure and function". *FASEB journal*, Vol. 29, No. 7, pp. 3040–53, 2015.

[Zain 15] A.-m. Zainana, J. Puoliväli, T. Heikkinen, R. Hodgson, and A. Nurmi. "Behavioral characterization of the cuprizone model of demyelination in mice". In: *45th annual meeting of the Society for Neuroscience (Neuroscience 2015)*, Chicago, 2015.

[Zhou 15] M. Zhou, W. Zhang, J. Chang, J. Wang, W. Zheng, Y. Yang, P. Wen, M. Li, and H. Xiao. "Gait analysis in three different 6-hydroxydopamine rat models of Parkinson's disease". *Neuroscience Letters*, Vol. 584, pp. 184–189, 2015.

[Zijl 96] W. Zijlstra, T. Prokop, and W. Berger. "Adaptability of leg movements during treadmill walking and split-belt walking in children". *Gait & Posture*, Vol. 4, No. 3, pp. 212–221, 1996.

[Zimp 18] A. Zimprich, M. A. Östereicher, L. Becker, P. Dirscherl, L. Ernst, H. Fuchs, V. Gailus-Durner, L. Garrett, F. Giesert, L. Glasl, A. Hummel, J. Rozman, M. H. de Angelis, D. Vogt-Weisenhorn, W. Wurst, and S. M. Hölter. "Analysis of locomotor behavior in the German mouse clinic". *Journal of Neuroscience Methods*, Vol. 300, pp. 77–91, 2018.

Index

List of Abbreviations

α-Syn	α-synuclein.
6-OHDA	6-hydroxydopamine.
AA	Alternate sequence (RF-RH-LF-LH).
AAV	adeno-associated viral.
AAV-NT3	AAV vector-mediated prolonged delivery of neurotrophin NT-3.
AB	Alternate sequence (LF-RH-RF-LH).
ACLT	anterior cruciate ligament transection.
AD	Alzheimer's disease.
AIMs	abnormal involuntary movement.
ALS	amyotrophic lateral sclerosis.
ANOVA	analysis of variance.
APP	amyloid precursor protein.
ATP7A	(also known as Menkes' protein or MNK) copper-transporting P-type ATPase.
b/w	black and white.
BAC	bacterial artificial chromosome.

BACHD bacterial artificial chromosome of mutant *HTT* gene (relevant to HD).

BBB Basso, Beattie, and Bresnahan.

BCE before the common era (also known as before Christ/BC).

BDNF brain-derived neurotrophic factor.

BLG combination of the BMS score, the modified Ladder climb, and the Grip walk.

blob binary large object.

BMS Basso mouse scale.

BOS base of support.

C cervical.

CA Cruciate sequence (RF-LF-RH-LH).

CAG cytosine, adenine, and guanine.

CB Cruciate sequence (LF-RF-LH-RH).

CCI chronic constriction injury.

CCI-score combined CatWalk index score.

CFA complete Freund's adjuvant.

ChABC Chondroitinase ABC enzyme.

CNS central nervous system.

COM center of mass.

CoP center of pressure.

CPC calcium phosphate cement.

CPU Caudate Putamen.

CST corticospinal tract.

CStat Circular statistic.

DCM degenerative cervical myelopathy.

DFT discrete Fourier transform.
dMCAO distal middle cerebral artery occlusion.
DMM destabilization of the medial meniscus.
DMSO dimethylsulfoxid.
dPDN dissociated predegenerated nerve.
dpi days post injury.
DTFT discrete-time Fourier transform.
DTW dynamic time warping.

EA2 episodic ataxia type-2.
EAE experimental autoimmune encephalomyelitis.
EN elastic net.
Epo epothilone.
EWN Eshkol Wachmann notation.

FCA Freund's complete adjuvant.
FDA Fisher discriminant analysis.
FFT fast Fourier transform.
FIR finite impulse response.
FL forelimb.
FLAS forelimb locomotor assessment scale.
FLS forelimb locomotor scale.
fps frames per second.

GBM gradient boosting machine.
GDA generalized discriminant analysis.
GFP green fluorescent protein.

H&Y Hoehn & Yahr.

HB9 (also known as MNX1) Motor neuron and pancreas homeobox 1.

hBACE1 human β-site APP cleaving enzyme 1.

HD Huntington disease.

HFS high frequency stimulation.

HL hindlimb.

HTT Huntingtin.

huWT/KO compensatory expression of human α-Syn protein, under the control of a BAC construct, on the mouse α-Syn knockout background.

Hz Hertz.

i.p. intraperitoneal.

IAI-HA intra-articular injection of hyaluronan.

ICH intracerebral hemorrhage.

IDA initial data analysis.

iDC incomplete dorsal column.

IH Infinite Horizon.

IIR infinite impulse response.

IVD intervertebral disc.

kDyn kilodynes.

KO knock out.

LD Leigh disease.

LDA linear discriminant analysis.

LF left front paw.

LH left hind paw.
LPF low pass filter.
LRRK2 leucine-rich repeat kinase 2.

MCAo middle cerebral artery occlusion.
MeCP2 methyl-CpG-binding protein 2.
MFB medial forebrain bundle.
mHTT mutant HTT.
MIA mono-iodoacetate.
MOG myelin oligodendrocyte glycoprotein.
MPS methylprednisolone.
MPTP methyl-4-phenyl-1,2,3,6-tetrahydropyridine.
MS multiple sclerosis.

NIH National Institute of Health.
NP nucleus pulposus.
NSSP normal step sequence pattern.

OA osteoarthritis.

PBS phosphate-buffered saline.
PCA principal component analysis.
PD Parkinson's disease.
pDNA plasmid deoxyribonucleic acid.
PFF synthetic pre formed fibrils.
PINK1 PTEN-induced putative kinase 1.
pixel picture elements.
pMMx partial medial menisectomy.

PT photothrombosis.

RA Rotary sequence (RF-LF-LH-RH).
Rand.For. random forest.
RB Rotary sequence (LF-RF-RH-LH).
RF right front paw.
RFID radio frequency identification.
RGB red green blue.
RH right hind paw.
RI regularity index.
RNA ribonucleic acid.
ROCK rho-associated kinase.

SC Schwann cell.
SCI spinal cord injury.
SD standard deviation.
SEM standard error of mean.
SHIRPA SmithKline Beecham, Harwell, Imperial College, and Royal London Hospital phenotype assessment.
shRNA short hairpin ribonucleic acid.
SNC substantia nigra compact.
SNP single nucleotide polymorphism.
SPF specific pathogen free.
STFFT short time fast Fourier transform.
STN subthalamic nucleus.
SWLS satisfaction with life scale.

TG transgenic.

Th thoracic.

TMS Toyama mouse score.

UHDRS unified Huntington disease rating scale.

UI uninjured.

UPDRS unified Parkinson's disease rating scale.

Val66Met valine to methionine at codon 66.

WT wild type.

YAC yeast artificial chromosome.

Gait analysis is important for the investigation of gait progression and the development of therapies in disorders characterized by gait impairments, such as Parkinson's disease (PD), Huntington disease (HD), and Spinal Cord Injury (SCI). Describing gait quantitatively helps researchers to analyze gait impairment in a more consistent, reliable, and precise manner compared to qualitative description. For this reason, apparatus and computation methods are continuously developed for both clinical and preclinical studies using animals.

One of the gait analysis apparatus for rodents is called CatWalk. The system is equipped with a transparent glass floor walkway, where rodents can walk from one to the opposite end. Using a camera located under the walkway, the system records a video, which contains the information of the paw contact positions. Based on the recorded video, this CatWalk system computes several gait parameters.

Here, several computational methods that enrich the information extracted from CatWalk data are presented. These methods improve the outcome of the current Catwalk data acquisition by providing methods in identifying gait patterns related to PD, providing a silhouette-length-based intra-assay scaling method, an initial data analysis method, and a parametric gait recovery progression score for rat SCI models.

ISBN 978-3-96147-320-5

9 783961 473205

FAU UNIVERSITY PRESS 2020